

2001

Synthesis and reactions of organometallic complexes featuring a doubly-linked dicyclopentadienyl ligand

Maxim V. Ovchinnikov
Iowa State University

Follow this and additional works at: <https://lib.dr.iastate.edu/rtd>

 Part of the [Inorganic Chemistry Commons](#), and the [Organic Chemistry Commons](#)

Recommended Citation

Ovchinnikov, Maxim V., "Synthesis and reactions of organometallic complexes featuring a doubly-linked dicyclopentadienyl ligand " (2001). *Retrospective Theses and Dissertations*. 1071.
<https://lib.dr.iastate.edu/rtd/1071>

This Dissertation is brought to you for free and open access by the Iowa State University Capstones, Theses and Dissertations at Iowa State University Digital Repository. It has been accepted for inclusion in Retrospective Theses and Dissertations by an authorized administrator of Iowa State University Digital Repository. For more information, please contact digirep@iastate.edu.

INFORMATION TO USERS

This manuscript has been reproduced from the microfilm master. UMI films the text directly from the original or copy submitted. Thus, some thesis and dissertation copies are in typewriter face, while others may be from any type of computer printer.

The quality of this reproduction is dependent upon the quality of the copy submitted. Broken or indistinct print, colored or poor quality illustrations and photographs, print bleedthrough, substandard margins, and improper alignment can adversely affect reproduction.

In the unlikely event that the author did not send UMI a complete manuscript and there are missing pages, these will be noted. Also, if unauthorized copyright material had to be removed, a note will indicate the deletion.

Oversize materials (e.g., maps, drawings, charts) are reproduced by sectioning the original, beginning at the upper left-hand corner and continuing from left to right in equal sections with small overlaps.

Photographs included in the original manuscript have been reproduced xerographically in this copy. Higher quality 6" x 9" black and white photographic prints are available for any photographs or illustrations appearing in this copy for an additional charge. Contact UMI directly to order.

ProQuest Information and Learning
300 North Zeeb Road, Ann Arbor, MI 48106-1346 USA
800-521-0600

UMI[®]

Synthesis and reactions of organometallic complexes featuring a doubly-linked
dicyclopentadienyl ligand

by

Maxim V. Ovchinnikov

A dissertation submitted to the graduate faculty
in partial fulfillment of the requirements for the degree of
DOCTOR OF PHILOSOPHY

Major: Organic Chemistry

Major Professor: Robert J. Angelici

Iowa State University

Ames, Iowa

2001

Copyright © Maxim V. Ovchinnikov, 2001. All rights reserved.

UMI Number: 3016736

Copyright 2001 by
Ovchinnikov, Maxim V.

All rights reserved.

UMI[®]

UMI Microform 3016736

Copyright 2001 by Bell & Howell Information and Learning Company.

All rights reserved. This microform edition is protected against
unauthorized copying under Title 17, United States Code.

Bell & Howell Information and Learning Company
300 North Zeeb Road
P.O. Box 1346
Ann Arbor, MI 48106-1346

Synthesis and reactions of organometallic complexes featuring a doubly-linked
dicyclopentadienyl ligand

Maxim V. Ovchinnikov

Major Professor: Robert J. Angelici

Iowa State University

This dissertation presents an overview of synthesis and chemical reactivity of a novel diruthenium complex $\{(\eta^5\text{-C}_5\text{H}_3)_2(\text{SiMe}_2)_2\}\text{Ru}_2(\text{CO})_4$ (**1**) and its derivatives. Complex 1H^+ , $\{[(\eta^5\text{-C}_5\text{H}_3)_2(\text{SiMe}_2)_2]\text{Ru}_2(\text{CO})_4(\mu\text{-H})\}^+$, with a protonated Ru-Ru bond, is deprotonated only very slowly (hours or days) by basic amines and phosphines although the proton in 1H^+ is acidic thermodynamically. This remarkable kinetic inertness of the bridging proton allows primary and secondary amines to react with 1H^+ by attacking the CO ligand to give a formamide and the CO-substituted ruthenium complex $\{(\eta^5\text{-C}_5\text{H}_3)_2(\text{SiMe}_2)_2\}\text{-Ru}_2(\text{NHR}_1\text{R}_2)(\text{CO})_3$. We have demonstrated that a CO ligand in the protonated complex $\{[(\eta^5\text{-C}_5\text{H}_3)_2(\text{SiMe}_2)_2]\text{Ru}_2(\text{CO})_4(\mu\text{-H})\}^+$ (1H^+) is the site of reaction with amines because of the high electrophilicity of the CO ligands and the low kinetic acidity of the bridging hydride – a unique combination of kinetic properties that are not found in the Fe and Os analogs. On the other hand, Γ , RS^- and phosphines add at one of the Ru centers in 1H^+ , resulting in cleavage of the Ru-H-Ru bond. The final type of addition to 1H^+ is that exhibited by MeO^- and F^- , which results in cleavage of Si-C(cyclopentadienyl) bonds. Except for the reaction with F^- , all of these types of reactions depend on the presence of the proton on the Ru-Ru bond. The unprotonated $(\eta^5\text{-C}_5\text{H}_3)_2(\text{SiMe}_2)_2\text{Ru}_2(\text{CO})_4$ (**1**) undergoes no reactions with these nucleophiles (except F^-) under the mild room-temperature conditions of these studies. The

protonated diruthenium alkene complexes $[\{(\eta^5\text{-C}_5\text{H}_3)_2(\text{SiMe}_2)_2\}\text{Ru}_2(\text{CO})_3(\eta^2\text{-CH}_2=\text{CH-R})(\mu\text{-H})]^+$ react with a variety of nucleophiles to give hydrofunctionalized alkenes with predominantly Markovnikov regioselectivity. The dinuclear ruthenium complex $\{(\eta^5\text{-C}_5\text{H}_3)_2(\text{SiMe}_2)_2\}\text{Ru}_2(\text{CO})_4$ (**1**) is a precursor for the synthesis of a variety of new dinuclear ruthenium complexes, in which the bridging $(\eta^5\text{-C}_5\text{H}_3)_2(\text{SiMe}_2)_2$ ligand controls the geometry of the final product. Thus, complex **1** reacts with diphenylacetylene to form a series of the unusual ruthenacarbocyclic complexes as major products.

Graduate College
Iowa State University

This is to certify that the Doctoral dissertation of
Maxim V. Ovchinnikov
has met the dissertation requirements of Iowa State University

Signature was redacted for privacy.

Major Professor

Signature was redacted for privacy.

For the Major Program

Signature was redacted for privacy.

For the Graduate College

Dedicated to my parents

Alla Ivanovna and Vasily Semenovich Ovchinnikov

TABLE OF CONTENTS

GENERAL INTRODUCTION	1
CHAPTER 1. A KINETICALLY-INERT PROTON ON A METAL-METAL BOND IN $[\{(\eta^5\text{-C}_5\text{H}_3)_2(\text{SiMe}_2)_2\}\text{Ru}_2(\text{CO})_4(\mu\text{-H})]^+$ THAT PROMOTES REACTIONS WITH AMINES	13
CHAPTER 2. AMINE ATTACK ON THE CARBONYL LIGANDS OF THE PROTONATED DICYCLOPENTADIENYL-BRIDGED DIRUTHENIUM COMPLEX $[\{(\eta^5\text{-C}_5\text{H}_3)_2(\text{SiMe}_2)_2\}\text{Ru}_2(\text{CO})_4(\mu\text{-H})]^+$	23
CHAPTER 3. REACTIONS OF THE DINUCLEAR RUTHENIUM COMPLEX $\{(\eta^5\text{-C}_5\text{H}_3)_2(\text{SiMe}_2)_2\}\text{Ru}_2(\text{CO})_4$ FEATURING A DOUBLY-LINKED DICYCLOPENTADIENYL LIGAND	50
CHAPTER 4. HYDROFUNCTIONALIZATION OF ALKENES PROMOTED BY DIRUTHENIUM COMPLEXES $[\{(\eta^5\text{-C}_5\text{H}_3)_2(\text{SiMe}_2)_2\}\text{Ru}_2(\text{CO})_3(\eta^2\text{-CH}_2\text{=CH-R})(\mu\text{-H})]^+$ FEATURING A KINETICALLY INERT PROTON ON A METAL-METAL BOND	92
CHAPTER 5. METAL CONTROL OF THE REACTION SITE IN REACTIONS OF $[\{(\eta^5\text{-C}_5\text{H}_3)_2(\text{SiMe}_2)_2\}\text{M}_2(\text{CO})_4(\mu\text{-H})]^+$ (M = Fe, Ru, Os) WITH NUCLEOPHILIC AMINES	107
CHAPTER 6. REACTIONS OF THE PROTONATED DINUCLEAR RUTHENIUM COMPLEX $[\{(\eta^5\text{-C}_5\text{H}_3)_2(\text{SiMe}_2)_2\}\text{Ru}_2(\text{CO})_4(\mu\text{-H})]^+$ WITH NUCLEOPHILES	121
GENERAL CONCLUSIONS	143
ACKNOWLEDGEMENTS	144

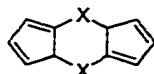
GENERAL INTRODUCTION

Dissertation Organization

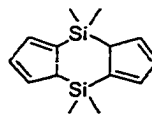
This dissertation contains six papers in the format required for journal publication, describing the research I have performed at Iowa State University. Preceding these papers is a literature review on bimetallic complexes with the doubly-linked cyclopentadiene ligand $(\eta^5\text{-C}_5\text{H}_3)_2(\text{SiMe}_2)_2$. In the literature review, as well as the papers, the literature citations, schemes, tables and figures pertain only to the chapters in which they appear.

Introduction

The study of bimetallic transition metal complexes in which the metal atoms are held in close proximity has been a topic of considerable interest. One of the rationales for the great interest in homo- and heterobimetallic organometallic complexes is the expectation that their chemical behavior both in stoichiometric and catalytic reactions may differ significantly from that of the analogous mononuclear complexes. A common assumption is that cooperative interactions between two metal centers might cause a significant increase or decrease in the reaction rates or lead to transformations which do not occur when monometallic complexes are involved. One of the most investigated classes of bimetallic complexes is that in which



X = alkyl, alkenyl, ER₂ etc.



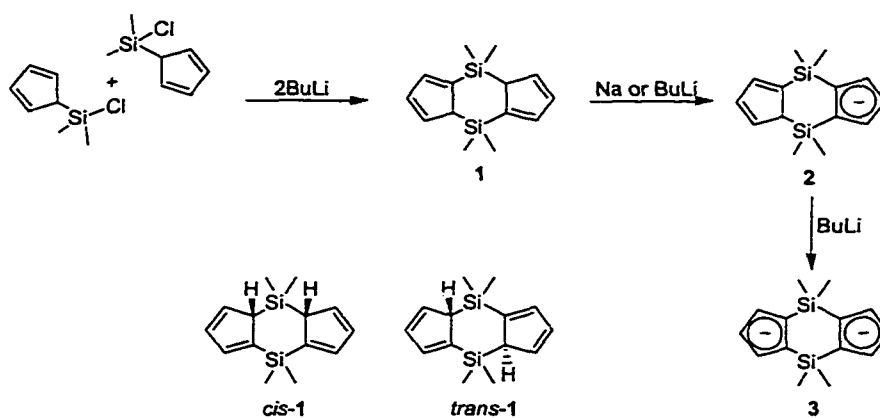
1

two cyclopentadienyl rings are directly connected by a single bond or by one or more saturated or unsaturated chains.¹

The purpose of this review is to summarize the presently available information relating to the synthesis and reactions of the bimetallic complexes featuring the doubly-linked cyclopentadiene ligand (η^5 -C₅H₃)₂(SiMe₂)₂.

Synthesis and Properties of the Doubly-linked Dicyclopentadiene Ligand (C₅H₄)₂(SiMe₂)₂

The first reliable synthesis of (C₅H₄)₂(SiMe₂)₂ (**1**) was reported in the early 1990s.² Compound **1** is conveniently prepared in 47-56% yield by the reaction of an ether solution of C₅H₅SiMe₂Cl with BuLi (Scheme 1). The reaction involves initial formation of dimethylsilafulvene C₅H₄=SiMe₂, which then undergoes dimerization in a [6+6] fashion to give **1**. In solution, two isomers (*cis*-**1** and *trans*-**1**) are present in an approximately 1:2 ratio,



Scheme 1

but only the trans isomer crystallizes from solution. It is well known that cyclopentadienylsilanes show fluxional NMR behavior.^{3, 4} Elementotropic (degenerate) and prototropic (non-degenerate) shifts result in the interconversion of different isomers (Si-allyl and Si-vinyl). The energy barrier for the prototropic shift is in the range of 24–168 J mol⁻¹,^{4b} suitable for studies using variable temperature NMR spectroscopy. Coalescence leads to broadening of several resonances at room temperature in the ¹H and ¹³C NMR spectra.

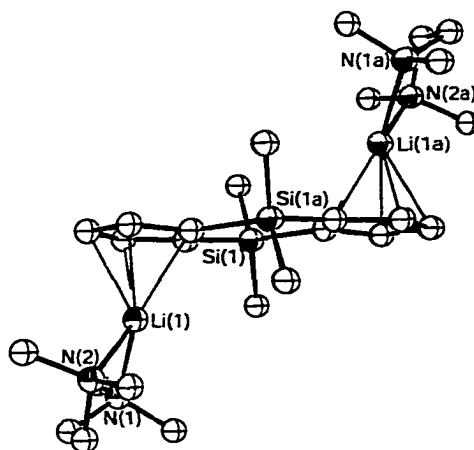
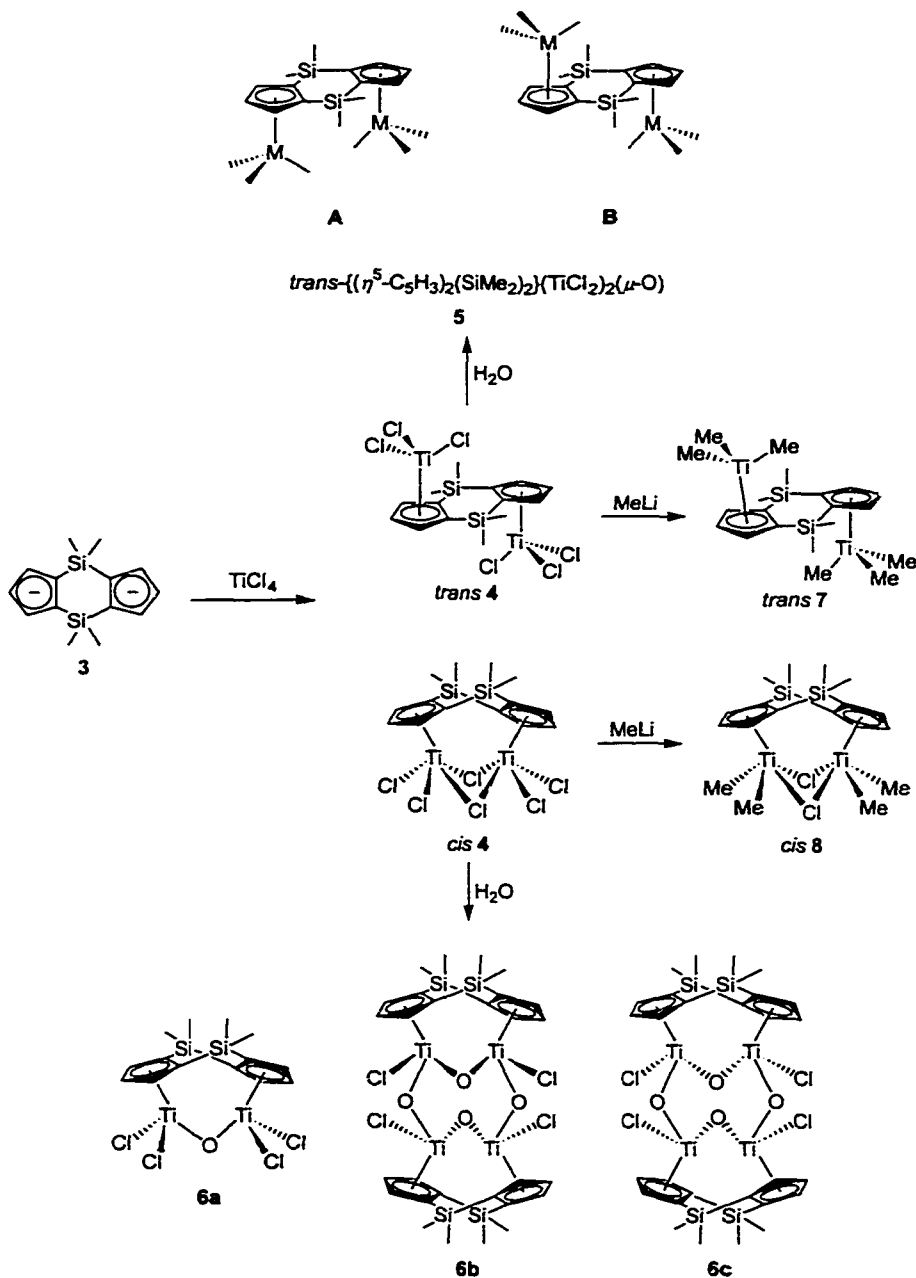


Figure 1. ORTEP representation of $[(\eta^5\text{-C}_5\text{H}_3)_2(\text{SiMe}_2)_2]\text{Li}_2(\text{TMEDA})_2$ (**3**).

Depending on the reaction conditions, only one or both acidic hydrogen atoms of **1** are removed to give the corresponding mono- and dianions **2** and **3**. The X-ray structure analysis of **3** (Figure 1)^{2b} shows that the dianion has a flat skeleton in which the interplanar angle between the six-membered ring and both Cp planes is 172.9°. The anti arrangement of **3** is expected from the electrostatic and steric repulsion of the Li ions.

Homodinuclear Complexes with Group 4 Metals

The doubly-linked dicyclopentadienyl $\{(\eta^5\text{-C}_5\text{H}_3)_2(\text{SiMe}_2)_2\}^{2-}$ (**3**) dianion is a rigid system that allows the coordination of two metal fragments that occupy *cis* or *trans* positions with respect to the faces of the rings, a quality that gives rise to the structural motifs A and B.

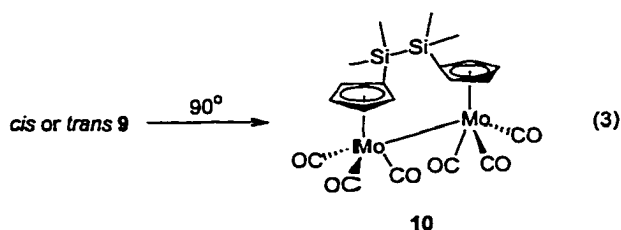
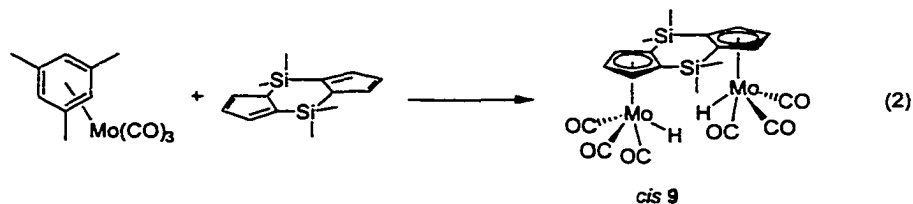
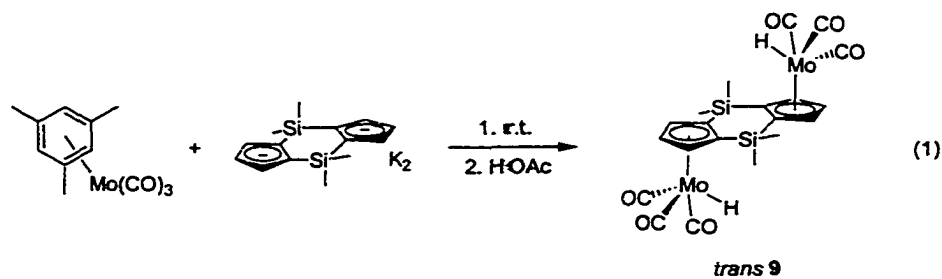


Scheme 2

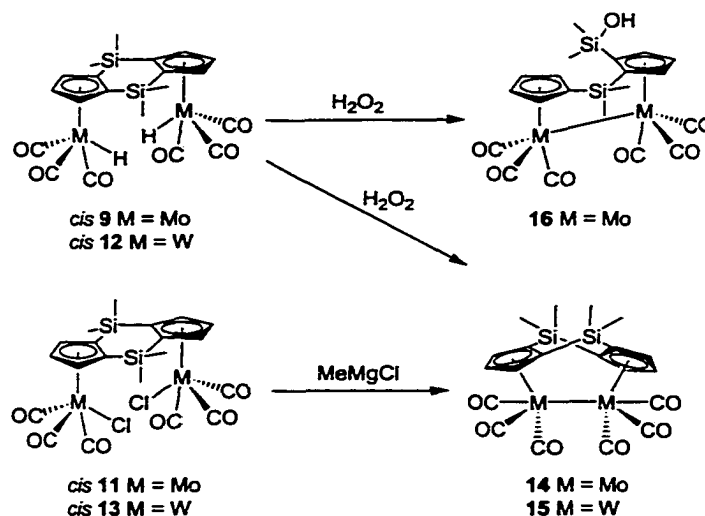
Royo and co-workers reported⁵ the isolation of the monocyclopentadienyl-type titanium complex $\{(\eta^5\text{-C}_5\text{H}_3)_2(\text{SiMe}_2)_2\}(\text{TiCl}_3)_2$ (**4**). Whereas the reaction of TiCl_4 with the dithallium salt of **1** in toluene led to the selective formation of *trans*- $\{(\eta^5\text{-C}_5\text{H}_3)_2(\text{SiMe}_2)_2\}(\text{TiCl}_3)_2$ (**4**) in 30 % yield, a similar reaction of the dilithium salt **1** in toluene (Scheme 2) always afforded a mixture having variable proportions of the *cis*-**3** and *trans*-**3** isomers, which can be separated by recrystallization from toluene. A similar behavior has been observed for the reaction of $(\eta^5\text{-C}_5\text{Me}_5)\text{TiCl}_3$ with the dilithium salt of **1**, which leads to a mixture of *cis* and *trans* mixed bent metallocenes $\{(\eta^5\text{-C}_5\text{H}_3)_2(\text{SiMe}_2)_2\}((\eta^5\text{-C}_5\text{Me}_5)\text{TiCl}_2)_2$, whereas the related $(\eta^5\text{-C}_5\text{H}_5)\text{TiCl}_3$ compound led only to the *trans* isomer.⁶ The complex *trans*- $\{(\eta^5\text{-C}_5\text{H}_3)_2(\text{SiMe}_2)_2\}(\text{TiCl}_3)_2$ (**4**) hydrolyzes immediately by the addition of H_2O to THF solution to give *trans*- $\{(\eta^5\text{-C}_5\text{H}_3)_2(\text{SiMe}_2)_2\}(\text{TiCl}_2)_2(\eta\text{-O})$ (**5**) as a solid insoluble in all organic solvents, whereas hydrolysis of *cis*- $\{(\eta^5\text{-C}_5\text{H}_3)_2(\text{SiMe}_2)_2\}(\text{TiCl}_3)_2$ (**4**) under different conditions led to the dinuclear μ -oxo complex *cis*- $\{(\eta^5\text{-C}_5\text{H}_3)_2(\text{SiMe}_2)_2\}(\text{TiCl}_2)_2(\mu\text{-O})$ (**6a**) and two oxo complexes of the same stoichiometry [$\{(\eta^5\text{-C}_5\text{H}_3)_2(\text{SiMe}_2)_2\}(\text{TiCl})_2(\mu\text{-O})\](\mu\text{-O})_2$ (**6b,c**) as crystalline solids.⁷ Alkylation of *cis*- and *trans*- $\{(\eta^5\text{-C}_5\text{H}_3)_2(\text{SiMe}_2)_2\}(\text{TiCl}_3)_2$ (**4**) with MeMgCl or MeLi led respectively to the partially alkylated *cis*- $\{(\eta^5\text{-C}_5\text{H}_3)_2(\text{SiMe}_2)_2\}(\text{TiMe}_2\text{Cl})_2$ (**8**) and the completely alkylated *trans*- $\{(\eta^5\text{-C}_5\text{H}_3)_2(\text{SiMe}_2)_2\}(\text{TiMe}_3)_2$ (**7**) compounds. The crystal structure of the tetranuclear oxo complex [$\{(\eta^5\text{-C}_5\text{H}_3)_2(\text{SiMe}_2)_2\}(\text{TiCl})_2(\mu\text{-O})\](\mu\text{-O})_2$ (**6b**) was determined by X-ray diffraction studies.

Homodinuclear Complexes with Group 6 Metals

The stereoselective synthesis of *cis* and *trans* isomers of $[\{(\eta^5\text{-C}_5\text{H}_3)_2(\text{SiMe}_2)_2\}\{\text{Mo}(\text{CO})_3(\text{H})\}_2]$ (**9**) (eqs 1 and 2) has been reported.⁸ Both isomers of complex **9** react with CCl_4 at room temperature to give complexes $[\{(\eta^5\text{-C}_5\text{H}_3)_2(\text{SiMe}_2)_2\}\{\text{Mo}(\text{CO})_3(\text{Cl})\}_2]$ (**11**).



Both isomers of complex **9** undergo thermal rearrangement in benzene solution leading to the monolinked complex **10**.⁹ In contrast to molybdenum chemistry, the related tungsten complex $[\{(\eta^5\text{-C}_5\text{H}_3)_2(\text{SiMe}_2)_2\}\{\text{W}(\text{CO})_3(\text{H})\}_2]$ (**12**) is always obtained as a mixture of *cis* and *trans* isomers from the reaction of $\text{W}(\text{CO})_3(\text{NCMe})_3$ and **1** and its dipotassium salt **3**.¹⁰ The reduction of the chloro derivatives **11** and **13** gives the dinuclear metal-metal bonded complexes **14** and **15** respectively (Scheme 3). The molybdenum complex **14** is also obtained in the reaction of the dihydride complex **9** with H_2O_2 , which also gives rise to the

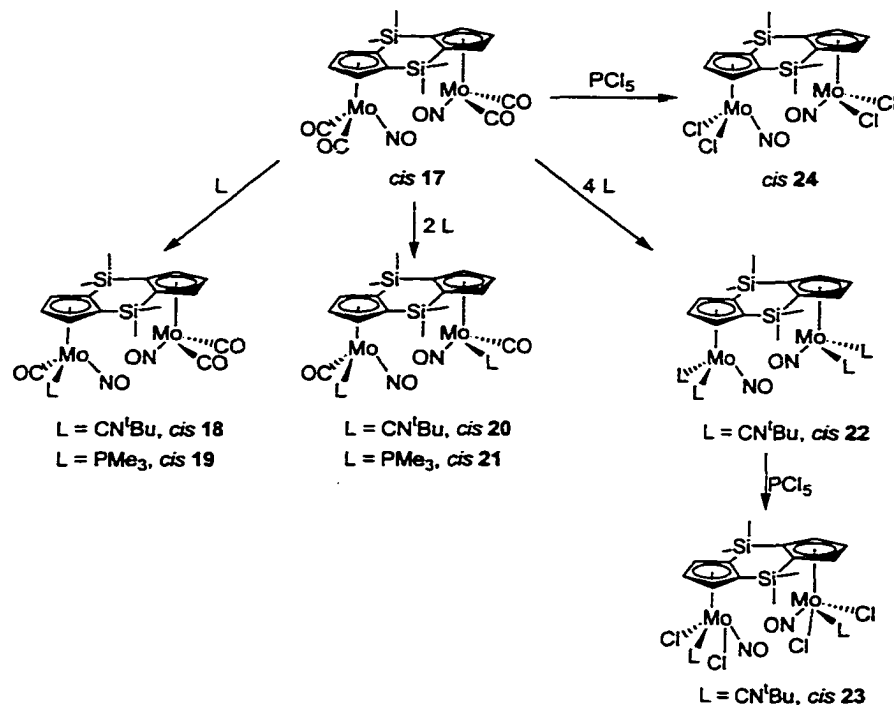


Scheme 3

monolinked complex **16**. The formation of complex **16** was rationalized by Royo and co-workers as the result of the hydrolysis of one of the SiMe_2 bridges of the ring system by H_2O from the H_2O_2 solution.

Also, the Royo group has reported¹¹ an oxidation of the chloro-tricarbonyl complexes **11** and **13** with PCl_5 to give paramagnetic *cis* and *trans* tetrachloro metal(V) $\{(\eta^5\text{-C}_5\text{H}_3)_2(\text{SiMe}_2)_2\}(\text{MCl}_4)_2$ ($\text{M} = \text{Mo}, \text{W}$) complexes, that react with primary amines to give paramagnetic dichloro-imido compounds $\{(\eta^5\text{-C}_5\text{H}_3)_2(\text{SiMe}_2)_2\}\{\text{MCl}_2(\text{NR})\}_2$ ($\text{M} = \text{Mo}, \text{W}$). The imido-tungsten derivative can be further oxidized with PCl_5 to the related tungsten(VI) trichloro-imido $\{(\eta^5\text{-C}_5\text{H}_3)_2(\text{SiMe}_2)_2\}\{\text{WCl}_3(\text{NR})\}_2$ compounds.

Recently, the same research group isolated and characterized¹² the dinuclear nitrosyl dicarbonyl molybdenum complexes $\{(\eta^5\text{-C}_5\text{H}_3)_2(\text{SiMe}_2)_2\}\text{Mo}_2(\text{CO})_4(\text{NO})_2$ (*cis* **17** and *trans* **17**; the *cis* isomer is shown in Scheme 4) from reactions of the corresponding tricarbonyl



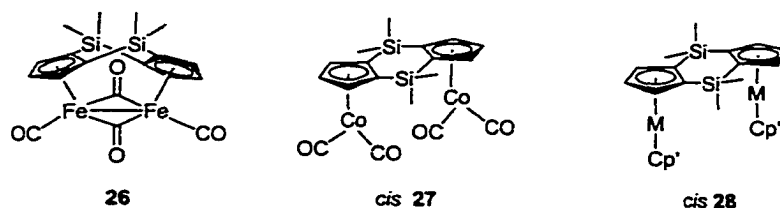
Scheme 4

hydride **9** or the anionic derivatives $[\{(\eta^5\text{-C}_5\text{H}_3)_2(\text{SiMe}_2)_2\}\text{Mo}_2(\text{CO})_3]^{2-}$ with diazald.

Complexes *cis* **17** and *trans* **17** react with different ligands in various molar ratios to give mono-, di-, and tetrasubstituted compounds **18-22**. Oxidation of the isocyanide adduct **22** with PCl_5 takes place with partial loss of the ligand, leading to the formation of the 18-electron dichloro-nitrosyl-isocyanide complex **23**, whereas the oxidation of the carbonyl derivatives produced the 16-electron dichloro-nitrosyl compounds *cis* **24** and *trans* **24** with a total loss of carbon monoxide (Scheme 4). All of these compounds were analytically identified and structurally characterized by NMR spectroscopy. The molecular structure of some were studied by X-ray diffraction methods.

Homodinuclear Complexes with Late Transition Metal

Relatively few synthesis of complexes of the $(\eta^5\text{-C}_5\text{H}_3)_2(\text{SiMe}_2)_2$ ligand with late transition metals have been reported. The thermal reaction of **1** and $\text{Fe}(\text{CO})_5$ leads to the complex $\{(\eta^5\text{-C}_5\text{H}_3)_2(\text{SiMe}_2)_2\}\text{Fe}_2(\text{CO})_4$ (**26**).^{2a} Complex **27** was isolated from the reaction



of **1** and $\text{Co}_2(\text{CO})_8$ as a mixture of *cis* and *trans* isomers in a 2:1 ratio.^{2a} Also, the synthesis of *cis* and *trans* metallocene complexes of type **28** ($\text{M} = \text{Fe}, \text{Ru}$; $\text{Cp}' = \text{C}_5\text{H}_5, \text{C}_5\text{Me}_5$) have appeared in the literature.^{2a,13} The macrocyclic heptamer complex $[\{(\eta^5\text{-C}_5\text{H}_3)_2(\text{SiMe}_2)_2\}\text{Fe}]_7$ (**29**) was isolated from the reaction of FeCl_2 and **3** in THF.^{13c} The structure of **29** (Figure 2)

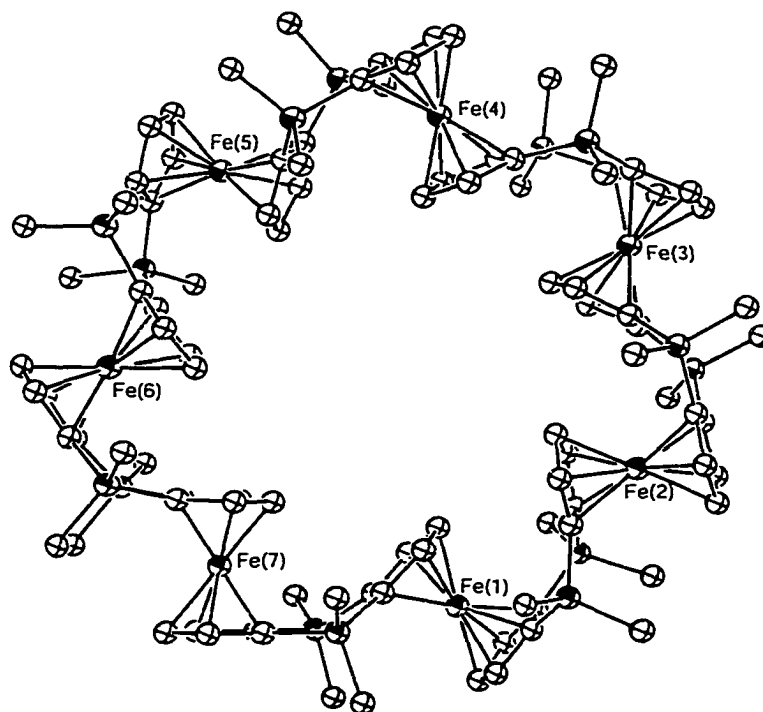
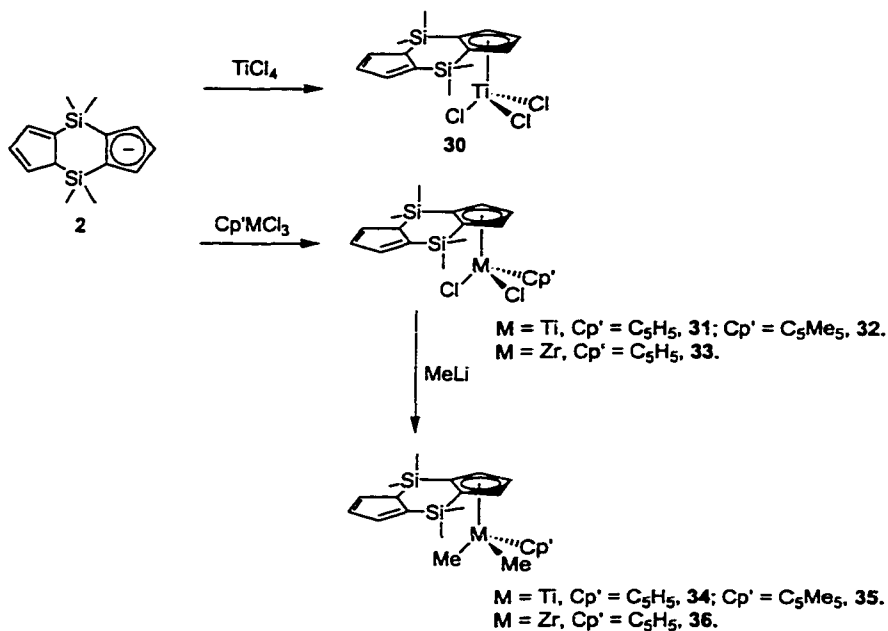


Figure 2. ORTEP representation of $[\{(\eta^5\text{-C}_5\text{H}_3)_2(\text{SiMe}_2)_2\}\text{Fe}]_7$ (**29**).

consists of seven ferrocene units linked by seven pairs of SiMe₂ groups in such a way that an almost regular cycle is formed.

Complexes with One Metal-coordinated Cyclopentadienyl Ring

Use of the (η^5 -C₅H₃)₂(SiMe₂)₂ ligand as a monoanion **2** has led to the isolation of several mixed dicyclopentadienyl titanium complexes.¹⁴ Complexes **30-36** of this type were isolated by the reaction represented in Scheme 5. The ¹H NMR spectra of all complexes show a common behavior; they exhibit four separate resonances arising from the four inequivalent methyl groups bonded to silicon, one singlet arising from the hydrogen on the cyclopentadiene sp³ carbon atom, and six multiplets arising from six inequivalent hydrogen



Scheme 5

atoms bonded to the cyclopentadiene and cyclopentadienyl rings between δ 5.50 and δ 7.70. Complexes **30-36** are potentially useful starting materials for the synthesis of heterobimetallic complexes.

References

- (1) For general reviews regarding linked cyclopentadienyl organometallic complexes, see:
(a) Barlow, S.; O'Hare, D. *Chem. Rev.* **1997**, *97*, 637. (b) Werner, H. *Inorg. Chim. Acta* **1992**, *198-200*, 715. (c) Bonifaci, C.; Ceccon, A.; Gambaro, A.; Mantovani, L.; Ganis, P.; Santi, S.; Venzo, A. *J. Organomet. Chem.* **1998**, *557*, 97. (d) Cuenca, T.; Royo, P. *Coord. Chem. Rev.* **1999**, *193-195*, 447. (e) Royo, P. *New J. Chem.* **1997**, *21*, 791.
- (2) (a) Siemeling, U.; Jutzi, P.; Neumann, B.; Stammler, H. G.; Hursthouse, M. B. *Organometallics* **1992**, *11*, 1328. (b) Hiermeier, J.; Köhler, F. H.; Mueller, G. *Organometallics* **1991**, *10*, 1787.
- (3) Yarnykh, V. L.; Mstyslavsky, V. I.; Zemlyanskii, N. N.; Borisova, I. V.; Roznyatovskii, V. A.; Ustynyuk, Yu. A. *Russ. Chem. Bull.* **1997**, *46*, 1228.
- (4) (a) Nifant'ev, I. E.; Yarnykh, V. L.; Borzov, M. V.; Mazurchik, B. A.; Mstislavskii, V. I.; Roznyatovskii, V. A.; Ustynyuk, Yu. A. *Organometallics* **1991**, *10*, 3739. (b) Nifant'ev, I. E.; Yarnykh, V. L.; Borzov, M. V.; Mazurchik, B. A.; Mstislavskii, V. I.; Roznyatovskii, V. A.; Ustynyuk, Yu. A. *Metalloorg. Khim.* **1991**, *4*, 1269.
- (5) Cano, A.; Cuenca, T.; Gómez-Sal, P.; Royo, B.; Royo, P. *Organometallics* **1994**, *13*, 1688.
- (6) Corey, J. Y.; Huhmann, J. L.; Rath, N. P. *Inorg. Chem.* **1995**, *34*, 3203.

- (7) Cano, A. M.; Cano, J.; Cuenca, T.; Gómez-Sal, P.; Manzanero, A.; Royo, P. *Inorg. Chim. Acta* **1998**, *280*, 1.
- (8) Amor, F.; Gómez-Sal, P.; de Jesús, E.; Royo, P.; Vázquez de Miguel, A. *Organometallics* **1994**, *13*, 4322.
- (9) Amor, F.; de Jesús, E.; Royo, P.; Vázquez de Miguel, A. *Inorg. Chem.* **1996**, *35*, 3440.
- (10) Amor, F.; de Jesús, E.; Pérez, A. I.; Royo, P.; Vázquez de Miguel, A. *Organometallics* **1996**, *15*, 365.
- (11) Amor, F.; Gómez-Sal, P.; de Jesús, E.; Martín, A.; Pérez, A. I.; Royo, P.; Vázquez de Miguel, A. *Organometallics* **1996**, *15*, 2103.
- (12) Calvo, M.; Galakhov, M. V.; Gómez-García, R.; Gómez-Sal, P.; Martín, A.; Royo, P.; Vázquez de Miguel, A. *J. Organomet. Chem.* **1997**, *548*, 157.
- (13) (a) Siemeling, U.; Jutzi, P. *Chem. Ber.* **1992**, *125*, 31. (b) Atzkern, H.; Hiermeier, J.; Kanellakopoulos, B.; Köhler, F. H.; Müller, G.; Steigelmann, O. *Chem. Commun.* **1991**, 997. (c) Grossmann, B.; Heinze, J.; Herdtweck, E.; Köhler, F. H.; Nöth, H.; Schwenk, H.; Spiegler, M.; Wachter, W.; Weber, B. *Angew. Chem., Int. Ed. Engl.* **1997**, *36*, 387.
- (14) Gómez-García, R.; Royo, P. *J. Organomet. Chem.* **1999**, *583*, 86.

CHAPTER 1. A KINETICALLY-INERT PROTON ON A METAL-METAL BOND IN $[\{(\eta^5\text{-C}_5\text{H}_3)_2(\text{SiMe}_2)_2\}\text{Ru}_2(\text{CO})_4(\mu\text{-H})]^+$ THAT PROMOTES REACTIONS WITH AMINES

A paper published in the Journal of the American Chemical Society¹

Maxim V. Ovchinnikov and Robert J. Angelici

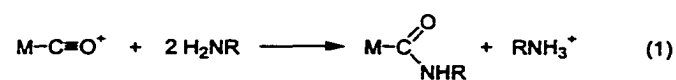
Abstract

Complex 1H^+ , $[\{(\eta^5\text{-C}_5\text{H}_3)_2(\text{SiMe}_2)_2\}\text{Ru}_2(\text{CO})_4(\mu\text{-H})]^+$, with a protonated Ru-Ru bond, was prepared as shown in the scheme. Although the proton in 1H^+ is acidic thermodynamically, it is deprotonated only very slowly (hours or days) by basic amines and phosphines. This remarkable kinetic inertness of the bridging proton allows amines to react with 1H^+ by attacking the CO ligand to give a formamide and the CO-substituted product **2**. Thus, protonation of the metal-metal bond in 1H^+ promotes reactions of the CO ligand that are not possible in the unprotonated **1**.

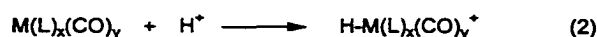
¹ Reproduced with permission from Journal of the American Chemical Society **2000**, *122*, 6130-6131. Copyright 2000 American Chemical Society.

Introduction

Unsaturated ligands in transition metal complexes can be activated to nucleophilic attack by creating a positive charge on the complex.¹ Carbon monoxide ligands are activated to attack by amine nucleophiles when the positive charge on a complex is sufficiently high to give C≡O stretching force constants, k_{CO} , that are higher than 16.5 mdyn/Å (or $\nu(\text{CO})$ values higher than approximately 2000 cm^{-1}).² These reactions lead to carbamoyl complexes (eq 1),



and some reactions give formamides and ureas catalytically.³ One approach to making a complex more positive is to add a proton (H^+) to the metal (eq 2). While numerous metal carbonyl complexes have been protonated,⁴ the CO ligands in these complexes either do not react with amines because their k_{CO} and $\nu(\text{CO})$ values are insufficiently high or the amine

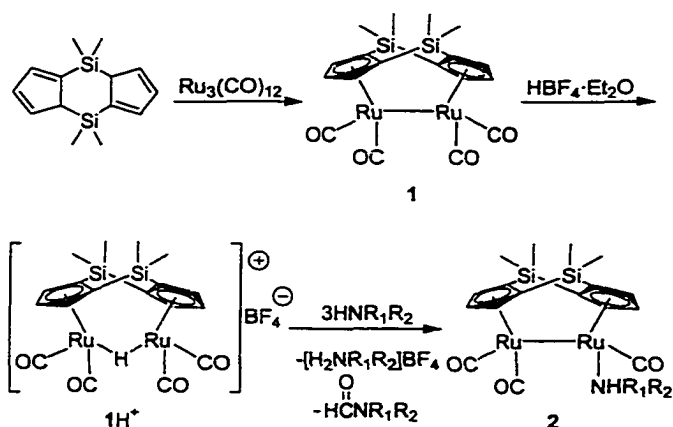


bases simply deprotonate the metal to give the unreactive neutral complex $\text{M}(\text{L})_x(\text{CO})_y$. This rapid deprotonation occurs for a wide range of cationic metal hydride complexes $\text{H-M}(\text{L})_x(\text{CO})_y^+$.^{5,4b} Neutral $\text{H-M}(\text{L})_x(\text{CO})_y$ complexes often undergo deprotonation much more slowly,⁶ but their k_{CO} and $\nu(\text{CO})$ values are not sufficiently high to promote attack by amines. Di- and polynuclear metal complexes with M-H-M bridging hydrides also undergo rapid deprotonation with bases.^{7,8} In this communication we describe a cationic dinuclear complex $[\{(\eta^5\text{-C}_5\text{H}_3)_2(\text{SiMe}_2)_2\}\text{Ru}_2(\text{CO})_4(\mu\text{-H})]^+ (\text{1H}^+)$ whose high $\nu(\text{CO})$ values promote amine attack but is only slowly deprotonated by amines. The bridging dicyclopentadienyl ($\eta^5\text{-C}_5\text{H}_3)_2(\text{SiMe}_2)_2$ ligand⁹ with two SiMe_2 groups linking the cyclopentadienyl rings is a key

contributor to the slow rate of deprotonation of 1H^+ thereby allowing nucleophilic attack on a CO ligand.

Results and Discussion

The reaction of $(\text{C}_5\text{H}_4)_2(\text{SiMe}_2)_2$ ¹⁰ with $\text{Ru}_3(\text{CO})_{12}$ in the presence of the hydrogen acceptor 1-dodecene furnished $\{(\eta^5\text{-C}_5\text{H}_3)_2(\text{SiMe}_2)_2\}\text{Ru}_2(\text{CO})_4$ (**1**) in 72% yield, as an air- and moisture-stable yellow solid (Scheme 1).¹¹ The hydride-bridged dinuclear Ru complex¹² 1H^+ was formed in quantitative yield upon addition of 1 equiv of $\text{HBF}_4\cdot\text{OEt}_2$ or $\text{CF}_3\text{SO}_3\text{D}$ to a solution of complex **1** in CH_2Cl_2 at room temperature. The Ru-H resonance in the ^1H NMR spectrum occurs as a singlet at δ -19.92 ppm. The CO stretching frequencies for 1H^+ are

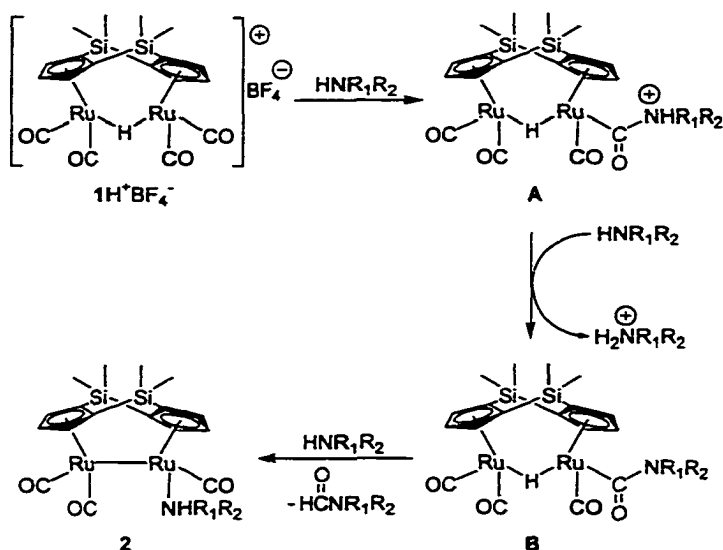


Scheme 1

approximately 67 cm^{-1} higher than those for **1** and fall within the range where amine attack on the CO groups is expected to occur.² An X-ray diffraction study of $1\text{H}^+\text{BF}_4^-$ reveals an eclipsed orientation of the terminal CO ligands on the two Ru atoms. The Ru-Ru distance is substantially longer in $1\text{H}^+\text{BF}_4^-$ ($3.1210(5)\text{ \AA}$) than in **1** ($2.8180(3)\text{ \AA}$).¹³

Compound $1H^+$ is exceptionally stable with respect to deprotonation by strong organic bases such as Et_3N , quinuclidine or pyridine. Less than 2% of the complex was deprotonated after 1 hour in CD_3NO_2 or CD_3CN solution in the presence of 10 fold excesses of these amines. Moreover, the deuterated complex $1D^+TfO^-$ in wet acetone solution (~10% H_2O) did not undergo measurable H-D exchange after 5 days at 25 °C. In contrast to $1H^+$, the unbridged and monobridged complexes $(\eta^5-C_5H_5)_2Ru_2(CO)_4(\mu-H)^{+14a}$ and $\{(\eta^5-C_5H_4)_2(SiMe_2)\}Ru_2(CO)_4(\mu-H)^{+14b}$ were deprotonated instantly and quantitatively by bases such as pyridine or diethylamine. The acidity of $1H^+BF_4^-$, estimated as pK_a^{AN} from studies of the equilibrium constant for the proton transfer reaction between **1** and $HPPH_3^+BF_4^-$ in CD_3CN at 25 °C,¹⁵ is $6.5(\pm 0.2)$ in CD_3CN . This pK_a^{AN} value clearly indicates that the above-noted amine bases will thermodynamically deprotonate $1H^+BF_4^-$ easily. Although it is not obvious why the $(\eta^5-C_5H_3)_2(SiMe_2)_2$ bridging ligand causes the bridging proton to be so slowly removed, it may be due to a combination of the bulkiness of the dimethylsilyl linkers and the rigidity of the molecule. The donor ability of the $(\eta^5-C_5H_3)_2(SiMe_2)_2$ ligand to the Ru atom is probably similar to that of the Cp ligand based on average $\nu(CO)$ values¹⁶ for $1H^+BF_4^-$ (2051 cm^{-1}) and $Cp_2Ru_2(CO)_4(\mu-H)^{+7a}$ (2046 cm^{-1}).

Reactions of $1H^+$ with secondary amines (Me_2NH , Et_2NH , morpholine, pyrrolidine), primary amines ($MeNH_2$, $EtNH_2$, $BnNH_2$) or ammonia furnished $\{(\eta^5-C_5H_3)_2(SiMe_2)_2\}-Ru_2(CO)_3(NHRR')$ (**2**) complexes and the corresponding formamides in a 1:1 ratio (Scheme 1). Complexes of type **2**¹⁷ were isolated in 78-94% yield as air- and moisture-sensitive dark-



Scheme 2

red solids. The other Ru-containing product in these reactions was the deprotonated complex **1** observed in 5-20% yields as a result of direct deprotonation of 1H^+ by amine. The yields of **1** appear to depend on the steric properties of the amine as less bulky amines (e.g. NH_3) give higher yields of **1**. Also, the yields of **1** were lower when the deuterated $1\text{D}^+\text{TfO}^-$ complex was used. Using a variety of amines, we determined that 1H^+ reacts when the amine has a $\text{p}K_a$ value equal to or greater than 8.33 (morpholine)¹⁸ and a cone angle θ that is equal to or less than 125° (diethylamine).¹⁹ Bulky amines (Bn_2NH , $i\text{-Pr}_2\text{NH}$, Cy_2NH) and weakly nucleophilic amines (aniline) failed to react with 1H^+ .

On the basis of studies described below, the amine reactions are proposed to occur by the mechanism shown in Scheme 2. This involves initial nucleophilic attack by the amine on a coordinated CO to produce the cationic intermediate **A**, which is rapidly deprotonated to **B**.^{2,20} Reductive elimination of the formamide from **B** gives an unsaturated di-ruthenium intermediate that coordinates an amine to give **2**. No intermediates were observed by FT-IR

or NMR spectroscopy during the course of the reaction. Experiments using the deuterium-labeled $1D^+TfO^-$ gave formamide products ($D(C=O)NRR'$) that are completely deuterated at the formyl position and no other. When $1D^+TfO^-$ rather than $1H^+BF_4^-$ was used in the reaction, substantially less deprotonation to **1** was observed, as expected for a deuterium isotope effect.

Rates of the reaction of $1D^+TfO^-$ ($[1D^+TfO^-] = 8.34 \times 10^{-3}$ to $11.12 \times 10^{-3} M^{-1}$) with morpholine ($[morpholine] = 8.56 \times 10^{-1}$ to $10.82 \times 10^{-1} M^{-1}$) in nitromethane solvent to give $\{(\eta^5-C_5H_3)_2(SiMe_2)_2\}Ru_2(CO)_3\{NH(CH_2CH_2)_2O\}$ were followed by monitoring the disappearance of the $\nu(CO)$ bands in the IR spectra or 1H NMR signals of $1D^+TfO^-$. The reaction was shown to follow the second-order rate law, $-d[1D^+TfO^-]/dt = k_2[1D^+TfO^-][morpholine]$, where $k_2 = (2.3 \pm 0.5) \times 10^{-3} M^{-1} s^{-1}$ at 20 °C. This rate law is consistent with the first step in the mechanism (Scheme 2) being rate-determining. The subsequent deprotonation of the nitrogen in **A** is likely to be fast and the reductive elimination of the formamide from **B** must be rapid because there is no spectroscopic evidence for intermediates in the reaction. Such a facile reductive elimination is surprising because removal of the bridging H^+ by bases is so slow. Reductive eliminations involving a μ -H have only recently been characterized, e.g. in the formation of alkanes and arenes from $Pd_2R_2(\mu-H)(dppm)_2^+$.²¹

Conclusions

In conclusion, we have discovered that protonation of the Ru-Ru bond in **1** gives a cationic complex ($1H^+$) in which the bridging proton is removed only very slowly by bases even though the proton is thermodynamically acidic ($pK_a^{AN} = 6.5(\pm 0.2)$). The low kinetic

acidity of 1H^+ allows it to react with alkyl amines, which attack a CO ligand that is activated to such an attack by the cationic nature of the complex. These amine reactions lead to the elimination of the $\mu\text{-H}$ which becomes incorporated into the formamide product.

Mechanistic studies support the pathway shown in Scheme 2. Further studies of reactions of 1H^+ with nucleophiles are in progress.

Acknowledgment

We appreciate the support of the National Science Foundation through Grant No. CHE-9816342.

References

- (1) Bush, R. C.; Angelici, R. J. *J. Am. Chem. Soc.* **1986**, *108*, 2735.
- (2) Angelici, R. J. *Acc. Chem. Res.* **1972**, *5*, 335.
- (3) (a) McCusker, J. E.; Logan, J.; McElwee-White, L. *Organometallics* **1998**, *17*, 4037.
(b) McCusker, J. E.; Abboud, K. A.; McElwee-White, L. *Organometallics* **1997**, *16*, 3863. (c) McCusker, J. E.; Grasso, C. A.; Main, A. D.; McElwee-White, L. *Org. Lett.* **1999**, *1*, 961. (d) Dombek, B. D.; Angelici, R. J. *J. Catal.* **1977**, *48*, 433.
- (4) (a) Angelici, R. J. *Acc. Chem. Res.* **1995**, *28*, 52. (b) Kristjánssdóttir, S. S.; Norton, J. R. *In Transition Metal Hydrides: Recent Advances in Theory and Experiments*; Dedieu, A., Ed.; VCH: New York, 1991; Chapter 10. (c) Pearson, R. G. *Chem. Rev.* **1985**, *85*,

41. (d) Martinho Simões, J. A.; Beauchamp, J. L. *Chem. Rev.* **1990**, *90*, 629. (e) Bullock, R. M. *Comments Inorg. Chem.* **1991**, *12*, 1.
- (5) Jia, G.; Morris, R. H. *Inorg. Chem.* **1990**, *29*, 582.
- (6) (a) Edidin, R. T.; Sullivan, J. M.; Norton, J. R. *J. Am. Chem. Soc.* **1987**, *109*, 3945. (b) Moore, E. J.; Sullivan, J. M.; Norton, J. R. *J. Am. Chem. Soc.* **1986**, *108*, 2257. (c) Jordan, R. F.; Norton, J. R. *J. Am. Chem. Soc.* **1982**, *104*, 1255.
- (7) (a) Nataro, C.; Thomas, L. M.; Angelici, R. J. *Inorg. Chem.* **1997**, *36*, 6000. (b) Nataro, C.; Angelici, R. J. *Inorg. Chem.* **1998**, *37*, 2975.
- (8) (a) Weberg, R. T.; Norton, J. R. *J. Am. Chem. Soc.* **1990**, *112*, 1105. (b) Kristjánsdóttir, S. S.; Moody, A. E.; Weberg, R. T.; Norton, J. R. *Organometallics* **1988**, *7*, 1983.
- (9) For recent examples of $(\eta^5\text{-C}_5\text{H}_3)_2(\text{SiMe}_2)_2$ complexes, see: (a) Sun, H.; Teng, X.; Huang, X.; Hu, Z.; Pan, Y. *J. Organomet. Chem.* **2000**, *595*, 268. (b) Cano, A. M.; Cano, J.; Cuenca, T.; Gómez-Sal, P.; Manzanero, A.; Royo, P. *Inorg. Chim. Acta* **1998**, *280*, 1.
- (10) (a) Siemeling, U.; Jutzi, P.; Neumann, B.; Stammer, H. G.; Hursthouse, M. B. *Organometallics* **1992**, *11*, 1328. (b) Hiermeier, J.; Koehler, F. H.; Mueller, G. *Organometallics* **1991**, *10*, 1787.
- (11) In a typical procedure, a solution of $\text{Ru}_3(\text{CO})_{12}$ (50.0 mg, 78.2 μmol), $(\text{C}_5\text{H}_4)_2(\text{SiMe}_2)_2$ (28.6 mg, 117.0 μmol) and 1-dodecene (260.0 mg, 2.4 mmol) in heptane (30 mL) was heated to reflux for 18 hours. The mixture was chromatographed on an alumina column (1 \times 20 cm) first with hexanes and then with a 1:10 (v/v) mixture of CH_2Cl_2 and hexanes which eluted a yellow band containing **1** (47 mg, 72%). ^1H NMR (400

- MHz, CDCl₃): δ 0.26 (s, 6 H, Si(CH₃)), 0.46 (s, 6 H, Si(CH₃)), 5.37 (d, $J = 1.6$ Hz, 4 H, Cp-H), 5.78 (t, $J = 1.6$ Hz, 2 H, Cp-H). ¹³C NMR (100 MHz, CDCl₃): δ -2.25 (CH₃), 4.53 (CH₃), 87.72, 93.95, 95.57 (Cp), 204.57 (CO). IR (CH₂Cl₂): ν (CO) (cm⁻¹) 2015 (vs), 1952 (vs). Anal. Calcd for C₁₈H₁₈O₄Ru₂Si₂: C, 38.84; H, 3.26. Found: C, 39.05; H, 3.32.
- (12) (1H⁺BF₄⁻): ¹H NMR (400 MHz, CD₂Cl₂): δ -19.92 (s, 1 H, Ru-H-Ru), 0.47 (s, 6 H, Si(CH₃)), 0.62 (s, 6 H, Si(CH₃)), 5.99 (d, $J = 2.0$ Hz, 4 H, Cp-H), 6.02 (t, $J = 2.0$ Hz, 2 H, Cp-H). ¹³C NMR (100 MHz, CD₂Cl₂): δ -2.57 (CH₃), 2.86 (CH₃), 88.97, 98.56, 98.81 (Cp), 195.19 (CO). IR (CH₂Cl₂): ν (CO) (cm⁻¹) 2077 (vs), 2050 (w), 2027 (s). Anal. Calcd for C₁₈H₁₉BF₄O₄Ru₂Si₂: C, 33.55; H, 2.97. Found: C, 33.19; H, 2.90.
- (13) Details of the X-ray diffraction studies of **1**, 1H⁺BF₄⁻ and **2a** will be published separately: Ovchinnikov, M. V.; Guzei, I. A.; Angelici, R. J. Manuscript in preparation.
- (14) (a) Ovchinnikov, M. V.; Angelici, R. J. Unpublished results. (b) Froehlich, R.; Gimeno, J.; Gonzalez, C. M.; Lastra, E.; Borge, J.; Garcia, G. S. *Organometallics* **1999**, *18*, 3008.
- (15) A solution of **1** (18.6 mg, 31.9 μ mol) and HPPPh₃⁺BF₄⁻ (11.2 mg, 32.0 μ mol) in CD₃CN (1 mL) was sealed in an NMR tube under an argon atmosphere. After following the reaction for 8 days, the ¹H NMR spectrum indicated a [**1**]/[1H⁺BF₄⁻] ratio of 2.35; and the ³¹P NMR spectrum established a [HPPPh₃⁺BF₄⁻]/[PPh₃] ratio of 2.47. From these two ratios and the pK_a^{AN} of HPPPh₃⁺ (8.0), the pK_a^{AN} of 1H⁺BF₄⁻ was calculated to be 6.5(\pm 0.2) in acetonitrile.
- (16) Jolly, W. L.; Avanzino, S. C.; Rietz, R. R. *Inorg. Chem.* **1977**, *16*, 964.

- (17) In a typical procedure, gaseous CH_3NH_2 was slowly bubbled through a suspension of yellow $1\text{H}^+\text{BF}_4^-$ (50.0 mg, 77.6 μmol) in hexanes (25 mL) for 5 min at ambient temperature. The color of the reaction mixture immediately changed to wine-red. Solvent was removed in vacuum, and the red residue was recrystallized from hexanes (10 mL) at $-25\text{ }^\circ\text{C}$ to give 39 mg (83%) of **2a** as dark-red, air- and moisture-sensitive crystals. ^1H NMR (400 MHz, C_6D_6): δ 0.24 (s, 6 H, $\text{Si}(\text{CH}_3)$), 0.38 (s, 6 H, $\text{Si}(\text{CH}_3)$), 1.58 (bs, 2 H, CH_3NH_2), 1.67 (t, $J = 6.4$ Hz, 3 H, CH_3NH_2), 4.52 (d, $J = 2.0$ Hz, 2 H, Cp- H), 4.77 (t, $J = 2.0$ Hz, 1 H, Cp- H), 5.11 (d, $J = 2.4$ Hz, 2 H, Cp- H), 5.76 (t, $J = 2.4$ Hz, 1 H, Cp- H). ^{13}C NMR (100 MHz, C_6D_6): δ -1.88 (CH_3), 5.38 (CH_3), 41.39 (CH_3NH_2), 79.20, 83.59, 90.10, 92.98, 94.37, 95.52 (Cp), 209.07 (CO), 211.98 (CO). IR (hexanes): $\nu(\text{CO})$ (cm^{-1}) 1973 (vs), 1907 (vs), 1884 (m). Anal. Calcd for $\text{C}_{18}\text{H}_{23}\text{NO}_3\text{Ru}_2\text{Si}_2 \cdot \frac{1}{4}\text{C}_6\text{H}_{14}$: C, 40.30; H, 4.60; N, 2.41. Found: C, 40.77; H, 4.57; N, 2.95.
- (18) Perrin, D. D. *Dissociation Constants of Organic Bases in Aqueous Solution*; Butterworths: London, 1972.
- (19) For amine cone angles, see: Seligson, A. L.; Trogler, W. C. *J. Am. Chem. Soc.* **1991**, *113*, 2520.
- (20) Semmelhack, M. F.; *J. Organomet. Chem., Libs.* **1976**, *1*, 361.
- (21) Stockland, R. A. Jr.; Anderson, G. K.; Rath, N. P. *J. Am. Chem. Soc.* **1999**, *121*, 7945.

**CHAPTER 2. AMINE ATTACK ON THE CARBONYL LIGANDS OF
THE PROTONATED DICYCLOPENTADIENYL-BRIDGED
DIRUTHENIUM COMPLEX $[\{(\eta^5\text{-C}_5\text{H}_3)_2(\text{SiMe}_2)_2\}\text{Ru}_2(\text{CO})_4(\mu\text{-H})]^+$**

A paper published in *Organometallics*¹

Maxim V. Ovchinnikov, Ilia A. Guzei,² and Robert J. Angelici

Abstract

Complexes $[\{(\eta^5\text{-C}_5\text{H}_3)_2(\text{SiMe}_2)_2\}\text{Ru}_2(\text{CO})_4(\mu\text{-H})]^+$ ($1\text{H}^+\text{BF}_4^-$, $1\text{D}^+\text{TfO}^-$), with a protonated Ru-Ru bond, were prepared by protonation of $\{(\eta^5\text{-C}_5\text{H}_3)_2(\text{SiMe}_2)_2\}\text{Ru}_2(\text{CO})_4$ (**1**) with $\text{HBF}_4\cdot\text{Et}_2\text{O}$ or $\text{CF}_3\text{SO}_3\text{D}$. The bridging proton in 1H^+ is removed only very slowly by amine bases even though it is thermodynamically acidic ($\text{p}K_a^{\text{AN}} = 6.5(\pm 0.2)$). This remarkable kinetic inertness of the bridging proton allows amines (NH_3 , NH_2CH_3 , $\text{NH}(\text{CH}_3)_2$, morpholine, piperidine, pyrrolidine) to react with 1H^+ by attacking the CO ligand to give a formamide ($\text{HC}(\text{=O})\text{NR}_2$) and the CO-substituted product $\{(\eta^5\text{-C}_5\text{H}_3)_2(\text{SiMe}_2)_2\}\text{-Ru}_2(\text{CO})_3(\text{NHR}_2)$ (**2**). Thus, protonation of the metal-metal bond in 1H^+ promotes reactions of the CO ligand that are not possible in the unprotonated **1**. A proposed mechanism for these reactions is supported by kinetic studies of the reaction of $1\text{D}^+\text{TfO}^-$ with morpholine in

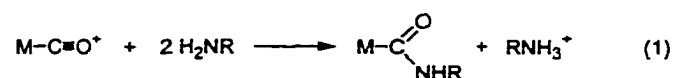
¹ Reproduced with permission from *Organometallics* **2001**, *20*, 691. Copyright 2000 American Chemical Society.

² Iowa State University, Molecular Structure Laboratory.

nitromethane at 20.0 °C, as well as by deuterium labeling experiments. The molecular structure of $\{(\eta^5\text{-C}_5\text{H}_3)_2(\text{SiMe}_2)_2\}\text{Ru}_2(\text{CO})_3(\text{NH}_2\text{CH}_3)$ (**2f**), as determined by an X-ray diffraction investigation, is also presented.

Introduction

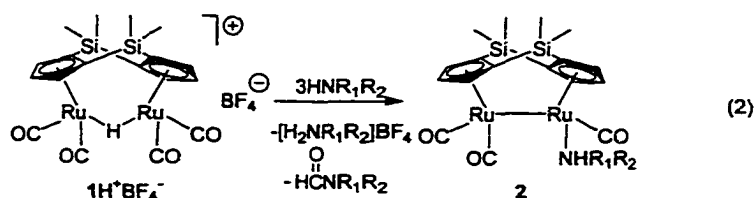
Metal-promoted nucleophilic attack on unsaturated ligands is a reaction common to a number of transition metal complexes and constitutes a transformation of synthetic importance.¹ Amines and alkoxides attack the carbon of carbon monoxide ligands in transition metal complexes if the positive charge on the complexes is sufficiently high to give $\text{C}\equiv\text{O}$ stretching force constants, k_{CO} , that are higher than 16.5 mdyn/Å (or $\nu(\text{CO})$ values higher than approximately 2000 cm^{-1}).² A common example of such a reaction is the formation of carbamoyl complexes (eq 1). Reactions of metal carbonyl complexes



with amines are also known to give formamides,³ carbamates,⁴ and ureas,⁵ either stoichiometrically or catalytically.

One of the simplest approaches to making a complex more positive is to add a proton (H^+) to the metal center.⁶ However, most protonated metal carbonyl complexes either do not react with amines because their k_{CO} and $\nu(\text{CO})$ values are insufficiently high or the amine bases simply deprotonate the metal to give the unreactive neutral metal complex. We recently communicated⁷ the synthesis of the cationic dinuclear complex $[\{(\eta^5\text{-C}_5\text{H}_3)_2(\text{SiMe}_2)_2\}\text{Ru}_2(\text{CO})_4(\mu\text{-H})]^+$ (1H^+) whose carbon monoxide ligands are activated to attack by amine nucleophiles because of the positive charge on the complex, which is

sufficiently high to give $\nu(\text{CO})$ values higher than 2000 cm^{-1} .² At the same time, complex 1H^+ is only slowly deprotonated by amines despite its high thermodynamic acidity.⁷ Treatment of 1H^+ with 3 equiv of nucleophilic amines resulted in the formation of $\{(\eta^5\text{-C}_5\text{H}_3)_2(\text{SiMe}_2)_2\}\text{Ru}_2(\text{CO})_3(\eta^1\text{-NHR}_1\text{R}_2)$ (**2**) and the corresponding formamide in a 1:1 ratio (eq 2). This paper provides details of the earlier study⁷ and new results that offer some understanding of the mechanism and scope of this reaction.



Experimental Section

General Procedures. All reactions were performed under an argon atmosphere in reagent grade solvents, using standard Schlenk or dry-box techniques.⁸ Hexanes, methylene chloride and diethyl ether were purified by the Grubbs method⁹ prior to use. All other solvents were purified by published methods.¹⁰ Gaseous amines were dried by passing them through a BaO column. Liquid amines were distilled from Na under an Ar atmosphere. Chemicals were purchased from commercial sources or prepared by literature methods, as referenced below. Alumina (neutral, activity I, Aldrich) was degassed under vacuum for 12 h and treated with 7.5 % of water. ^1H and ^{13}C NMR spectra were recorded on a Bruker DRX-400 spectrometer. Solution infrared spectra were recorded on a Nicolet-560 spectrometer using NaCl cells with 0.1 mm spacers. Elemental analyses were performed on a Perkin Elmer 2400 series II CHNS/O analyzer.

Synthesis of $\{(\eta^5\text{-C}_5\text{H}_3)_2(\text{SiMe}_2)_2\}\text{Ru}_2(\text{CO})_4(\mu\text{-D})\}^+\text{CF}_3\text{SO}_3^-$ ($1\text{D}^+\text{TfO}^-$). By reacting $\text{CF}_3\text{SO}_3\text{D}$ (8 μL , 90.4 μmol) (Aldrich) with **1** (50 mg, 89.8 μmol) in CH_2Cl_2 (30 mL), $1\text{D}^+\text{TfO}^-$ was prepared using the same method as in the preparation of $1\text{H}^+\text{BF}_4^-$. Complex $1\text{D}^+\text{TfO}^-$ was found to be spectroscopically (^1H , ^{13}C NMR, FT-IR) identical to $1\text{H}^+\text{BF}_4^-$ except for the near absence¹¹ of the $\mu\text{-H}$ resonance at -19.92 ppm.⁷ Anal. Calcd for $\text{C}_{19}\text{H}_{18}\text{BDF}_3\text{O}_7\text{Ru}_2\text{SSi}_2$: C, 32.29; H, 2.71; S, 4.54. Found: C, 32.18; H, 2.65; S, 4.48.

Synthesis of $\{(\eta^5\text{-C}_5\text{H}_3)_2(\text{SiEt}_2)_2\}\text{Ru}_2(\text{CO})_4$ (3**).** A solution of $\text{Ru}_3(\text{CO})_{12}$ (200.0 mg, 312.8 μmol), $(\text{C}_5\text{H}_4)_2(\text{SiEt}_2)_2$ ¹² (143 mg, 475.7 μmol) and methylisobutylketone (1.0 mL, 10.0 mmol) in heptane (100 mL) was heated to reflux for 30 hours. The mixture was cooled to ambient temperature and chromatographed on an alumina column (1x20 cm) first using hexanes as the eluent and then a 1:5 (v/v) mixture of CH_2Cl_2 and hexanes which eluted a yellow band containing **3** (170 mg, 58 %). ^1H NMR (400 MHz, CDCl_3): δ 0.73 (m, 4 H, $\text{Si}(\text{CH}_2\text{CH}_3)$), 0.91 (m, 4 H, $\text{Si}(\text{CH}_2\text{CH}_3)$), 0.97 (m, 6 H, $\text{Si}(\text{CH}_2\text{CH}_3)$), 1.10 (m, 6 H, $\text{Si}(\text{CH}_2\text{CH}_3)$), 5.39 (d, $J=2.2$ Hz, 4 H, Cp-*H*), 5.79 (t, $J=2.2$ Hz, 2 H, Cp-*H*). ^{13}C NMR (100 MHz, CDCl_3): δ 5.21, 8.20, 8.23, 9.94 (Et); 87.81, 92.21, 96.04 (Cp); 204.58 (CO). IR (hexanes): $\nu(\text{CO})$ (cm^{-1}) 2025 (vs), 1967 (vs). Anal. Calcd for $\text{C}_{22}\text{H}_{26}\text{O}_4\text{Ru}_2\text{Si}_2$: C, 43.12; H, 4.28. Found: C, 43.09; H, 4.21.

Synthesis of $\{(\eta^5\text{-C}_5\text{H}_3)_2(\text{SiEt}_2)_2\}\text{Ru}_2(\text{CO})_4(\mu\text{-H})\}^+\text{BF}_4^-$ ($3\text{H}^+\text{BF}_4^-$). A solution of **3** (100.0 mg, 161.2 μmol) in CH_2Cl_2 (20 mL) was treated with $\text{HBF}_4\cdot\text{Et}_2\text{O}$ (24.0 μL , 174.1 μmol) at room temperature. A yellow precipitate of $3\text{H}^+\text{BF}_4^-$ was obtained in nearly quantitative yield (111.0 mg, 100%) by diluting the reaction solution with a 10-fold excess of ether (200 mL). ^1H NMR (400 MHz, CD_3NO_2): δ -19.76 (s, 1 H, Ru-*H*-Ru), 0.95-1.30 (m,

20 H, Si(CH₂CH₃)), 6.13 (t, *J*=2.2 Hz, 2 H, Cp-*H*), 6.19 (d, *J*=2.2 Hz, 4 H, Cp-*H*). ¹³C NMR (100 MHz, CD₃NO₂): δ 5.73, 8.05, 8.24, 9.50 (Et); 90.13, 97.41, 100.48 (Cp); 196.81, 196.86 (CO). IR (CH₂Cl₂): ν(CO) (cm⁻¹) 2077 (vs), 2050 (w), 2027 (s). Anal. Calcd for C₂₂H₂₇BF₄O₄Ru₂Si₂: C, 37.72; H, 3.88. Found: C, 37.65; H, 3.95.

Reactions of 1H⁺BF₄⁻ and 1D⁺TfO⁻ with Amines. In a typical experiment, amine (3-5 equiv) was added to a mixture of 1H⁺BF₄⁻ (or 1D⁺TfO⁻) (~10 mg) and triphenylmethane (~3 mg, internal standard) in deuterated benzene (1 mL) in an NMR tube (gaseous amines were bubbled through the suspension for 5 min; then a stream of dry argon was bubbled through the solution in order to remove the excess amine). During the addition of amine, the reaction mixture immediately changed color from colorless to wine-red. The 1H⁺BF₄⁻ or 1D⁺TfO⁻ reacted completely, and yields of the formamides were determined by means of ¹H NMR spectroscopy. Yields of the formamides¹³ and characterizations of 2a-f are given below.

Reactions of 1H⁺BF₄⁻ and 1D⁺TfO⁻ with NH₃. 72%, (84%).¹⁴ {(η⁵-C₅H₃)₂(SiMe₂)₂}Ru₂(CO)₃(NH₃) (2a): ¹H NMR (400 MHz, C₆D₆): δ 0.29 (s, 6 H, Si(CH₃)), 0.36 (s, 6 H, Si(CH₃)), 3.54 (bs, 3 H, NH₃), 4.67 (d, *J*=2.0 Hz, 2 H), 4.78 (t, *J*=2.0 Hz, 1 H), 5.10 (d, *J*=2.4 Hz, 2 H), 5.73 (t, *J*=2.4 Hz, 1 H). IR (hexanes): ν(CO) (cm⁻¹) 1974 (vs), 1903 (vs), 1879 (m).

Reactions of 1H⁺BF₄⁻ and 1D⁺TfO⁻ with NH₂CH₃. 84%, 88%. Isolation and characterization of {(η⁵-C₅H₃)₂(SiMe₂)₂}Ru₂(CO)₃(NH₂CH₃) (2b) were reported earlier.⁷ Crystals of 2b suitable for X-ray diffraction analysis were obtained by slow cooling of a saturated solution of 2b in hexanes to -20°C.

Reactions of $1\text{H}^+\text{BF}_4^-$ and $1\text{D}^+\text{TfO}^-$ with $\text{NH}(\text{CH}_3)_2$. 85%, 90%. $\{(\eta^5-$

$\text{C}_5\text{H}_3)_2(\text{SiMe}_2)_2\}\text{Ru}_2(\text{CO})_3(\text{NH}(\text{CH}_3)_2)$ (2c): ^1H NMR (400 MHz, C_6D_6): δ 0.28 (s, 6 H, $\text{Si}(\text{CH}_3)$), 0.34 (s, 6 H, $\text{Si}(\text{CH}_3)$), 1.53 (m, 6 H, $(\text{CH}_3)_2\text{NH}$), 1.99 (bs, 1 H, $(\text{CH}_3)_2\text{NH}$), 4.42 (d, $J=2.0$ Hz, 2 H), 4.79 (t, $J=2.0$ Hz, 1 H), 5.03 (d, $J=2.4$ Hz, 2 H), 5.69 (t, $J=2.4$ Hz, 1 H). IR (hexanes): $\nu(\text{CO})$ (cm^{-1}) 1975 (vs), 1907 (vs), 1882 (m).

Reactions of $1\text{H}^+\text{BF}_4^-$ and $1\text{D}^+\text{TfO}^-$ with $\text{NH}(\text{CH}_2\text{CH}_2)_2\text{O}$. 89%, 91%. $\{(\eta^5-$

$\text{C}_5\text{H}_3)_2(\text{SiMe}_2)_2\}\text{Ru}_2(\text{CO})_3\{\text{NH}(\text{CH}_2\text{CH}_2)_2\text{O}\}$ (2d): ^1H NMR (400 MHz, C_6D_6): δ 0.31 (s, 6 H, $\text{Si}(\text{CH}_3)$), 0.39 (s, 6 H, $\text{Si}(\text{CH}_3)$), 2.95 (m, 2 H, $\{\text{O}(\text{CH}_2\text{CH}_2)_2\text{NH}\}$), 3.33 (m, 2 H, $\{\text{O}(\text{CH}_2\text{CH}_2)_2\text{NH}\}$), 3.66 (m, 4 H, $\{\text{O}(\text{CH}_2\text{CH}_2)_2\text{NH}\}$), 3.71 (bs, 1 H, (NH)), 4.48 (d, $J=2.0$ Hz, 2 H), 4.81 (t, $J=2.0$ Hz, 1 H), 5.11 (d, $J=2.4$ Hz, 2 H), 5.77 (t, $J=2.4$ Hz, 1 H). IR (hexanes): $\nu(\text{CO})$ (cm^{-1}) 1981 (vs), 1909 (vs), 1889 (m).

Reactions of $1\text{H}^+\text{BF}_4^-$ and $1\text{D}^+\text{TfO}^-$ with $\text{NH}(\text{CH}_2\text{CH}_2)_2\text{CH}_2$. 82%, 88%. $\{(\eta^5-$

$\text{C}_5\text{H}_3)_2(\text{SiMe}_2)_2\}\text{Ru}_2(\text{CO})_3\{\text{NH}(\text{CH}_2\text{CH}_2)_2\text{CH}_2\}$ (2e): ^1H NMR (400 MHz, C_6D_6): δ 0.26 (s, 6 H, $\text{Si}(\text{CH}_3)$), 0.43 (s, 6 H, $\text{Si}(\text{CH}_3)$), 1.76 (m, 2 H, $\{\text{CH}_2(\text{CH}_2\text{CH}_2)_2\text{NH}\}$), 2.21 (m, 4 H, $\{\text{CH}_2(\text{CH}_2\text{CH}_2)_2\text{NH}\}$), 3.01 (m, 4 H, $\{\text{CH}_2(\text{CH}_2\text{CH}_2)_2\text{NH}\}$), 3.20 (bs, 1 H, (NH)), 4.40 (d, $J=2.1$ Hz, 2 H), 4.73 (t, $J=2.1$ Hz, 1 H), 5.01 (d, $J=2.4$ Hz, 2 H), 5.55 (t, $J=2.4$ Hz, 1 H). IR (hexanes): $\nu(\text{CO})$ (cm^{-1}) 1976 (vs), 1909 (vs), 1879 (m).

Reactions of $1\text{H}^+\text{BF}_4^-$ and $1\text{D}^+\text{TfO}^-$ with $\text{NH}(\text{CH}_2\text{CH}_2)_2$. 77%, 84%. $\{(\eta^5-$

$\text{C}_5\text{H}_3)_2(\text{SiMe}_2)_2\}\text{Ru}_2(\text{CO})_3\{\text{NH}(\text{CH}_2\text{CH}_2)_2\}$ (2f): ^1H NMR (400 MHz, C_6D_6): δ 0.19 (s, 6 H, $\text{Si}(\text{CH}_3)$), 0.32 (s, 6 H, $\text{Si}(\text{CH}_3)$), 1.66 (m, 4 H, $(\text{CH}_2\text{CH}_2)_2\text{NH}$), 2.15 (m, 4 H, $(\text{CH}_2\text{CH}_2)_2\text{NH}$), 2.99 (bs, 1 H, (NH)), 4.35 (d, $J=2.0$ Hz, 2 H), 4.78 (t, $J=2.0$ Hz, 1 H), 5.08

(d, $J=2.4$ Hz, 2 H), 5.73 (t, $J=2.4$ Hz, 1 H). IR (hexanes): $\nu(\text{CO})$ (cm^{-1}) 1973 (vs), 1907 (vs), 1887 (m).

Reaction between $1\text{H}^+\text{BF}_4^-$ and PhNHLi^+ . A suspension of $1\text{H}^+\text{BF}_4^-$ (156 mg, 0.24 mmol) in diethyl ether (50 mL) was treated with a freshly prepared ether (10 mL) solution of PhNHLi^{+15} (0.26 mmol) at -78°C . The mixture was gradually warmed to room temperature and filtered through a short pad of Celite. Removing the solvent under reduced pressure gave an oily brown residue, which was found to be a mixture of **1** and formanilide (49% yield) by ^1H NMR spectroscopy. The reaction with $1\text{D}^+\text{TfO}^-$ was conducted in a similar fashion (61% yield of formanilide).

Synthesis of $[(\eta^5\text{-C}_5\text{H}_3)_2(\text{SiMe}_2)_2]\text{Ru}_2(\text{CO})_3\{\text{NH}(\text{CH}_2\text{CH}_2)_2\}(\mu\text{-H})^+\text{BF}_4^-$ (2fH⁺BF₄⁻**).** A suspension of yellow $1\text{H}^+\text{BF}_4^-$ (50.0 mg, 77.6 μmol) in hexanes (25 mL) was treated with neat pyrrolidine (32 μL , 0.4 mmol). The color of the reaction mixture immediately changed to wine-red. Solvent was removed in vacuum, and the red residue was recrystallized from hexanes (10 mL) at -25°C to give 41 mg (85%) of **2f** as dark-red, air- and moisture-sensitive crystals. A solution of **2f** (25 mg, 41.7 μmol) in CH_2Cl_2 (10 mL) treated with $\text{HBF}_4\cdot\text{OEt}_2$ (6 μL , 43.5 μmol) immediately gave a bright red solution, which was diluted with diethyl ether (50 mL) to give **2fH⁺BF₄⁻** (28 mg, 98%) as a red crystalline precipitate. ^1H NMR (400 MHz, CD_2Cl_2): δ -19.18 (s, 1 H, Ru-*H*-Ru), 0.38 (s, 3 H, Si(CH_3)), 0.47 (s, 3 H, Si(CH_3)), 0.51 (s, 3 H, Si(CH_3)), 0.53 (s, 3 H, Si(CH_3)), 1.71 (m, 2 H, (CH_2)), 1.86 (m, 2 H, (CH_2)), 2.33 (m, 2 H, (CH_2)), 3.19 (m, 1 H, (CH_2)), 3.34 (m, 1 H, (CH_2)), 4.96 (bs, 1 H, NH), 5.17 (m, 1 H, Cp), 5.64 (m, 1 H, Cp), 5.71 (m, 1 H, Cp), 5.87 (m, 2 H, Cp), 6.01 (m, 1 H, Cp). IR (CH_2Cl_2): $\nu(\text{CO})$ (cm^{-1}) 2050 (vs), 2002 (s), 1954 (m).

Anal. Calcd for $C_{21}H_{28}BF_4NO_3Ru_2Si_2$: C, 36.68; H, 4.10; N, 2.04. Found: C, 36.42; H, 3.80; N, 2.06.

Kinetic Studies of the Reaction (eq 2) of $1D^+TfO^-$ with Morpholine. In a typical NMR experiment, $1D^+TfO^-$ (3-6 mg) and triphenylmethane (~3 mg, internal standard) were dissolved in dry CD_3NO_2 (1 mL) under an argon atmosphere in an NMR tube. The tube was placed in the NMR spectrometer and the probe temperature was set at 20.0 ± 0.5 °C. The temperature of the solution was allowed to equilibrate for at least 30 min. The tube was taken out, an amount of neat morpholine to give a 7.72×10^{-2} M to 9.40×10^{-2} M solution was injected into the NMR tube, and the tube was returned to the NMR spectrometer. In a typical IR experiment, $1D^+TfO^-$ (30-50 mg) was dissolved in dry CH_3NO_2 (10 mL) under an argon atmosphere in a Schlenk flask equipped with a constant-temperature water jacket. The jacket was connected to a constant-temperature water circulator, and the temperature of the solution was allowed to equilibrate for at least 30 min. Then, an amount of neat morpholine to give a 4.10×10^{-1} M to 15.1×10^{-1} M solution was added. Samples were periodically withdrawn from the flask and their IR spectra were obtained in a constant-temperature IR cell.

The reactions were monitored by the disappearance of the 2075 cm^{-1} $\nu(\text{CO})$ band in the IR spectra or the 6.11 and 6.17 ppm bands in the ^1H NMR spectra of $1D^+TfO^-$. Rate constants were calculated from the 10-60 spectra taken during the first two (second-order conditions) or three (pseudo-first-order conditions) half-lives of the reaction. Rate data, which were obtained by the IR method under pseudo-first-order conditions, where a ~100-fold excess of morpholine was utilized, were fit to the equation¹⁶ $\text{Rate} = k_{\text{obs}}[1D^+TfO^-]$ to obtain the pseudo-first-order rate constants k_{obs} (s^{-1}). Second order rate constants k_2 ($\text{M}^{-1}\cdot\text{s}^{-1}$)

were calculated using the expression $k_2 = k_{\text{obs}} / [\text{morpholine}]_{\text{av}}$, where $[\text{morpholine}]_{\text{av}}$ is the average of the $[\text{morpholine}]$ at the beginning and the end of the reaction.

Rate data, which were obtained by the ^1H NMR method, when $[\text{morpholine}]_0$ was less than 30 times larger than $[\text{1D}^+\text{TfO}^-]$, were fit to a second-order equation¹⁶ by plotting $\ln([\text{morpholine}]_t / [\text{1D}^+\text{TfO}^-]_t)$ vs t . The second-order rate constants k_2 ($\text{M}^{-1}\text{s}^{-1}$) were determined from the slope of the best fit straight line.

X-ray Crystallography of $\{(\eta^5\text{-C}_5\text{H}_3)_2(\text{SiMe}_2)_2\}\text{Ru}_2(\text{CO})_3(\text{NH}_2\text{CH}_3)$ (2b). A red crystal with approximate dimensions $0.40 \times 0.18 \times 0.06 \text{ mm}^3$ was selected under oil under ambient conditions and attached to the tip of a glass capillary. The crystal was mounted in a stream of cold nitrogen at 173(2) K and centered in the X-ray beam by using a video camera. The crystal evaluation and data collection were performed on a Bruker CCD-1000 diffractometer with Mo K_α ($\lambda = 0.71073 \text{ \AA}$) radiation and a diffractometer to crystal distance of 5.08 cm. The initial cell constants were obtained from three series of ω scans at different starting angles. Each series consisted of 20 frames collected at intervals of 0.3° in a 6° range about ω with an exposure time of 10 seconds per frame. A total of 47 reflections was obtained. The reflections were successfully indexed by an automated indexing routine in the SMART program. The final cell constants were calculated from a set of 4927 strong reflections from the actual data collection. The data were collected by using the hemisphere data collection routine. Reciprocal space was surveyed to the extent of 1.9 hemisphere to a resolution of 0.80 \AA . A total of 10630 data were harvested by collecting three sets of frames with 0.3° scans in ω with an exposure time of 60 sec per frame. These highly redundant datasets were corrected for Lorentz and polarization effects. The absorption correction was based on fitting a function to the empirical transmission surface as sampled by multiple

equivalent measurements.¹⁷ Systematic absences in the diffraction data were consistent with the space groups $P\bar{1}$ and $P1$.¹⁸ The E -statistics strongly suggested the centrosymmetric space group $P\bar{1}$ that yielded chemically reasonable and computationally stable results of refinement. A successful solution by the direct method provided most non-hydrogen atoms from the E -map. The remaining non-hydrogen atoms were located in an alternating series of least-squares cycles and difference Fourier maps. All non-hydrogen atoms except for N(1), N(2), C(7), and C(19) were refined with anisotropic displacement coefficients. All hydrogen atoms were included in the structure factor calculation at idealized positions and were allowed to ride on the neighboring atoms with relative isotropic displacement coefficients. There is occupational disorder present in the structure. One coordination site of each Ru atom is 50% occupied by a CO ligand and 50% occupied by a MeNH₂ ligand. The disordered groups were refined with idealized geometries. There is also half a molecule of solvate hexane per molecule of complex present in the asymmetric unit. The final least-squares refinement of 289 parameters against 4878 data resulted in residuals R (based on F^2 for $I \geq 2\sigma$) and wR (based on F^2 for all data) of 0.0464 and 0.1107, respectively.

Results and Discussion

Synthesis and Protonation of $\{(\eta^5\text{-C}_5\text{H}_3)_2(\text{SiMe}_2)_2\}\text{Ru}_2(\text{CO})_4$ (1). The reaction of $(\text{C}_5\text{H}_4)_2(\text{SiMe}_2)_2$ ¹⁹ with $\text{Ru}_3(\text{CO})_{12}$ in the presence of the hydrogen acceptor (1-dodecene or methylisobutylketone) furnished $\{(\eta^5\text{-C}_5\text{H}_3)_2(\text{SiMe}_2)_2\}\text{Ru}_2(\text{CO})_4$ (**1**) in 72% yield, as an air- and moisture-stable yellow solid. When the reaction was carried out in the absence of a

hydrogen acceptor, a considerable amount of $\text{Ru}_4(\text{CO})_{12}(\mu\text{-H})_4$ ²⁰ (15-25 % based on Ru equiv) was formed and lower yields of **1** were obtained.

The hydride-bridged dinuclear Ru complex $[\{(\eta^5\text{-C}_5\text{H}_3)_2(\text{SiMe}_2)_2\}\text{Ru}_2(\text{CO})_4(\mu\text{-H})]^+$ (**1H⁺**) was prepared in quantitative yield upon addition of 1 equiv of $\text{HBF}_4\cdot\text{OEt}_2$ or $\text{CF}_3\text{SO}_3\text{D}$ to a CH_2Cl_2 solution of complex **1** at room temperature. The Ru-H resonance in the ¹H NMR spectrum occurs as a singlet at $\delta -19.92$ ppm. The CO stretching frequencies for **1H⁺** are approximately 67 cm^{-1} higher than those for **1** and fall within the range where amine attack on the CO groups is expected to occur.² Complex **1H⁺** is kinetically inert with respect to deprotonation by organic bases such as Me_3N . Less than 2% of the complex was deprotonated after 1 hour in CD_3NO_2 or CD_3CN solution in the presence of 10 fold excesses of Me_3N ($\text{pK}_a(\text{H}_2\text{O})=10.35$) or pyridine ($\text{pK}_a(\text{H}_2\text{O})=5.25$). In contrast, the unbridged^{21a} and monobridged^{21b} analogs of **1H⁺**, $(\eta^5\text{-C}_5\text{H}_5)_2\text{Ru}_2(\text{CO})_4(\mu\text{-H})^+$ and $\{(\eta^5\text{-C}_5\text{H}_4)_2(\text{SiMe}_2)\}\text{-Ru}_2(\text{CO})_4(\mu\text{-H})^+$, undergo fast and quantitative deprotonation by bases such as pyridine or diethylamine. In order to understand whether the slow rate of deprotonation of $\text{1H}^+\text{BF}_4^-$ was caused by kinetic or thermodynamic factors, we estimated the pK_a^{AN} value ($6.5(\pm 0.2)$ in CD_3CN) for $\text{1H}^+\text{BF}_4^-$ from studies of the equilibrium constant for the proton transfer reaction between **1** and $\text{HPPPh}_3^+\text{BF}_4^-$ in CD_3CN at $25\text{ }^\circ\text{C}$.⁷ The pK_a^{AN} value for complex $\text{1H}^+\text{BF}_4^-$ clearly indicates that the above-noted amine bases²² will thermodynamically deprotonate $\text{1H}^+\text{BF}_4^-$ easily. Although it is not obvious why **1H⁺** undergoes slow deprotonation, it is perhaps a combination of the bulkiness of the dimethylsilyl linkers and the rigidity of the dicyclopentadienyl bridging ligand.

Reaction of $[\{(\eta^5\text{-C}_5\text{H}_3)_2(\text{SiMe}_2)_2\}\text{Ru}_2(\text{CO})_4(\mu\text{-H})]^+\text{BF}_4^-$ (1H⁺BF₄⁻**) with Amines.**

Complex **1H⁺** reacts with 3 equiv of nucleophilic amines (NH_3 , NH_2CH_3 , $\text{NH}(\text{CH}_3)_2$,

morpholine, piperidine, pyrrolidine) at ambient temperature to the yield complexes $\{(\eta^5\text{-C}_5\text{H}_3)_2(\text{SiMe}_2)_2\}\text{Ru}_2(\text{CO})_3(\text{NHR}_1\text{R}_2)$ (**2**) and the corresponding formamides in a 1:1 ratio (eq 2). The only other Ru-containing product was the deprotonated complex $\{(\eta^5\text{-C}_5\text{H}_3)_2(\text{SiMe}_2)_2\}\text{Ru}_2(\text{CO})_4$ (**1**). The yields of formamides, established for most cases by ^1H NMR spectroscopy, vary from 72% for the reaction of ammonia with 1H^+ to 91% for morpholine with 1D^+ . The only other product of these reactions was **1** which was observed in 5-20% yields. The least bulky amine (ammonia) gave the lowest yield of formamide due to the faster rate of direct deprotonation of 1H^+ by amine to give complex $\{(\eta^5\text{-C}_5\text{H}_3)_2(\text{SiMe}_2)_2\}\text{Ru}_2(\text{CO})_4$ (**1**). Also, yields of the formamides were generally higher when the deuterated 1D^+ complex was used, since 1D^+ presumably undergoes slower deprotonation compared to 1H^+ because of the deuterium isotope effect. Unfortunately, we were unable to measure the magnitude of the deuterium isotope effect for proton transfer from 1H^+ because we did not find a base that will deprotonate 1H^+ without side reactions²³ at rates sufficiently fast for kinetic studies. Experiments using the deuterium-labeled $1\text{D}^+\text{TfO}^-$ and amines (NHMe_2 , morpholine) gave formamide products ($\text{D}(\text{C}=\text{O})\text{NRR}'$) that are >95% deuterated at the formyl position and no other. Bulky nucleophilic amines (Bn_2NH , $i\text{-Pr}_2\text{NH}$, Cy_2NH) and weakly nucleophilic amines (aniline) failed to react with 1H^+ under the same reaction conditions.

Second-order rate constants (k_2) for the reaction (eq 2) of morpholine²⁴ with $1\text{D}^+\text{TfO}^-$ were determined from rate studies conducted under pseudo-first-order conditions (~ 100 -fold excess of amine; $[1\text{D}^+\text{TfO}^-] = 8.50 \times 10^{-3}$ - 8.95×10^{-3} M, $[\text{morpholine}] = 4.10 \times 10^{-1}$ - 15.10×10^{-1} M, by the IR method) or second order conditions (< 30 -fold excess of amine; $[1\text{D}^+\text{TfO}^-] = 9.09 \times 10^{-3}$ - 9.89×10^{-3} M, $[\text{morpholine}] = 7.72 \times 10^{-2}$ - 9.40×10^{-2} M, by the ^1H NMR method) in

nitromethane at 20 °C. The reactions were followed by monitoring the disappearance of the $\nu(\text{CO})$ bands in the IR spectra or the ^1H NMR signals of $1\text{D}^+\text{TfO}^-$. The rate constants k_2 (Table S1) were obtained either indirectly from the equation $k_2 = k_{\text{obs}}/[\text{morpholine}]_{\text{av}}$ or directly from a linear plot, $\ln([\text{morpholine}]_t/[1\text{D}^+\text{TfO}^-]_t)$ vs t , for a second order reaction. A plot (Figure 4) of k_{obs} vs $[\text{morpholine}]_0$ gave a straight line with a near-zero intercept. Thus, the reaction follows the second-order rate law, $-\text{d}[1\text{D}^+\text{TfO}^-]/\text{d}t = k_2[1\text{D}^+\text{TfO}^-][\text{morpholine}]$, where $k_2 = (2.2 \pm 0.5) \times 10^{-3} \text{ M}^{-1}\text{s}^{-1}$. Although the rate constant k_2 includes the rate of deprotonation of $1\text{D}^+\text{TfO}^-$ by morpholine, the contribution of this concurrent reaction (5%) to the overall rate is smaller than the experimental error in the kinetic studies.

This rate law is consistent with the mechanism proposed in Figure 1. Initial nucleophilic attack by the amine on a coordinated CO produces the cationic intermediate **A**. Subsequent deprotonation of the nitrogen in **A** is likely to be fast, and reductive elimination of the formamide from **B** must be rapid because there is no spectroscopic evidence (^1H NMR or IR) for intermediates in the reaction. Such a facile reductive elimination from **B** is surprising because removal of the bridging H^+ in 1H^+ by bases is so slow. Reductive elimination of the formamide from **B** gives an unsaturated di-ruthenium intermediate that coordinates an amine to give **2**. The observed first order dependence on amine concentration and the absence of measurable quantities of intermediates means that the first step, nucleophilic attack on a CO ligand, is rate-determining.

Since the bulkiness of the dimethylsilyl linkers in the $(\eta^5\text{-C}_5\text{H}_3)_2(\text{SiMe}_2)_2$ ligand is a possible reason for the unusually low kinetic acidity of 1H^+ , it is conceivable that a more bulky linker would make the proton even less kinetically acidic and presumably increase yields of the formamide products in reactions of 1H^+ with amines. We therefore synthesized

the more bulky tetraethyl analog of $1H^+$, $[\{(\eta^5-C_5H_3)_2(SiEt_2)_2\}Ru_2(CO)_4(\mu-H)]^+$ ($3H^+$), which was successfully characterized by elemental analysis and 1H , ^{13}C NMR and IR spectroscopies. However, the reactions of amines (NH_3 , NH_2Me , $NHMe_2$, morpholine) with complex $3H^+$ gave essentially the same yields of formamides and **3** (the result of direct deprotonation of $3H^+$ by amine) as those for the reactions of $1H^+$.

Weakly nucleophilic amines, such as aniline, with $pK_a(H_2O)$ values lower than ~ 8 failed to react with $1H^+$. In contrast to aniline, the corresponding lithium anilide $PhNHLi^+$ readily reacted with $1H^+$ and $1D^+$ to give formanilide ($H(C=O)NHPH$) in 49% and 61% isolated yields, respectively. As observed in reactions of the alkyl amines with $1D^+$, the formanilide product ($D(C=O)NHPH$) from the reaction of $1D^+$ with $PhNHLi^+$ was found by 1H NMR studies to be almost completely ($>95\%$) deuterated at the formyl position and no other. Complex **1**, rather than **2**, was observed as the only identifiable ruthenium-containing product of the reaction of $PhNHLi^+$ with both $1H^+$ and $1D^+$. The formation of **1** clearly also requires the formation of other Ru products which were not identified. The direct deprotonation of $1H^+$ by $PhNHLi^+$ also may lead to complex **1**.

Characterization of complexes $\{(\eta^5-C_5H_3)_2(SiMe_2)_2\}Ru_2(CO)_3(NHR_1R_2)$ (2**).** The cyclopentadienyl hydrogens of the $(\eta^5-C_5H_3)Ru(CO)(NHR_1R_2)$ fragment in **2** are observed as a well-resolved doublet and triplet, shifted approximately 0.7 ppm upfield from the cyclopentadienyl hydrogens of the $(\eta^5-C_5H_3)Ru(CO)_2$ part of the molecule. It is worth noting that at room temperature the 1H NMR spectra of the **2** complexes show only four signals in the cyclopentadienyl region instead of the expected six and only two singlets for the $Si(CH_3)_2$ groups instead of four, required by the structure of the molecules. The ^{13}C NMR spectrum of **2b** exhibits only two signals for the CO ligands and six signals in

cyclopentadienyl region.⁷ Although these observations suggest that these compounds are fluxional, variable temperature NMR studies of $\{(\eta^5\text{-C}_5\text{H}_3)_2(\text{SiMe}_2)_2\}\text{Ru}_2(\text{CO})_3(\text{NH}_2\text{CH}_3)$ (**2b**) in CD_3NO_2 at temperatures down to -25°C did not reveal any broadening or splitting of the cyclopentadienyl resonances.

However, it is known²⁵ that $\text{Cp}_2\text{Ru}_2(\text{CO})_4$ is fluxional even at low temperatures which suggests that **2** is fluxional according to the mechanism in Figure 2 which involves the pairwise exchange of two carbonyl ligands between the two metal atoms *via* a bridging carbonyl intermediate. This mechanism requires the movement of the NHR_1R_2 ligand from one side of the molecule to the other, but not from one Ru to the other; this motion accounts for the relatively simple ^1H and ^{13}C NMR spectra of the $(\eta^5\text{-C}_5\text{H}_3)_2(\text{SiMe}_2)_2$ ligand. If CO groups on opposite sides of the Ru-Ru bond are involved in forming the carbonyl-bridged intermediate, only two of the three CO groups can participate in the exchange process, which accounts for the observation of two ^{13}C CO signals. The IR spectra in the $\nu(\text{CO})$ region for all complexes of type **2** exhibit a medium band in the 1890 cm^{-1} region and two strong bands in the 1910 cm^{-1} and 1980 cm^{-1} regions, which are typical for group 8 $\text{Cp}_2\text{M}_2(\text{CO})_3\text{L}$ complexes without bridging CO ligands.²⁶

The structure of **2b** (Figure 3), established by X-ray crystallography, shows the presence of occupational disorder. One coordination site of each Ru atom is 50% occupied by a CO (C(19), O(4)) ligand and 50% by a NH_2Me ligand. The Ru-Ru distance in **2b** ($2.8955(6)\text{ \AA}$) is longer than that in **1** ($2.8180(3)\text{ \AA}$).²⁷ The C(6)-Ru(1)-Ru(2)-C(18) torsion angle (1.0°) confirms the eclipsed orientation of the CO ligands. Both Ru atoms of complex **2b** have pseudo-octahedral geometry, with angles of approximately 90° between adjacent

carbonyls, methylamine and the Ru-Ru bond (Figure 3). As one would expect, the Cp-Cp fold angle²⁸ (125.9°) is larger than in **1** (120.5(7) °) because of the longer Ru-Ru distance.

The lability of the amine ligand in complex **2** was established by observing the substitution of this ligand (NH₃, NH₂Me, NHMe₂) by CO in a hexanes solution of complex **2** under a flow of CO gas (1 atm) at ambient temperature (*t*_{1/2}=40-75 min) to give {(η⁵-C₅H₃)₂(SiMe₂)₂}Ru₂(CO)₄ (**1**). As expected, the bulky NHMe₂ ligand was the most labile (*t*_{1/2}=40 min) as compared with the less bulky NH₃ and NH₂Me. Complexes **2** are extremely air-sensitive and undergo slow decomposition in solution under inert atmosphere to give **1** as the only identifiable product.

Protonation of {(η⁵-C₅H₃)₂(SiMe₂)₂}Ru₂(CO)₃{NH(CH₂CH₂)₂} (**2f**). The Ru-Ru bond in **2f** is protonated with 1 equiv of acid (HBF₄·OEt₂) to give the air-stable cationic complex [{(η⁵-C₅H₃)₂(SiMe₂)₂}Ru₂(CO)₃{NH(CH₂CH₂)₂}(μ-H)]⁺BF₄⁻ (**2fH⁺BF₄⁻**). The cyclopentadienyl hydrogens in **2fH⁺BF₄⁻**, appearing in the ¹H NMR spectrum as five sets of well-resolved multiplets, are shifted approximately 0.4 ppm downfield compared to the cyclopentadienyl hydrogens of **2f** due to the positive charge on the molecule. In contrast to **2f**, the complicated resonances in the cyclopentadienyl region of **2fH⁺**, as well as the four separate methyl resonances of the dimethylsilyl groups, indicate the absence of fluxional behavior of the type observed for **2** (Figure 2). The Ru-H-Ru resonance in the ¹H NMR spectrum occurs as a singlet at -19.18 ppm. The presence of the strongly donating pyrrolidine ligand in **2fH⁺BF₄⁻**, as one would expect, lowers the carbonyl stretching frequencies in **2fH⁺BF₄⁻** (2050, 2002, 1954 cm⁻¹) as compared to those in **1H⁺BF₄⁻** (2077, 2050, 2027 cm⁻¹), thereby deactivating the remaining CO ligands in **2fH⁺BF₄⁻** to nucleophilic attack by alkyl amines, which confirms the usefulness of *ν*(CO) values for determining the

reactivity of CO groups with amines. Bulky alkyl amines (NMe₃) deprotonate 2fH⁺BF₄⁻ (*t*_{1/2}≈30 min) slowly, although much faster than the deprotonation of 1H⁺, whereas less bulky amines (NH₃) deprotonate 2fH⁺BF₄⁻ quickly. (*t*_{1/2}≈1.5 min).

Conclusions

We have prepared a cationic complex [{(η⁵-C₅H₃)₂(SiMe₂)₂}Ru₂(CO)₄(μ-H)]⁺ (1H⁺) in which the bridging proton is removed only very slowly by amine bases even though it is thermodynamically acidic (pK_a^{AN}=6.5(±0.2)). Although it is not obvious why complex 1H⁺ is kinetically stable with respect to deprotonation, it may be due to a combination of the bulkiness of the dimethylsilyl linkers and the rigidity of the dicyclopentadienyl bridging ligand. The low kinetic acidity and the positive charge in 1H⁺ allows its CO ligands to undergo attack by alkyl amines. To our knowledge, this is the only system in which protonation of metal centers in a complex activates CO ligands to nucleophilic attack. The amine reactions lead to the elimination of the μ-H ligand which becomes incorporated into the formamide product, as shown in Figure 1. The facile reductive elimination in the product-forming step is surprising because removal of the bridging H⁺ by bases is so slow.²⁹ Weakly nucleophilic amines (*e.g.*, aniline) with pK_a(H₂O) values lower than ~8.00³⁰ and bulky amines with cone angles (Θ) larger than 125° (*e.g.*, Bn₂NH, *i*-Pr₂NH, Cy₂NH)³¹ do not react with 1H⁺. Although aniline does not react with 1H⁺, its amide (RNH⁻) does react to give the formanilide.

Acknowledgment

This work was supported by the National Science Foundation through Grant No. CHE-9816342.

References

- (1) Collman, J. P.; Hehedus, L. S.; Norton, J. R.; Finke, R. G. *Principles and Applications of Organotransition Metal Chemistry*; University Science Books: Mills Valley, CA, 1987; Chapter 7.
- (2) Angelici, R. J. *Acc. Chem. Res.* **1972**, *5*, 335.
- (3) (a) Jenner, J.; Bitsu, G.; Schleiffer, E. *J. Mol. Catal.* **1987**, *39*, 233.
- (4) (a) Valli, V. L. K.; Alper, H. *Organometallics* **1995**, *14*, 80.
- (5) (a) McCusker, J. E.; Grasso, C. A.; Main, A. D.; McElwee-White, L. *Org. Lett.* **1999**, *1*, 961. (b) McCusker, J. E.; Logan, J.; McElwee-White, L. *Organometallics* **1998**, *17*, 4037. (c) McCusker, J. E.; Abboud, K. A.; McElwee-White, L. *Organometallics* **1997**, *16*, 3863. (d) Giannocaro, P.; Nobile, C. F.; Mastroilli, P.; Ravasio, N. *J. Organomet. Chem.* **1991**, *419*, 251. (e) Srivastava, S. C.; Shrimal, A. K.; Srivastava, A. *J. Organomet. Chem.* **1991**, *414*, 65. (f) Bassoli, A.; Rindone, B.; Tollari, S.; Chioccare, F. *J. Mol. Catal.* **1990**, *60*, 41.
- (6) (a) Angelici, R. J. *Acc. Chem. Res.* **1995**, *28*, 52. (b) Kristjánisdóttir, S. S.; Norton, J. R. *In Transition Metal Hydrides: Recent Advances in Theory and Experiments*; Dedieu, A., Ed.; VCH: New York, 1991; Chapter 10. (c) Pearson, R. G. *Chem. Rev.* **1985**, *85*,

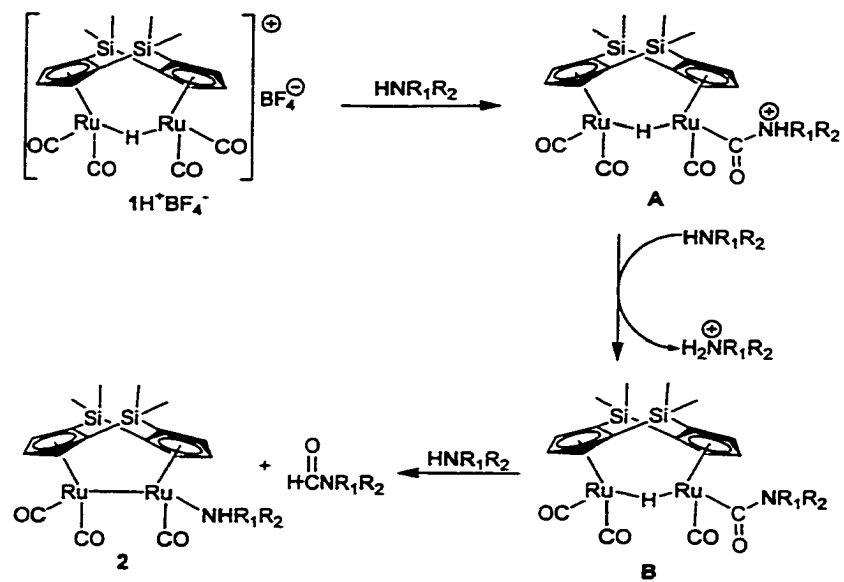
41. (d) Martinho Simões, J. A.; Beauchamp, J. L. *Chem. Rev.* **1990**, *90*, 629. (e) Bullock, R. M. *Comments Inorg. Chem.* **1991**, *12*, 1.
- (7) Ovchinnikov, M. V.; Angelici, R. J. *J. Am. Chem. Soc.* **2000**, *122*, 6130.
- (8) Errington, R. J. *Advanced Practical Inorganic and Metalorganic Chemistry*, 1st ed.; Chapman & Hall: New York, 1997.
- (9) Pangborn, A. B.; Giardello, M. A.; Grubbs, R. H.; Rosen, R. C.; Timmers, F. J. *Organometallics* **1996**, *15*, 1518.
- (10) Perrin, D. D.; Armarego, W. L. F.; Perrin, D. R. *Purification of Laboratory Chemicals*, 2nd ed.; Pergamon: New York, 1980.
- (11) The ^1H NMR spectrum of $1\text{D}^+\text{TfO}^-$ in CD_3NO_2 revealed a small peak for the Ru-H resonance at -19.98 ppm (s, 0.02 H), which corresponds to $1\text{H}^+\text{TfO}^-$ as a ~2% impurity.
- (12) Köhler, F. H.; Schell, A.; Weber, B. *J. Organomet. Chem.* **1999**, *575*, 33.
- (13) Yield values correspond to the reactions of $1\text{H}^+\text{BF}_4^-$ and $1\text{D}^+\text{TfO}^-$, respectively.
- (14) Yield was estimated from the yield of $\{(\eta^5\text{-C}_5\text{H}_3)_2(\text{SiMe}_2)_2\}\text{Ru}_2(\text{CO})_3(\text{NH}_3)$
- (15) (a) Dorta, R.; Togni, A. *Helv. Chim. Acta* **2000**, *83*, 119. (b) Matsuzaka, H.; Kamura, T.; Ariga, K.; Watanabe, Y.; Okubo, T.; Ishii, T.; Yamashita, M.; Kondo, M.; Kitagawa, S. *Organometallics* **2000**, *19*, 216.
- (16) Espenson, J. *Chemical Kinetics and Reaction Mechanisms*, 1st ed; McGraw-Hill: New-York, 1981.
- (17) Blessing, R. H. *Acta Cryst.* **1995**, *A51*, 33-38.

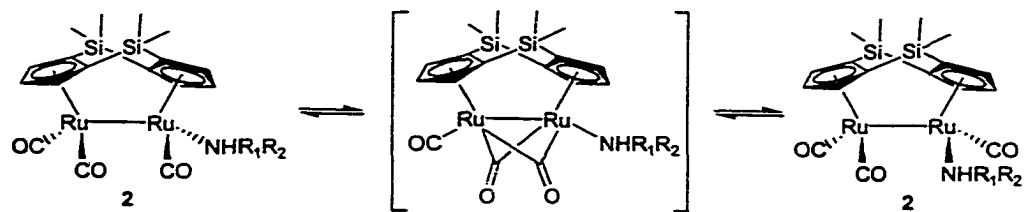
- (18) All software and sources of the scattering factors are contained in the SHELXTL (version 5.1) program library (G. Sheldrick, Bruker Analytical X-Ray Systems, Madison, WI).
- (19) (a) Siemeling, U.; Jutzi, P.; Neumann, B.; Stammer, H. G.; Hursthouse, M. B. *Organometallics* **1992**, *11*, 1328. (b) Hiermeier, J.; Koehler, F. H.; Mueller, G. *Organometallics* **1991**, *10*, 1787.
- (20) Wilson, R. D.; Wu, S. M.; Love, R. A.; Bau, R. *Inorg. Chem.* **1978**, *17*, 1271.
- (21) (a) Ovchinnikov, M. V.; Angelici, R. J. Unpublished results. (b) Froehlich, R.; Gimeno, J.; Gonzalez, C. M.; Lastra, E.; Borge, J.; Garcia, G. S. *Organometallics* **1999**, *18*, 3008.
- (22) pK_a^{AN} values for NMe_3 (17.61) and pyridine (12.33) were reported earlier: Coetzee, J. F.; Padmanabhan, G. R. *J. Am. Chem. Soc.* **1965**, *87*, 5005.
- (23) NMe_3 causes slow decomposition of 1H^+ to a mixture of unidentifiable products at rates that are faster than the rate of direct deprotonation.
- (24) The rate of the reaction of $1\text{D}^+\text{TfO}^-$ with morpholine was the only rate suitable for kinetic studies by ^1H NMR and FT-IR spectroscopies. More nucleophilic amines (NH_3 , NH_2CH_3 , $\text{NH}(\text{CH}_3)_2$, piperidine, pyrrolidine) reacted with $1\text{D}^+\text{TfO}^-$ very fast ($t_{1/2} < 1$ sec).
- (25) (a) Bullitt, J. G.; Cotton, F. A.; Marks, T. J. *J. Am. Chem. Soc.* **1970**, *92*, 2155. (b) Gansow, O. A.; Burke, A. R.; Vernon, W. D. *J. Am. Chem. Soc.* **1976**, *98*, 5817.
- (26) $(\eta^5, \eta^5\text{-C}_{10}\text{H}_8)\text{Ru}_2(\text{CO})_3(\text{PMe}_3)$ in: Boese, R.; Tolman, W. B.; Vollhardt, K. C. P. *Organometallics* **1986**, *7*, 582.

- (27) Ovchinnikov, M. V.; Guzei, I. A.; Angelici, R. J. Manuscript in preparation.
- (28) The angle between the two cyclopentadienyl planes.
- (29) Reductive eliminations involving a μ -H have only recently been characterized, *e.g.*, in the formation of alkanes and arenes from $\text{Pd}_2\text{R}_2(\mu\text{-H})(\text{dppm})_2^+$: Stockland, R. A. Jr.; Anderson, G. K.; Rath, N. P. *J. Am. Chem. Soc.* **1999**, *121*, 7945.
- (30) Perrin, D. D. *Dissociation Constants of Organic Bases in Aqueous Solution*; Butterworths: London, 1972.
- (31) For amine cone angles, see: Seligson, A. L.; Trogler, W. C. *J. Am. Chem. Soc.* **1991**, *113*, 2520.

Table 1. Crystal Data and Structure Refinement for **2b**.

Empirical formula	$C_{21}H_{30}NO_3Ru_2Si_2$
Formula weight	602.78
Temperature	173(2) K
Wavelength	0.71073 Å
Crystal system	Triclinic
Space group	$P\bar{1}$
Unit cell dimensions	$a = 8.8046(5)$ Å $b = 8.9523(5)$ Å $c = 16.6067(9)$ Å $\alpha = 89.721(1)^\circ$ $\beta = 88.199(1)^\circ$ $\gamma = 66.777(1)^\circ$
Volume	1202.27(12) Å ³
Z	2
Density (calculated)	1.665 Mg/m ³
Absorption coefficient	1.377 mm ⁻¹
F(000)	606
Crystal size	0.40 x 0.18 x 0.06 mm ³
Theta range for data collection	2.45 to 26.37°.
Index ranges	-10 ≤ h ≤ 10, -11 ≤ k ≤ 11, 0 ≤ l ≤ 20
Reflections collected	10630
Independent reflections	4878 [R(int) = 0.0349]
Completeness to theta = 26.37°	99.0 %
Absorption correction	Empirical with SADABS
Max. and min. transmission	0.9219 and 0.6089
Refinement method	Full-matrix least-squares on F ²
Data / restraints / parameters	4878 / 6 / 289
Goodness-of-fit on F ²	1.008
Final R indices [I > 2σ(I)]	R1 = 0.0464, wR2 = 0.1107
R indices (all data)	R1 = 0.0662, wR2 = 0.1189
Largest diff. peak and hole	1.563 and -0.958 e.Å ⁻³

**Figure 1**

**Figure 2**

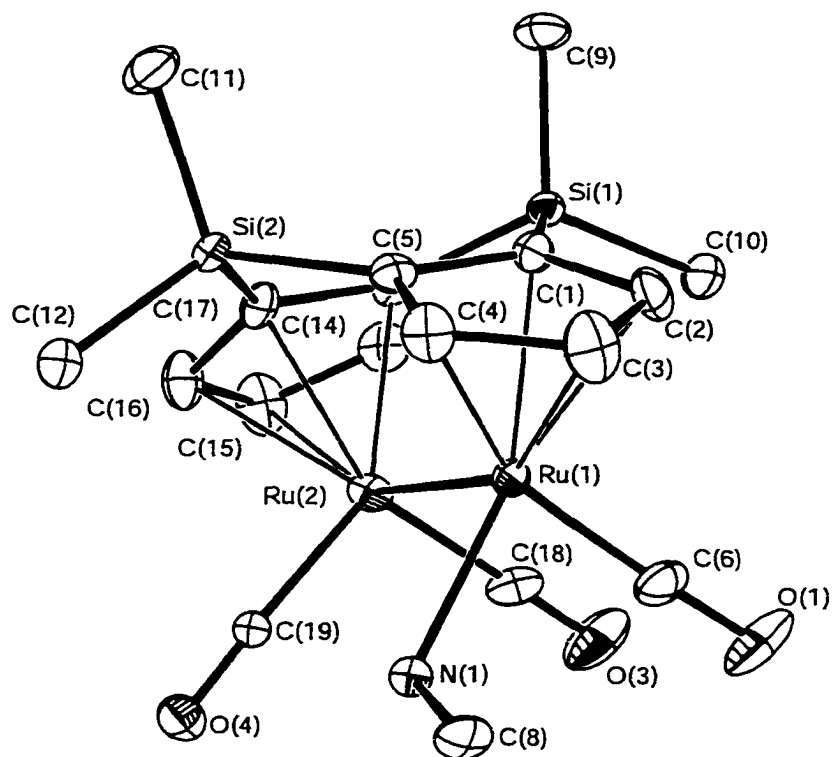


Figure 3. Thermal ellipsoid drawing of $\{(\eta^5\text{-C}_5\text{H}_3)_2(\text{Me}_2\text{Si})_2\}\text{Ru}_2(\text{CO})_3(\text{NH}_2\text{CH}_3)$ (**2b**) showing the labeling scheme at 50% probability ellipsoids; hydrogens are omitted for clarity. Selected bond distances (Å) and angles (deg) are as follows: Ru(1)-Ru(2), 2.8955(6); Ru(1)-N(1), 2.148(9); N(1)-C(8), 1.4691(10); Ru(1)-Cp(centroid), 1.887; Ru(2)-Cp(centroid), 1.889; $\angle\text{C}(8)\text{-N}(1)\text{-Ru}(1)$, 112.5(7); $\angle\text{C}(18)\text{-Ru}(2)\text{-C}(19)$, 99.4(4); $\angle\text{C}(6)\text{-Ru}(1)\text{-N}(1)$, 85.3(3); $\angle\text{Ru}(1)\text{-Ru}(2)\text{-C}(18)$, 88.50(17); $\angle\text{C}(6)\text{-Ru}(1)\text{-Ru}(2)$, 90.94(18); $\angle\text{C}(6)\text{-Ru}(1)\text{-Ru}(2)\text{-C}(18)$, 1.0; $\angle\text{C}(6)\text{-Ru}(1)\text{-Ru}(2)\text{-C}(19)$, 98.4; $\angle\text{Cp-Cp}$ fold angle, 125.9.

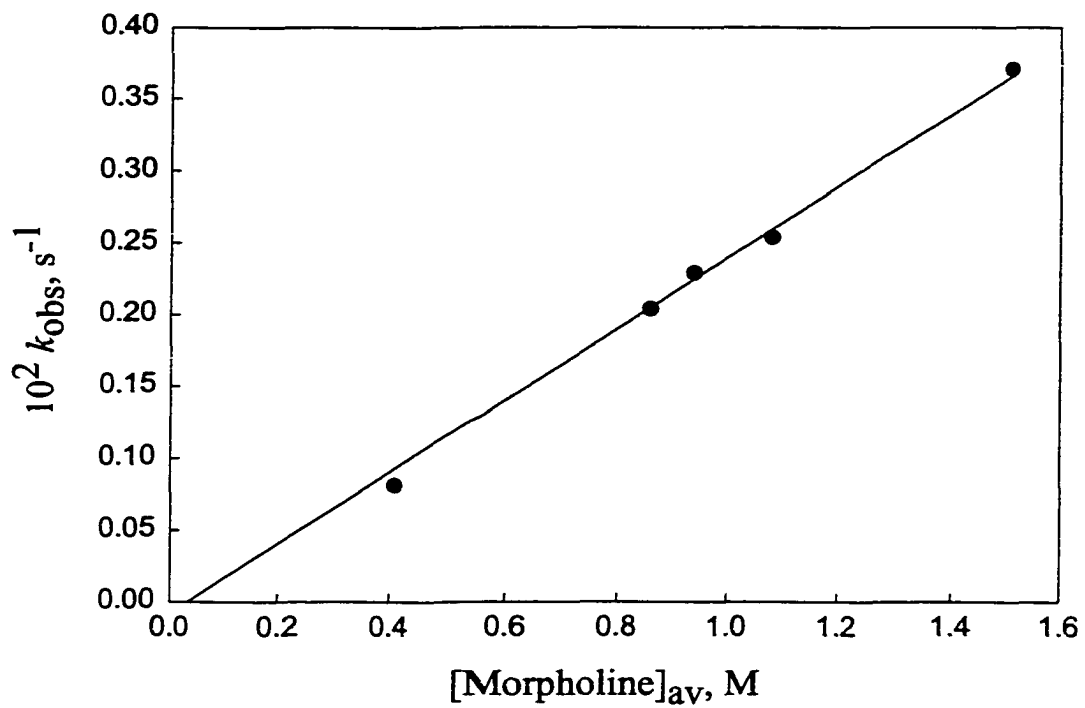


Figure 4. Plot of k_{obs} vs $[\text{morpholine}]_{\text{av}}$ for reaction (eq 2) of $1\text{D}^+\text{TfO}^-$ with morpholine at $20.0\text{ }^\circ\text{C}$.

Table S1. Rate constants for the reaction (eq 2) of $1D^+TfO^-$ with morpholine in nitromethane at 20 °C

$10^3 [1D^+TfO^-]$, M	10^2 [morpholine], M	$10^4 k_{obs}$, s^{-1}	$10^3 k_2$, $M^{-1}s^{-1}$
9.09	7.72	-	1.81
9.89	9.40	-	2.56
8.95	41	8.14	1.98
8.67	86	20.4	2.37
8.50	94	22.9	2.44
8.55	108	25.4	2.35
8.89	151	37.1	2.46

**CHAPTER 3. REACTIONS OF THE DINUCLEAR RUTHENIUM
COMPLEX $\{(\eta^5\text{-C}_5\text{H}_3)_2(\text{SiMe}_2)_2\}\text{Ru}_2(\text{CO})_4$ FEATURING A DOUBLY-
LINKED DICYCLOPENTADIENYL LIGAND[†]**

A paper to be submitted to the Organometallics¹

Maxim V. Ovchinnikov, Ilia A. Guzei, Moon-Gun Choi and Robert J. Angelici

Abstract

Complex $\{(\eta^5\text{-C}_5\text{H}_3)_2(\text{SiMe}_2)_2\}\text{Ru}_2(\text{CO})_4$ (**1**), which features the doubly-linked dicyclopentadienyl ligand $(\eta^5\text{-C}_5\text{H}_4)_2(\text{SiMe}_2)_2$, reacts with phosphines (PMe_3 , PCy_3 , PPh_3) to give $\{(\eta^5\text{-C}_5\text{H}_3)_2(\text{SiMe}_2)_2\}\text{Ru}_2(\text{CO})(\mu\text{-CO})_2(\text{PR}_3)$ (**2a-c**), with halogens X_2 ($\text{X} = \text{Cl}, \text{Br}, \text{I}$) to give Ru-Ru cleaved products $\{(\eta^5\text{-C}_5\text{H}_3)_2(\text{SiMe}_2)_2\}\text{Ru}_2(\text{CO})_4(\text{X})_2$ (**3a-c**), with X_2 and AgTfO to give complexes $[\{(\eta^5\text{-C}_5\text{H}_3)_2(\text{SiMe}_2)_2\}\text{Ru}_2(\text{CO})_4(\mu\text{-X})]^+\text{TfO}^-$ ($\text{X} = \text{Cl}, \text{Br}, \text{I}$; **4a-c**), and with SnCl_2 to give $\{(\eta^5\text{-C}_5\text{H}_3)_2(\text{SiMe}_2)_2\}\text{Ru}_2(\text{CO})_4(\mu\text{-SnCl}_2)$ (**5**) resulting from the insertion of SnCl_2 into the Ru-Ru bond. Reduction of **1** with Na/Hg generates $[\{(\eta^5\text{-C}_5\text{H}_3)_2(\text{SiMe}_2)_2\}\text{Ru}_2(\text{CO})_4]^{2-}$ (**6**), which reacts with $(\eta^5\text{-C}_5\text{H}_5)_2\text{TiCl}_2$ to give $\{(\eta^5\text{-C}_5\text{H}_3)_2(\text{SiMe}_2)_2\}\text{Ru}_2(\text{CO})_4\{\mu\text{-Ti}(\eta^5\text{-C}_5\text{H}_5)_2\}$ (**7**). Ultraviolet photolysis of **1** with

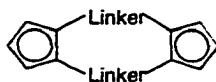
[†] Dedicated to Professor Jiabi Chen, a good friend and colleague, on the occasion of his 60th birthday.

¹ Reproduced with permission from Organometallics, to be submitted for publication.

diphenylacetylene and phenylacetylene yields a series of five dinuclear Ru complexes (**8-13**) containing one or two bridging acetylene units. The rigidity of the doubly-linked (η^5 -C₅H₃)₂(SiMe₂)₂ ligand substantially influences the reactivity and structures of the complexes. Molecular structures of **1**, **2a**, **3c**, **5**, **9**, **10** and **12** as determined by X-ray diffraction studies are also presented.

Introduction

The doubly-linked bis(cyclopentadienyl) ligands (η^5 -C₅H₃)(Linker)₂ (Linker = CH, CH₂, CH₂CH₂, SiMe₂, GeMe₂, etc.) have been extensively explored as frameworks for dinuclear metal complexes that are resistant to fragmentation and have two metal centers in close proximity.¹ The latter feature is especially attractive for studying cooperative effects between two reactive

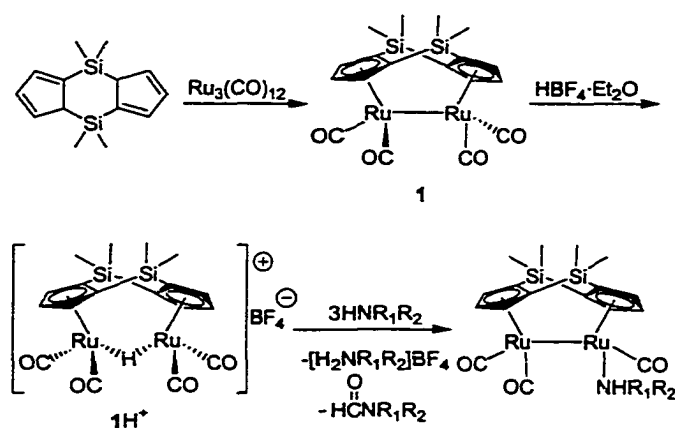


metal sites since free rotation cannot occur around the Cp-(Linker)₂-Cp linker unit. Most of the known (η^5 -C₅H₃)₂(SiMe₂)₂-bridged bimetallic complexes contain group 4² or 6³ metals. To the best of our knowledge only one example of a non-metallocene complex ($\{(\eta^5$ -C₅H₃)₂(SiMe₂)₂\}Fe₂(CO)₄) is known for group 8 metals,^{4a} and little chemistry of this compound has been reported.

We recently reported⁵ the synthesis (Scheme 1) of the cationic dinuclear complex [$\{(\eta^5$ -C₅H₃)₂(SiMe₂)₂\}Ru₂(CO)₄(μ -H)]⁺ (1H⁺) whose carbon monoxide ligands are activated to attack by amine nucleophiles because of the positive charge on the complex and the slow

rate of deprotonation of the bridging hydride by the amines.

In order to develop a general understanding of the effect of the doubly-linked (η^5 - $C_5H_3)_2(SiMe_2)_2$ ligand on the reactivity of $\{(\eta^5-C_5H_3)_2(SiMe_2)_2\}Ru_2(CO)_4$ (**1**), we have explored the reactions of **1** with phosphines, halogens, $SnCl_2$, Na/Hg , phenylacetylene and diphenylacetylene to give a variety of new complexes. These reactions also demonstrate the robustness of the bridging system which remains unchanged throughout the transformations.



Scheme 1

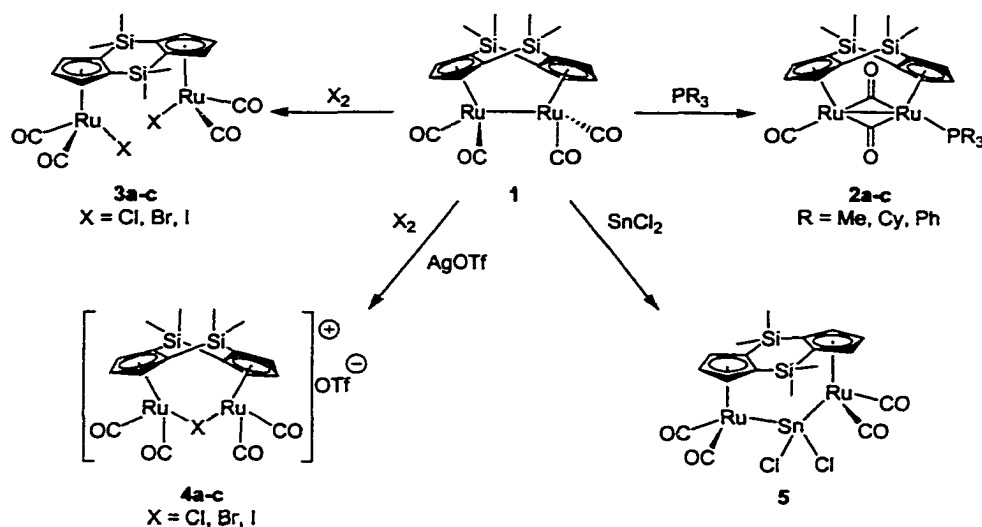
Results and Discussion

Crystal Structure of $\{(\eta^5-C_5H_3)_2(SiMe_2)_2\}Ru_2(CO)_4$ (1**).** The starting complex **1**, whose synthesis (Scheme 1) was recently published,⁵ has a structure (Figure 1, Table 1) that contains a pair of ruthenium atoms linked by a metal-metal bond and a bridging (η^5 - $C_5H_3)_2(SiMe_2)_2$ ligand, with four terminal carbonyls bound in a symmetrical and staggered array ($\angle C(7)-Ru(1)-Ru(1A)-C(6A) = 32.3^\circ$). The staggered character of the molecule is also reflected by a significant twist around the $Ru(1)-Ru(1A)$ axis ($\angle Cp(\text{centroid})-Ru(1)-Ru(1A)-$

Cp(centroid) = 24.2°). The bend of the (η^5 -C₅H₃)₂(SiMe₂)₂ ligand, defined as the fold angle between the planes of the Cp rings, is relatively large (122.86°), suggesting that the normally planar (η^5 -C₅H₃)₂(SiMe₂)₂ moiety (e.g. in *trans*-{ η^5 -C₅H₃)₂(SiMe₂)₂}Li₂(TMEDA)₂)^{4b} is somewhat strained leading to the expectation of a longer than normal Ru-Ru single bond distance. This hypothesis is based on X-ray structural data for (η^5 , η^5 -Fulvalene)Ru₂(CO)₄,⁶ where fulvalene is η^5 , η^5 -C₅H₄-C₅H₄, in which the Ru-Ru distance (2.821(1) Å) is significantly greater than that in the corresponding non-linked complex Cp₂Ru₂(μ -CO)₂(CO)₂ (2.735(2) Å).⁷ Avoidance of nonbonding contacts between the carbonyl ligands and alleviation of strain by decreasing the (η^5 , η^5 -Fulvalene) bend were cited to account for these lengthened bonds. In part, similar arguments may be applied to **1**. Thus, the Ru-Ru distance in **1** (2.8180(3) Å) is longer than that observed in Cp₂Ru₂(CO)₂(μ -CO)₂ (2.735(2) Å). This difference is partially due to the preference of the carbonyl ligands in **1** for an all-terminal arrangement that favors a longer Ru-Ru distance which also relieves the strain in the folded (η^5 -C₅H₃)₂(SiMe₂)₂ ligand. Avoidance of nonbonding contacts between the carbonyl ligands is probably also responsible for elongation of the Ru-Ru bond and for the staggered conformation of the CO ligands in **1**. It is worth noting that (η^5 , η^5 -Fulvalene)Ru₂(CO)₄ adopts an eclipsed conformation of the CO ligands, presumably, because the twist around the Ru-Ru axis would lead to an energetically unfavorable further elongation of the Ru-Ru bond and/or to an increase in the non-planarity of the (η^5 , η^5 -Fulvalene) ligand. The Ru-Ru separation in **1** is also greater than that reported for the bis(cyclopentadienyl)methane complex (η^5 , η^5 -C₅H₄CH₂C₅H₄)Ru₂(CO)₄ (2.766 (1) Å),⁸ perhaps a more appropriate comparison because it contains exclusively terminal carbonyl ligands and exhibits a

staggered arrangement of carbonyl ligands.

Substitution of a CO in 1 by Phosphines. Complex **1** reacts at 200 °C with phosphines PR_3 ($\text{R} = \text{Me}, \text{Cy}, \text{Ph}$) to give monosubstituted complexes of the type $\{(\eta^5\text{-C}_5\text{H}_3)_2(\text{SiMe}_2)_2\}\text{Ru}_2(\text{CO})(\mu\text{-CO})_2(\text{PR}_3)$ (**2a-c**) (Scheme 2). No disubstituted products were observed. Also, it is worth noting that the same reaction did not give the clean formation of **2a** under UV photolysis conditions. The IR spectra of the compounds **2a-c** exhibit $\nu(\text{CO})$



Scheme 2

bands at $1934\text{-}1872\text{ cm}^{-1}$ and $1805\text{-}1778\text{ cm}^{-1}$ which are consistent with the presence of terminal and bridging CO ligands. The additional electron density provided by the PR_3 ligands is presumably responsible for the CO-bridged structure of **2a-c** as compared with the unbridged structure of **1**. The molecular structure of **2a** determined by X-ray diffraction (Figure 2, Table 1) shows an almost symmetrical disposition of the bridging CO ligands, which are responsible for the shorter Ru(1)-Ru(2) distance ($2.6579(2)\text{ \AA}$) compared to that observed in **1** ($2.8180(3)\text{ \AA}$), and, surprisingly, to that observed in $\text{Cp}_2\text{Ru}_2(\text{CO})(\mu\text{-$

CO)₂(PMe₃) (2.722(2) Å).⁹ The shorter Ru(1)-Ru(2) distance in **2a** may also be favored by the doubly-linked (η^5 -C₅H₃)₂(SiMe₂)₂ ligand which adopts a smaller \angle Cp-Cp fold angle (119.0°), compared to that (122.86°) in complex **1**, which relieves unfavorable steric interactions between the bridging CO ligands and the equatorial SiMe₂ methyl groups. This argument is also supported by the smaller dihedral angle between the Ru(1)-C(7)-Ru(2) and Ru(1)-C(8)-Ru(2) planes (130.5°), compared to that found in Cp₂Ru₂(CO)(μ -CO)₂(PMe₃) (155.5°). The Ru(2)-C(7) and Ru(2)-C(8) distances (1.992(2) Å, 1.998(2) Å) are shorter than the Ru(1)-C(7) and Ru(1)-C(8) distances (2.104(2) Å, 2.088(2) Å) as expected for the more electron-rich Ru(2) center. There is no twist around Ru-Ru bond as indicated by torsion angles \angle Cp(centroid)-Ru(1)-Ru(2)-Cp(centroid) (0.1°) and \angle C(6)-Ru(1)-Ru(2)-P (0.5°).

Reactions of $\{(\eta^5\text{-C}_5\text{H}_3)_2(\text{SiMe}_2)_2\}\text{Ru}_2(\text{CO})_4$ (1**) with Halogens. Synthesis of $\{(\eta^5\text{-C}_5\text{H}_3)_2(\text{SiMe}_2)_2\}\text{Ru}_2(\text{CO})_4(\text{X})_2$ (**3a-c**) and $[\{(\eta^5\text{-C}_5\text{H}_3)_2(\text{SiMe}_2)_2\}\text{Ru}_2(\text{CO})_4(\mu\text{-X})]^+\text{TfO}^-$ (**4a-c**).** It is well-known¹⁰ that the dimeric Cp'₂M₂(CO)₄ (M = Fe, Ru, Os) complexes react with halogens (X₂) to give metal (II) halide carbonyl complexes Cp'M(CO)₂X. Similarly, complex **1** reacts with X₂ (X = Cl, Br, I) in CH₂Cl₂ at room temperature to give complexes **3a-c** (Scheme 2) (71-85% yield), which were isolated as yellow air-stable solids. Their IR spectra in hexanes solutions show the expected two strong $\nu(\text{CO})$ absorptions in the ranges 2052-2060 cm⁻¹ and 2000-2006 cm⁻¹. Their ¹H NMR spectra at room temperature show a doublet and a triplet in the range δ 5.21-5.49 ppm for the protons of each cyclopentadienyl ring, consistent with an ABB' spin system. This pattern remains unchanged at low temperature (-50 °C). An X-ray structural determination of **3c** shows (Figure 3, Table 1) that

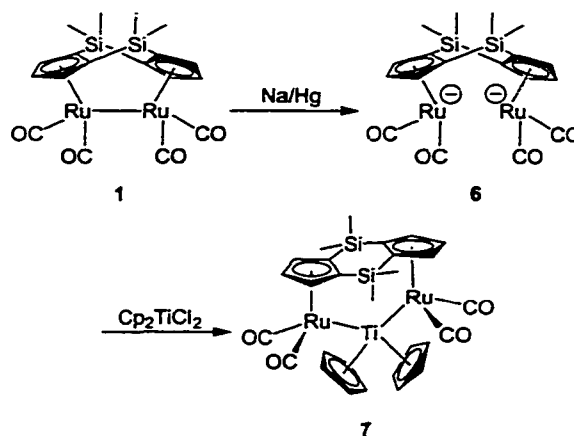
the asymmetric unit contains *three* different molecules. In each of these molecules the Ru atoms exhibit a three-legged piano-stool geometry. The most interesting feature of the structure is the almost flat conformation of the $(\eta^5\text{-C}_5\text{H}_3)_2(\text{SiMe}_2)_2$ ligand ($\angle\text{Cp-Cp}$ fold angle = 175.9°), which is consistent with the long Ru-Ru nonbonding distance (4.9762 Å). The cyclopentadienyl rings of the bridging ligand are slightly twisted with respect to each other, which is evident in the torsion angle $\angle\text{Cp}(\text{centroid})\text{-Ru}(1)\text{-Ru}(2)\text{-Cp}(\text{centroid})$ (5.3°). This twist may reflect steric repulsions between the cisoid $\text{Ru}(\text{CO})_2\text{X}$ units.

The halide-bridged cationic complexes $\{\text{Cp}_2\text{Ru}_2(\text{CO})_4(\mu\text{-X})\}^+$ can be isolated from aromatic solvents as intermediates from reactions of $\text{Cp}_2\text{Ru}_2(\text{CO})_4$ and halogens (X_2) in the presence of large counterions.¹¹ Although we did not observe similar intermediates in the reactions of **1** with halogens, the corresponding cationic, halide-bridged complexes $[\{(\eta^5\text{-C}_5\text{H}_3)_2(\text{SiMe}_2)_2\}\text{Ru}_2(\text{CO})_4(\mu\text{-X})\text{]}^+\text{TfO}^-$ (**4a-c**) were readily accessible as air-stable solids (65-82% yield) by the reaction of complex **1** and X_2 ($\text{X} = \text{Cl}, \text{Br}, \text{I}$) in the presence of a large excess of AgTfO at room temperature. It is worth mentioning that, in contrast to the corresponding mono-linked ($[\{(\eta^5\text{-C}_5\text{H}_4)_2(\text{SiMe}_2)\}\text{Ru}_2(\text{CO})_4(\mu\text{-X})\text{]}^+$)¹² and non-linked ($\{\text{Cp}_2\text{Ru}_2(\text{CO})_4(\mu\text{-X})\}^+$)¹⁰ Ru complexes, compounds **4a-c** do not react with an excess of AgTfO further in acetonitrile to give dicationic complexes $[\{(\eta^5\text{-C}_5\text{H}_3)_2(\text{SiMe}_2)_2\}\text{Ru}_2(\text{CO})_4(\text{MeCN})_2\text{]}^{+2}$; this indicates an unusual stability of the bridging halide in the complexes with the doubly-linked $(\eta^5\text{-C}_5\text{H}_3)_2(\text{SiMe}_2)_2$ ligand. The ^1H NMR spectra of **4a-c** show a doublet and a triplet (AB_2 spin system) for the equivalent cyclopentadienyl rings and two singlets for the methyl groups in the SiMe_2 groups of the ligand, as expected for a symmetrical structure.

Insertion of SnCl₂ into the Ru-Ru Bond in 1. Stannous chloride (SnCl₂) has been reported¹³ to react with Cp₂M₂(CO)₄ (M = Fe, Ru) complexes to give products Cp₂M₂(CO)₄(μ-SnCl₂) in which the Sn inserts into the M-M bond. When **1** and SnCl₂ are refluxed in THF for 30 h, {(η⁵-C₅H₃)₂(SiMe₂)₂}Ru₂(CO)₄(μ-SnCl₂) (**5**) is obtained in 74% yield as an air-stable yellow crystalline solid. The ¹H NMR spectrum of **5** shows a doublet and a triplet at δ 5.58, 5.64 ppm for the protons in the equivalent cyclopentadienyl rings and two singlets for the different CH₃ protons in the SiMe₂ groups. The IR spectrum exhibits three strong ν(CO) bands in the 1986-2038 cm⁻¹ region. A single crystal X-ray structural determination (Figure 4, Table 1) of **5** shows that *three* different molecules are present in the asymmetric unit. In all three molecules, each Ru has a three-legged piano-stool structure. The Ru-Sn bond distances are almost identical in all three molecules (2.6034(4)-2.6066(4) Å). The presence of the bridging SnCl₂ ligand leads to a Ru-Ru distance of 4.625 Å, much longer than that (2.8180(3) Å) in complex **1** but shorter than that (4.9762 Å) in **3c**. The long Ru-Ru distance in **5** leads to a Cp-Cp fold angle that is significantly larger (171.1°) than that (122.86°) in complex **1**, but smaller than that (175.9°) in **3c**. The twist around the Ru-Ru axis is minimal, which is reflected in the small ∠Cp(centroid)-Ru(1)-Ru(2)-Cp(centroid) torsion angle (3.1°).

Generation of [(η⁵-C₅H₃)₂(SiMe₂)₂}Ru₂(CO)₄]²⁻ (6**) and Synthesis {(η⁵-C₅H₃)₂(SiMe₂)₂}Ru₂(CO)₄{μ-Ti(η⁵-C₅H₅)₂} (**7**).** It is known¹⁰ that the dimeric Cp'₂Ru₂(CO)₄ complexes react with Na amalgam to give anionic complexes Cp'₂Ru(CO)₂⁻, which can react with various electrophiles (MeI, Me₃SnCl, etc.). The related anionic complex [(η⁵-C₅H₃)₂(SiMe₂)₂}Ru₂(CO)₄]²⁻ (**6**) was generated *in situ* from the reaction of **1**

with Na/Hg but was too reactive to be isolated. However, **6** reacts with 1 equiv of $(\eta^5\text{-C}_5\text{H}_5)_2\text{TiCl}_2$ at room temperature in THF to give $\{(\eta^5\text{-C}_5\text{H}_5)_2(\text{SiMe}_2)_2\}\text{Ru}_2(\text{CO})_4\{\mu\text{-Ti}(\eta^5\text{-C}_5\text{H}_5)_2\}$ (**7**) (Scheme 3; 53%), which was isolated as extremely moisture-sensitive pale-yellow crystals. The $\nu(\text{CO})$ bands of **7** at 1938, 1876 cm^{-1} are shifted to lower energy from the corresponding bands (2025, 1967 cm^{-1}) of **1**, as expected for complexes of this type,

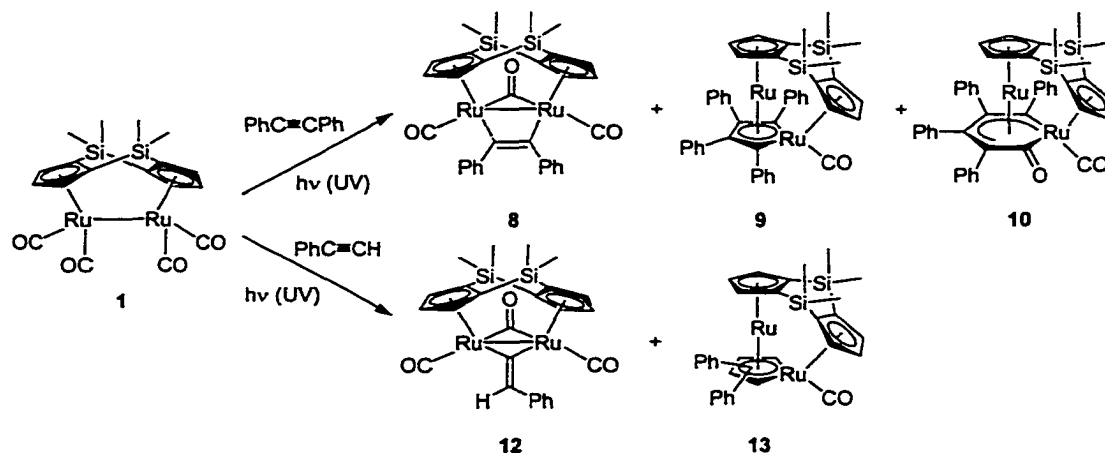


Scheme 3

for example $(\eta^5\text{-C}_5\text{H}_5)_2\text{Ru}_2(\text{CO})_4\{\mu\text{-Zr}(\eta^5\text{-C}_5\text{H}_5)_2\}$.¹⁴ The two Ti-Cp groups are equivalent in the ^1H NMR spectrum. Unfortunately, we were unable to obtain X-ray quality crystals of (**7**).

Reaction of $\{(\eta^5\text{-C}_5\text{H}_5)_2(\text{SiMe}_2)_2\}\text{Ru}_2(\text{CO})_4$ (1**) with diphenylacetylene. Synthesis of $\{(\eta^5\text{-C}_5\text{H}_5)_2(\text{SiMe}_2)_2\}\text{Ru}_2(\text{CO})_2(\mu\text{-CO})\{\eta^1:\eta^1\text{-}\mu_2\text{-C}(\text{Ph})\text{C}(\text{Ph})\}$ (**8**), $\{(\eta^5\text{-C}_5\text{H}_5)_2(\text{SiMe}_2)_2\}\text{Ru}_2(\text{CO})\{\eta^2:\eta^4\text{-}\mu_2\text{-C}(\text{Ph})\text{C}(\text{Ph})\text{C}(\text{Ph})\text{C}(\text{Ph})\}$ (**9**) and $\{(\eta^5\text{-C}_5\text{H}_5)_2(\text{SiMe}_2)_2\}\text{Ru}_2(\text{CO})\{\eta^2:\eta^4\text{-}\mu_2\text{-C}(\text{=O})\text{C}(\text{Ph})\text{C}(\text{Ph})\text{C}(\text{Ph})\text{C}(\text{Ph})\}$ (**10**). Ultraviolet irradiation of a benzene solution containing **1** and 4 equivalents of diphenylacetylene for 25 h produces the bimetallic Ru complexes **8**, **9** and **10** (Scheme 4), which were successfully separated by chromatography.**

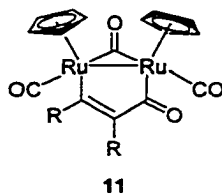
There was no evidence for the formation of a $\{(\eta^5\text{-C}_5\text{H}_3)_2(\text{SiMe}_2)_2\}$ -based diruthenacyclopentenone analogous to **11**, which is obtained upon photolysis of



Scheme 4

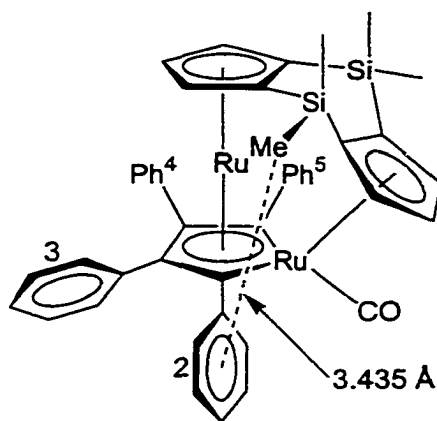
$\text{Cp}_2\text{Ru}_2(\text{CO})_4$ in the presence of alkynes (e.g. mono- and diphenylacetylene).¹⁵

Complex **8**, which was obtained as dark-red, air-sensitive crystals, was identified by characteristic patterns in its ^1H NMR and IR spectra, which are similar to those of the known analogous complexes $\{(\eta^5\text{-C}_5\text{H}_4)_2(\text{CMe}_2)\}\text{Ru}_2(\text{CO})_2(\mu\text{-CO})\{\eta^1:\eta^1\text{-}\mu_2\text{-C(Ph)C(Ph)}\}$ and $\{(\eta^5\text{-C}_5\text{H}_4)_2\}\text{Ru}_2(\text{CO})_2(\mu\text{-CO})\{\eta^1:\eta^1\text{-}\mu_2\text{-C(Ph)C(Ph)}\}$.¹⁶ In the ^1H NMR spectrum, the presence of



three signals in the cyclopentadienyl region and four signals corresponding to the $\text{Si}(\text{CH}_3)_2$ methyl groups are consistent with the proposed structure of **8**. Its IR spectrum ($\nu(\text{CO})$: 1983, 1935 and 1753 cm^{-1}) indicates the presence of both terminal and bridging CO ligands.

Complex **9** is an air-stable orange crystalline solid that is soluble in benzene and CH_2Cl_2 and moderately soluble in non-polar solvents (hexanes). The IR spectrum of **9** in hexanes shows only one sharp $\nu(\text{CO})$ band at 1969 cm^{-1} which corresponds to the terminal CO ligand coordinated to one of the Ru atoms. The ^1H NMR spectrum of **9** exhibits resonances for the inequivalent Cp rings (each displays a unique ABB' splitting pattern) and two signals for the $\text{Si}(\text{CH}_3)_2$ methyl groups at δ -0.62 and 0.36. The δ -0.62 signal is approximately 0.7 ppm upfield from the typical $\text{Si}(\text{CH}_3)_2$ region and indicates a pronounced shielding of the equatorial methyl groups by the nearby phenyl rings. The X-ray structure of **9** (Figure 5, Table 1), which is discussed in more detail below, confirms a close non-bonding interaction (3.435 \AA) between the SiMe_2 equatorial methyl groups and the π -systems of phenyl groups 2 and 5.



The variable-temperature ^1H NMR spectrum of **9** in CD_2Cl_2 in the aromatic region is shown in Figure 6. At $-50\text{ }^\circ\text{C}$, the spectrum consists of ten (δ 6.42, 6.58, 6.65, 6.77, 6.83, 6.88, 7.03, 7.09, 7.12, 7.62) well-resolved resonances of equal intensity. As the temperature is increased to $-20\text{ }^\circ\text{C}$, four of the ten resonances (δ 6.58, 6.77, 7.09, 7.62) coalesce to a single broad resonance, which is almost indistinguishable from the base line. At $+25\text{ }^\circ\text{C}$ a

new broad signal is observed at δ 7.25 ppm and the signal at δ 6.88 ppm gains intensity and broadens, while the other five resonances at δ 7.12, 7.03, 6.83, 6.65 and 6.42 remain virtually unchanged. We can assign the latter set of five resonances to the equivalent phenyl rings 2 and 5 adjacent to the Ru atoms, which are not fluxional with respect to rotation around the C(2 or 5)-phenyl bond in the -50 to +25 °C temperature range. An ^1H - ^1H COSY experiment demonstrates the mutual coupling of these 5 signals, and an NOE experiment indicates the presence of a weak through-space interaction between the equatorial SiMe_2 methyl groups and phenyl rings 2 and 5. Broad resonances at δ 7.25 and 6.88 ppm (+25 °C) are assigned to the ortho and meta protons of the equivalent phenyl groups 3 and 4, indicating fluxionality at room temperature on the NMR time scale. The simplest explanation for the temperature-dependent appearance of phenyl groups 3 and 4 in the ^1H NMR spectra is the lack of free rotation around the C(3 or 4)-phenyl bond at -50 °C, when five signals are observed. As the temperature is increased to +25 °C, this rotational motion becomes semi-restricted. Further sharpening of resonances at δ 7.25 and 6.88 ppm in the ^1H NMR spectra was observed at temperatures up to +50 °C.

In the molecular structure of **9** (Figure 5, Table 1), there is an approximate (non-crystallographic) mirror plane containing Ru(1), Ru(2) and the centroids of the two Cp rings. The Ru(1)-Ru(2) distance is 2.6221(6) Å, corresponding to a single Ru-Ru bond. The two ruthenium atoms are bridged by a $\{\eta^2:\eta^4-\mu_2-\text{C}(\text{Ph})\text{C}(\text{Ph})\text{C}(\text{Ph})\text{C}(\text{Ph})\}$ fragment, the ends of which are σ -bonded to Ru(1), forming a metallacyclopentadiene ring. The Ru(1)-C(2) and Ru(1)-C(5) distances of 2.100(4) and 2.096(4) Å are consistent with Ru-C single bonds, as are the Ru(2)-C(2) and Ru(2)-C(5) lengths of 2.133(5) and 2.130(4) Å. The Ru(1)-C(2)-

C(3)-C(4)-C(5) ring may be viewed as being π -bound to Ru(2), but this bonding does not result in the geometry observed for other related dinuclear complexes, such as $(\eta^2\text{-MeCCMe})\text{W}_2(\text{OPr}^i)_5(\mu_2\text{-OPr}^i)(\eta^2:\eta^4\text{-}\mu_2\text{-C}_4\text{Me}_4)$, which contain planar rings.¹⁷ Instead, the Ru(1)-C(2)-C(3)-C(4)-C(5) ring is puckered, with Ru(1) lying 0.41 Å out of the least-squares plane defined by carbon atoms C(2)-C(5) and away from Ru(2). The angle between the C(2)-C(3)-C(4)-C(5) and Ru(1)-C(2)-C(5) planes is 166.78°. The mean plane of the C(2)-C(3)-C(4)-C(5) fragment is nearly parallel ($\angle\text{Cp}(\text{centroid})\text{-Ru(2)-Ruthenacyclopentadiene}(\text{Ru(1), C(2)-C(5)})(\text{centroid}) = 172.17^\circ$) to the plane of the cyclopentadienyl ring bound to Ru(2), giving Ru(2) a pseudo-metallocene coordination environment. The phenyl groups C(31)-C(36) and C(41)-C(46) are almost orthogonal to the C(2)-C(3)-C(4)-C(5) plane (76.4° and 80.6°), while the phenyl groups C(21)-C(26) and C(51)-C(56) have tilt angles of 50.7° and 51.5° due to close through-space interactions with the equatorial methyl groups of the SiMe₂ linkers. Structural features of **9** are similar to those of other dinuclear ruthenacyclopentadiene complexes $(\eta^5\text{-C}_5\text{Me}_5)\text{Cl}_2\text{Ru}_2(\eta^2:\eta^4\text{-}\mu_2\text{-C}_4\text{H}_4)(\eta^5\text{-C}_5\text{Me}_5)$ ¹⁸, $(\eta^5\text{-C}_5\text{Me}_5)(\text{CO})\text{Ru}\{\eta^2:\eta^4\text{-}\mu_2\text{-C}(\text{Tol})\text{CHC}(\text{Tol})\text{CH}\}\text{Co}(\text{CO})_2$ ¹⁹ and $[(\eta^5\text{-C}_5\text{Me}_5)(\text{MeCN})\text{Ru}(\eta^2:\eta^4\text{-}\mu_2\text{-C}_4\text{H}_2\text{Ph}_2)\text{Ru}(\eta^5\text{-C}_5\text{Me}_5)](\text{CF}_3\text{SO}_3)$.²⁰

Spectroscopic and structural features of $\{(\eta^5\text{-C}_5\text{H}_3)_2(\text{SiMe}_2)_2\}\text{Ru}_2(\text{CO})\{\eta^2:\eta^4\text{-}\mu_2\text{-C}(=\text{O})\text{C}(\text{Ph})\text{C}(\text{Ph})\text{C}(\text{Ph})\text{C}(\text{Ph})\}$ (**10**) are similar to those of complex **9**. Compound **10** differs from **9** only by the insertion of a CO group into a Ru(1)-C(2 or 5) bond of **9**. This leads to the lack of the mirror plane, that was present in complex **9**. As a result of the lower symmetry, the ¹H NMR spectrum of **10** exhibits resonances for the inequivalent Cp rings (each displays a unique ABC splitting pattern) and four signals for the Si(CH₃)₂ methyl

groups at δ -1.00, 0.31, 0.36 and 0.57. The upfield signal indicates shielding of an equatorial methyl group by a nearby phenyl ring. The X-ray structure of **10** (Figure 7, Table 1) supports this close non-bonding interaction (3.476 Å) between the equatorial methyl C(10) and the plane of phenyl ring C(51)-C(56). The η^5 binding mode of the ruthenacyclohexadienone fragment to Ru(2) is supported by a long C(1)-C(2) bond (1.482(6) Å) compared to the C-C bonds in the delocalized C(2)-C(3)-C(4)-C(5) (1.444(5), 1.431(5), 1.431(5) Å) π -system and a non-bonding Ru(1)-C(1) distance (2.796 Å). The conformation of the ruthenacyclohexadienone Ru(1)-C(1)-C(2)-C(3)-C(4)-C(5) ring (Figure 8) cannot be described simply because of significant out-of-plane deviations of each atom; the smallest dihedral angle in the Ru(1)-C(1)-C(2)-C(3)-C(4)-C(5) ring is \angle C(2)-C(3)-C(4)-C(5) (10.3°). The IR spectrum of **10** in hexanes shows one sharp CO band at 1973 cm^{-1} which corresponds to the terminal CO ligand coordinated to Ru(1) and a weak broad band at 1601 cm^{-1} which may be assigned to the acyl CO group in the ruthenacyclohexadienone fragment.

Reaction of $\{(\eta^5\text{-C}_5\text{H}_3)_2(\text{SiMe}_2)_2\}\text{Ru}_2(\text{CO})_4$ (1**) with Phenylacetylene. Synthesis of $\{(\eta^5\text{-C}_5\text{H}_3)_2(\text{SiMe}_2)_2\}\text{Ru}_2(\text{CO})_2(\mu\text{-CO})(\mu\text{-C}=\text{CHPh})$ (**12**) and $\{(\eta^5\text{-C}_5\text{H}_3)_2(\text{SiMe}_2)_2\}\text{Ru}_2(\text{CO})\{\eta^2:\eta^4\text{-}\mu_2\text{-C(H)C(Ph)C(H)C(Ph)}\}$ (mixture of isomers) (**13**).**

Ultraviolet irradiation of a solution containing **1** and 4 equivalents of phenylacetylene (Scheme 4) in benzene solvent yields a mixture of products, which were identified as complexes **12** and **13** on the basis of spectral evidence. In contrast, ultraviolet irradiation of $\text{Cp}_2\text{Ru}_2(\text{CO})_4$ and phenylacetylene gives exclusively a complex of type **11** (R, R = H, Ph), which undergoes thermal (110 °C, toluene) rearrangement to the bridging vinylidene complex $\text{Cp}_2\text{Ru}_2(\text{CO})_2(\mu\text{-CO})(\mu\text{-C}=\text{CHPh})$.²¹ The structure of **12** (Figure 9, Table 1) was

conclusively established by an X-ray crystallographic analysis. The bridging μ -C=CHPh vinylidene ligand is planar (\angle Ru(1)-C(18)-C(19)-C(20) = 0.2°) and bound almost symmetrically to both Ru atoms (Ru(1)-C(18) = 2.049(6) Å; Ru(2)-C(18) = 2.028(7) Å). As in complex **2a**, the Ru(1)-Ru(2) distance (2.6551(7) Å) is shorter compared to that (2.696(1) Å) in the non-linked analog, complex Cp₂Ru₂(CO)₂(μ -CO)(μ -C=CH₂).²¹ The Cp-Cp fold angle (118.5°) is smaller compared to the same parameter (122.86°) for **1**. In fact the structures of **12** and **2a**, especially the geometries around the Ru atoms, are very similar.

In the ¹H NMR spectrum of **12**, the cyclopentadienyl hydrogens occur as six sets of well-resolved multiplets; in addition there are four singlet methyl resonances for the SiMe₂ groups, which are consistent with the symmetry of the solid-state molecule and indicate the absence of rotation around the C(18)-C(19) bond of the vinylidene ligand. In the IR spectrum of **12**, bands for both terminal (2008, 1982 cm⁻¹) and bridging (1819 cm⁻¹) carbonyl absorptions are evident.

We were unable to obtain X-ray quality crystals of **13** due in part to the fact that this compound is formed as a mixture of three geometrical isomers. However, the patterns in the ¹H NMR and IR spectra are very similar to those of complex **9**, which suggests that **13** has the structure shown in Scheme 4. Attempts to isolate individual isomers of **13** by means of column chromatography were unsuccessful.

Conclusions

In summary, the dinuclear ruthenium complex $\{(\eta^5\text{-C}_5\text{H}_3)_2(\text{SiMe}_2)_2\}\text{Ru}_2(\text{CO})_4$ (**1**) is a precursor for the synthesis of a variety of new dinuclear ruthenium complexes, in which the bridging $(\eta^5\text{-C}_5\text{H}_3)_2(\text{SiMe}_2)_2$ ligand controls the geometry of the final product. This influence is particularly pronounced in the reactions of **1** and phenylacetylenes which give (Scheme 4) the unexpected complexes $\{(\eta^5\text{-C}_5\text{H}_3)_2(\text{SiMe}_2)_2\}\text{Ru}_2(\text{CO})\{\eta^2:\eta^4\text{-}\mu_2\text{-C(Ph)C(Ph)C(Ph)C(Ph)}\}$ (**9**), $\{(\eta^5\text{-C}_5\text{H}_3)_2(\text{SiMe}_2)_2\}\text{Ru}_2(\text{CO})\{\eta^2:\eta^4\text{-}\mu_2\text{-C(=O)C(Ph)C(Ph)C(Ph)C(Ph)}\}$ (**10**) and $\{(\eta^5\text{-C}_5\text{H}_3)_2(\text{SiMe}_2)_2\}\text{Ru}_2(\text{CO})\{\eta^2:\eta^4\text{-}\mu_2\text{-C(H)C(Ph)C(H)C(Ph)}\}$ (**13**) as major products. It is apparent that the $(\eta^5\text{-C}_5\text{H}_3)_2(\text{SiMe}_2)_2$ ligand stabilizes these unique structural motifs, which were not reported for non-linked or mono-linked dicyclopentadienyl Ru complexes. The steric properties and rigidity of the bridging $(\eta^5\text{-C}_5\text{H}_3)_2(\text{SiMe}_2)_2$ ligand are presumably also responsible for the unusual inertness of the X⁻ ligand in the complexes $[\{(\eta^5\text{-C}_5\text{H}_3)_2(\text{SiMe}_2)_2\}\text{Ru}_2(\text{CO})_4(\mu\text{-X})]^+\text{TfO}^-$ (X = Cl, Br, I; **4a-c**) upon reaction with AgTfO. We have also demonstrated the robustness of the $(\eta^5\text{-C}_5\text{H}_3)_2(\text{SiMe}_2)_2$ ligand which remains unchanged in reactions of $\{(\eta^5\text{-C}_5\text{H}_3)_2(\text{SiMe}_2)_2\}\text{-Ru}_2(\text{CO})_4$ (**1**) with phosphines, halogens, SnCl₂, Na/Hg to give a variety of new dinuclear doubly-linked ruthenium (II) complexes.

Experimental Part

General Procedures. All reactions were performed under an argon atmosphere in reagent grade solvents, using standard Schlenk or dry-box techniques.²² Hexanes, methylene

chloride and diethyl ether were purified by the Grubbs method prior to use.²³ All other solvents were purified by published methods.²⁴ Chemicals were purchased from Aldrich Chemical Co., unless otherwise mentioned, or prepared by literature methods, as referenced below. Alumina (neutral, activity I, Aldrich) was degassed under vacuum for 12 h and treated with Ar-saturated water (7.5 % w/w). ¹H and ¹³C NMR spectra were recorded on a Bruker DRX-400 spectrometer using deuterated solvents as internal references. Solution infrared spectra were recorded on a Nicolet-560 spectrometer using NaCl cells with 0.1 mm spacers. Elemental analyses were performed on a Perkin Elmer 2400 series II CHNS/O analyzer.

All photochemical reactions were carried out in 60 or 300 mL quartz Schlenk photolysis tubes fitted with a coldfinger condenser (which is immersed in the reaction solution) and using a Hanovia 450 W medium pressure Hg lamp with a quartz jacket as the ultraviolet light source. The temperature of each reaction was controlled using an Isotemp 1013P refrigerated circulating bath (Fisher Scientific) with the circulating hoses connected to the coldfinger.

Synthesis of $\{(\eta^5\text{-C}_5\text{H}_3)_2(\text{SiMe}_2)_2\}\text{Ru}_2(\text{CO})_3(\text{PMe}_3)$ (2a**).** To a solution of **1** (30 mg; 0.05 mmol) in THF (1 mL) in a NMR tube was added PMe_3 (15 μL ; 0.15 mmol). The mixture was degassed, sealed under vacuum, heated to 200°C for 20 h, and cooled to room temperature; and the volatiles were removed under vacuum. The resulting orange residue was redissolved in THF (3 mL), and the solution was filtered through a short pad (3 cm) of alumina. Subsequent addition of hexanes (5 mL) and cooling (-20 °C) afforded crystalline **2a** (23 mg, 58%) as orange blades. ¹H NMR (400 MHz, C_6D_6): δ 0.14 (s, 6 H, Si(CH₃)), 0.42

(s, 6 H, Si(CH₃)), 1.58 (d, 9 H, *J*=9.5 Hz, P-CH₃), 4.48 (m, 2 H, Cp-*H*), 5.12 (m, 2 H, Cp-*H*), 5.23 (m, 1 H, Cp-*H*), 5.38 (m, 1 H, Cp-*H*). ¹³C NMR (100 MHz, C₆D₆): δ 1.03 (CH₃), 5.97 (CH₃), 24.3 (d, *J*=37.2 Hz, P-CH₃), 64.59, 85.76, 87.98, 91.76, 95.78, 101.27 (Cp), 202.45, 213.56 (CO). IR (hexanes): ν(CO) (cm⁻¹) 1926 (vs), 1889 (m), 1782 (m). Anal. Calcd for C₂₀H₂₇O₃PRu₂Si₂: C, 39.72; H, 4.50. Found: C, 39.38; H, 4.13.

Synthesis of {(η⁵-C₅H₃)₂(SiMe₂)₂}Ru₂(CO)₃(PCy₃) (2b). A solution of **1** (30 mg, 0.050 mmol) in THF (1 mL) was reacted with PCy₃ (48 mg, 0.17 mmol) at 200°C for 36 h, as in the preparation of **2a**. Two crystallizations of the resulting orange oil from THF-hexanes gave **2b** (29 mg, 74%) as orange prisms. ¹H NMR (400 MHz, C₆D₆): δ 0.15 (s, 6 H, Si(CH₃)), 0.33 (s, 6 H, Si(CH₃)), 1.03 (m, 18 H, P-Cy), 1.58 (m, 15 H, P-Cy), 4.39 (m, 2 H, Cp-*H*), 5.01 (m, 2 H, Cp-*H*), 5.12 (m, 1 H, Cp-*H*), 5.23 (m, 1 H, Cp-*H*). ¹³C NMR (100 MHz, C₆D₆): δ 0.93 (CH₃), 4.56 (CH₃), 20.21, 23.67, 31.56, 31.39, 32.67, 35.67, 41.02 (P-Cy), 64.32, 82.45, 83.88, 90.54, 93.23, 99.37 (Cp), 201.78, 213.01 (CO). IR (hexanes): ν(CO) (cm⁻¹) 1916 (vs), 1872 (m), 1778 (m).

Synthesis of {(η⁵-C₅H₃)₂(SiMe₂)₂}Ru₂(CO)₃(PPh₃) (2c). A solution of **1** (30 mg, 0.050 mmol) in THF (1 mL) was reacted with PPh₃ (60 mg, 0.23 mmol) at 200°C for 80 h, as in the preparation of **2a**. Two crystallizations of the resulting orange oil from THF-hexanes gave **2c** (25 mg, 67%) as orange crystals. ¹H NMR (400 MHz, C₆D₆): δ 0.14 (s, 6 H, Si(CH₃)), 0.38 (s, 6 H, Si(CH₃)), 4.89 (m, 2 H, Cp-*H*), 5.24 (m, 2 H, Cp-*H*), 5.38 (m, 1 H, Cp-*H*), 5.62 (m, 1 H, Cp-*H*), 7.04 (m, 15 H, Ph). IR (hexanes): ν(CO) (cm⁻¹) 1934 (vs), 1889 (m), 1805 (m).

Synthesis of {(η⁵-C₅H₃)₂(SiMe₂)₂}Ru₂(CO)₄(Cl)₂ (3a). A solution of Cl₂, prepared

by passing gaseous chlorine through CH₂Cl₂ (30 mL) for ~ 1 min, was added dropwise to a solution of complex **1** (120 mg, 0.22 mmol) in CH₂Cl₂ (60 mL). The reaction was monitored by IR spectroscopy and stopped when complex **1** was used up completely. The resulting solution was then concentrated at reduced pressure to ~5 mL, and hexanes (20 mL) was added to give complex **3a** (102 mg, 72%) as a yellow solid. ¹H NMR (400 MHz, CDCl₃): δ 0.24 (s, 6 H, Si(CH₃)), 0.59 (s, 6 H, Si(CH₃)), 5.34 (d, *J*=2.6 Hz, 4 H, Cp-*H*), 5.49 (t, *J*=2.6 Hz, 2 H, Cp-*H*). IR (hexanes): ν(CO) (cm⁻¹) 2060 (vs), 2006 (vs). Anal. Calcd for C₁₈H₁₈Cl₂O₄Ru₂Si₂: C, 34.45; H, 2.89. Found: C, 34.87; H, 2.81.

Synthesis of {(η⁵-C₅H₃)₂(SiMe₂)₂}Ru₂(CO)₄(Br)₂ (3b**).** By reacting Br₂ (~5% solution in CH₂Cl₂) with complex **1** (120 mg, 0.22 mmol) in CH₂Cl₂ (60 mL), **3b** (141 mg, 85%; yellow solid) was prepared using the same method as in the preparation of **3a**. ¹H NMR (400 MHz, CDCl₃): δ 0.21 (s, 6 H, Si(CH₃)), 0.60 (s, 6 H, Si(CH₃)), 5.21 (d, *J*=2.6 Hz, 4 H, Cp-*H*), 5.42 (t, *J*=2.6 Hz, 2 H, Cp-*H*). IR (hexanes): ν(CO) (cm⁻¹) 2058 (vs), 2004 (vs).

Synthesis of {(η⁵-C₅H₃)₂(SiMe₂)₂}Ru₂(CO)₄(I)₂ (3c**).** By reacting I₂ (~5% solution in CH₂Cl₂) with complex **1** (120 mg, 0.22 mmol) in CH₂Cl₂ (60 mL), **3c** (132 mg, 71%; yellow solid) was prepared using the same method as in the preparation of **3a**. ¹H NMR (400 MHz, CDCl₃): δ 0.27 (s, 6 H, Si(CH₃)), 0.56 (s, 6 H, Si(CH₃)), 5.32 (d, *J*=2.6 Hz, 4 H, Cp-*H*), 5.45 (t, *J*=2.6 Hz, 2 H, Cp-*H*). IR (hexanes): ν(CO) (cm⁻¹) 2052 (vs), 2000 (vs).

Synthesis of [{(η⁵-C₅H₃)₂(SiMe₂)₂}Ru₂(CO)₄(μ-Cl)]⁺TfO⁻ (4a**).** A yellow solution of **1** (175 mg, 0.31 mmol) and AgOTf (89 mg, 0.35 mmol) in CH₂Cl₂ (30 mL) was titrated with a solution of chlorine in CH₂Cl₂, prepared as described in the synthesis of **3a**. The reaction was followed by IR until the starting complex **1** disappeared. The resulting red-

brown suspension was filtered through a short pad of Celite, and the filtrate was layered with Et₂O (100 mL) to precipitate (**4a**) as bright-orange cubic crystals (199 mg, 85%). ¹H NMR (400 MHz, CD₂Cl₂): δ 0.65 (s, 6 H, Si(CH₃)), 0.69 (s, 6 H, Si(CH₃)), 5.08 (t, *J*=2.0 Hz, 2 H, Cp-*H*), 5.93 (d, *J*=2.0 Hz, 4 H, Cp-*H*). ¹³C NMR (100 MHz, CD₂Cl₂): δ -3.57 (CH₃), 0.02 (CH₃), 79.89, 94.76, 106.27 (Cp), 194.17, 204.95 (CO). IR (CH₂Cl₂): ν(CO) (cm⁻¹) 2077 (vs), 2069 (m), 2029 (s). Anal. Calcd for C₁₉H₁₈O₇ClF₃Ru₂SSi₂: C, 30.79; H, 2.45. Found: C, 30.68; H, 2.43.

Synthesis of [{(η⁵-C₅H₃)₂(SiMe₂)₂}Ru₂(CO)₄(μ-Br)]⁺TfO⁻ (4b**).** By reacting Br₂ (~5% solution in CH₂Cl₂) with complex **1** (175 mg, 0.31 mmol) and AgOTf (89 mg, 0.35 mmol) in CH₂Cl₂ (30 mL), **4b** (141 mg, 51%; orange solid) was prepared using the same method as in the preparation of **4a**. ¹H NMR (400 MHz, CD₂Cl₂): δ 0.60 (s, 6 H, Si(CH₃)), 0.68 (s, 6 H, Si(CH₃)), 5.11 (t, *J*=2.0 Hz, 2 H, Cp-*H*), 5.91 (d, *J*=2.0 Hz, 4 H, Cp-*H*). IR (CH₂Cl₂): ν(CO) (cm⁻¹) 2074 (vs), 2065 (m), 2026 (s).

Synthesis of [{(η⁵-C₅H₃)₂(SiMe₂)₂}Ru₂(CO)₄(μ-I)]⁺TfO⁻ (4c**).** By reacting I₂ (~5% solution in CH₂Cl₂) with complex **1** (175 mg, 0.31 mmol) and AgOTf (89 mg, 0.35 mmol) in CH₂Cl₂ (30 mL), **4c** (191 mg, 78%; orange solid) was prepared using the same method as in the preparation of **4a**. ¹H NMR (400 MHz, CD₂Cl₂): δ 0.59 (s, 6 H, Si(CH₃)), 0.66 (s, 6 H, Si(CH₃)), 5.13 (t, *J*=2.0 Hz, 2 H, Cp-*H*), 5.89 (d, *J*=2.0 Hz, 4 H, Cp-*H*). IR (CH₂Cl₂): ν(CO) (cm⁻¹) 2072 (vs), 2061 (m), 2025 (s).

Synthesis of *cis*-{(η⁵-C₅H₃)₂(SiMe₂)₂} (CO)₄(μ-SnCl₂) (5**).** A solution of **1** (200.0 mg, 0.31 mmol) and SnCl₂ (300 mg, 1.0 mmol) in THF (100 mL) was heated to reflux for 30 hours. The mixture was cooled to ambient temperature and chromatographed on an alumina

column (20 × 1 cm) first using hexanes as the eluent and then a 1:5 (v/v) mixture of CH₂Cl₂ and hexanes which eluted a yellow band containing **5** (193 mg, 74 %). ¹H NMR (400 MHz, CDCl₃): δ 0.36 (s, 6 H, Si(CH₃)), 0.58 (s, 6 H, Si(CH₃)), 5.58 (d, *J*=2.6 Hz, 4 H, Cp-*H*), 5.64 (t, *J*=2.6 Hz, 2 H, Cp-*H*). ¹³C NMR (100 MHz, CDCl₃): δ -0.52 (CH₃), 0.73 (CH₃), 88.09, 94.97, 95.26 (Cp), 196.95 (CO). IR (hexanes): ν(CO) (cm⁻¹) 2038 (s), 2023 (s), 1986 (vs), 1954 (w). Anal. Calcd for C₁₈H₁₈Cl₂O₄Ru₂Si₂Sn: C, 28.97; H, 2.43. Found: C, 28.95; H, 2.52.

Generation of [{(η⁵-C₅H₃)₂(SiMe₂)₂}Ru₂(CO)₄]²⁻ (6**) and Synthesis of {(η⁵-C₅H₃)₂(SiMe₂)₂}Ru₂(CO)₄{μ-Ti(η⁵-C₅H₅)₂} (**7**). A solution of **1** (100.0 mg, 0.18 mmol) in THF (50 mL) was added to Na/Hg (50 mg/2 mL) and THF (20 mL). After the mixture was stirred for 20 h at ambient temperature, the resulting yellow-green solution contained mainly [{(η⁵-C₅H₃)₂(SiMe₂)₂}Ru₂(CO)₄]²⁻ (**6**), as indicated by IR bands at 1928 (vs) and 1808 (vs) cm⁻¹. The solution was cannulated from the amalgam layer and added to a solution of (η⁵-C₅H₅)₂TiCl₂ (37 mg, 0.15 mmol) in THF (30 mL). The resulting solution was stirred for 1 h; volatiles were removed under reduced pressure and the residue was recrystallized from hexanes (20 mL) to give **7** as pale-yellow crystals (83 mg, 53 %). ¹H NMR (400 MHz, CDCl₃): δ 0.41 (s, 6 H, Si(CH₃)), 0.61 (s, 6 H, Si(CH₃)), 4.89 (br s, 10 H, Cp-*H*), 5.21 (m, 4 H, Cp-*H*), 5.42 (m, 2 H, Cp-*H*). IR (hexanes): ν(CO) (cm⁻¹) 1938 (vs), 1876 (vs).**

Reaction of {(η⁵-C₅H₃)₂(SiMe₂)₂}Ru₂(CO)₄ with diphenylacetylene. Synthesis of {(η⁵-C₅H₃)₂(SiMe₂)₂}Ru₂(CO)₂(μ-CO){η¹:η¹-μ₂-C(Ph)C(Ph)} (8**), {(η⁵-C₅H₃)₂(SiMe₂)₂}Ru₂(CO){η²:η⁴-μ₂-C(Ph)C(Ph)C(Ph)C(Ph)} (**9**) and {(η⁵-C₅H₃)₂(SiMe₂)₂}Ru₂(CO){η²:η⁴-μ₂-C(=O)C(Ph)C(Ph)C(Ph)C(Ph)} (**10**). The photolysis tube, equipped with a magnetic stir**

bar, was charged with **1** (200 mg, 0.36 mmol) and diphenylacetylene (140 mg, 0.79 mmol). Benzene (120 mL) was added, and the reaction tube was then fit with the coldfinger (10 °C) and an oil bubbler. A slow flow of argon was maintained through the solution using a teflon cannula while it was irradiated with stirring for 25 h. During this time the solution turned from yellow to red. Solvent was removed under vacuum; the resulting orange-brown residue was dissolved in hexanes (10 mL) and chromatographed on an alumina column (20 × 3 cm) with hexanes/CH₂Cl₂ (5:1) as the eluent. A yellow band was eluted and collected. Then, a pale-orange band was eluted with hexanes/CH₂Cl₂ (1:1). Finally, a red-orange band was eluted with hexanes/CH₂Cl₂ (1:20). After vacuum removal of the solvents from the above three eluates, the residues were recrystallized from hexanes (eluates 1 and 3) or hexanes/CH₂Cl₂ (1:1) (eluate 2) at -20°C. From the first fraction, 123 mg (58%, based on **1**) of orange crystalline **9** were obtained. ¹H NMR (400 MHz, C₆D₆): δ -0.62 (s, 6 H, Si(CH₃)), 0.36 (s, 6 H, Si(CH₃)), 4.89 (d, *J*=2.0 Hz, 2 H, Cp-*H*), 5.00 (d, *J*=2.0 Hz, 2 H, Cp-*H*), 5.52 (t, *J*=2.0 Hz, 1 H, Cp-*H*), 6.01 (t, *J*=2.0 Hz, 1 H, Cp-*H*), 6.52 (t, *J*=7.6 Hz, 2 H, Ph), 6.72 (t, *J*=7.6 Hz, 2 H, Ph), 6.82 (d, *J*=7.6 Hz, 2 H, Ph), 6.87 (br s, 12 H, Ph), 7.09 (t, *J*=7.6 Hz, 2 H, Ph), 7.31 (d, *J*=7.6 Hz, 2 H, Ph), 7.46 (br s, 8 H, Ph). ¹³C NMR (100 MHz, C₆D₆): δ -4.60 (CH₃), 8.13 (CH₃), 82.49, 85.71, 90.39, 92.41, 93.71, 104.49 (Cp), 121.08, 126.01, 126.42, 126.51, 126.62 (br), 127.79, 131.65, 132.98 (br), 135.05, 139.88, 152.26, 158.90 (Ph, C-Ph), 208.54 (CO). IR (hexanes): ν(CO) (cm⁻¹) 1969 (vs). Anal. Calcd for C₄₃H₃₈ORu₂Si₂·½C₅H₁₂: C, 63.17; H, 5.13. Found: C, 63.08; H, 5.16. From the second fraction, 27 mg (12%, based on **1**) of orange crystalline **8** were obtained. ¹H NMR (400 MHz, C₆D₆): δ 0.12 (s, 3 H, Si(CH₃)), 0.23 (s, 3 H, Si(CH₃)), 0.26 (s, 3 H, Si(CH₃)), 0.21 (s,

3 H, Si(CH₃)), 4.41 (m, 2 H, Cp-H), 4.89 (m, 2 H, Cp-H), 5.23 (m, 2 H, Cp-H), 6.56 (m, 4 H, Ph), 6.79 (m, 2 H, Ph), 6.91 (m, 4 H, Ph). IR (hexanes): $\nu(\text{CO})$ (cm⁻¹) 1983 (vs), 1935 (m), 1753 (m). From the third fraction, 41 mg (21%, based on 1) of red crystalline **10** were obtained. ¹H NMR (400 MHz, CDCl₃): δ -1.00 (s, 3 H, Si(CH₃)), 0.31 (s, 3 H, Si(CH₃)), 0.36 (s, 3 H, Si(CH₃)), 0.57 (s, 3 H, Si(CH₃)), 4.80 (m, 1 H, Cp-H), 5.18 (m, 1 H, Cp-H), 5.43 (m, 1 H, Cp-H), 5.89 (t, $J=2.2$ Hz, 1 H, Cp-H), 6.02 (m, 1 H, Cp-H), 6.89 (t, $J=2.2$ Hz, 1 H, Cp-H), 6.40-7.15 (complex array of signals, 19 H, Ph), 7.86 (d, $J=8.4$ Hz, 1 H, Ph). ¹³C NMR (100 MHz, C₆D₆): δ -4.42, -1.22, 6.76, 8.27 (CH₃), 63.21, 81.53, 86.78, 89.02, 89.06, 93.87, 96.93, 98.71, 98.78, 104.99 (Cp; 10 peaks), 110.19, 116.27, 117.20, 126.84, 125.90, 125.95, 126.00, 126.08, 126.49, 126.70, 127.36, 127.72, 131.33, 131.54, 132.47, 134.25, 134.99, 135.20, 139.88, 140.74, 141.95, 155.11, 175.58 (Ph, C-Ph; 23 out of 24 peaks), 203.10, 211.40 (CO, C(=O)-Ph). IR (hexanes): $\nu(\text{CO})$ (cm⁻¹) 1973 (vs), 1601 (w). Anal. Calcd for C₄₄H₃₈O₂Ru₂Si₂·½CH₂Cl₂: C, 59.42; H, 4.37. Found: C, 59.19; H, 4.59.

Reaction of $\{(\eta^5\text{-C}_5\text{H}_3)_2(\text{SiMe}_2)_2\}\text{Ru}_2(\text{CO})_4$ with phenylacetylene. Synthesis of $\{(\eta^5\text{-C}_5\text{H}_3)_2(\text{SiMe}_2)_2\}\text{Ru}_2(\text{CO})_3(\mu\text{-C}=\text{CHPh})$ (12**) and $\{(\eta^5\text{-C}_5\text{H}_3)_2(\text{SiMe}_2)_2\}\text{Ru}_2(\text{CO})\{\eta^2:\eta^4\text{-}\mu_2\text{-C}(\text{H})\text{C}(\text{Ph})\text{C}(\text{H})\text{C}(\text{Ph})\}$ (mixture of isomers) (**13**).**

The photolysis tube, equipped with a magnetic stir bar, was charged with **1** (200 mg, 0.36 mmol) and phenylacetylene (160 mg, 1.23 mmol). Benzene (120 mL) was added, and the reaction tube was then fitted with the coldfinger (10 °C) and an oil bubbler. A slow flow of argon was maintained through the solution using a teflon cannula while it was irradiated with stirring for 30 h. During this time the solution turned from yellow to red. Solvent was removed under vacuum; the resulting orange-brown residue was redissolved in hexanes (10

mL) and chromatographed on an alumina column (20 × 3 cm) with hexanes/CH₂Cl₂ (5:1) as the eluent. A yellow band was eluted and collected. Then, a pale-orange band was eluted with hexanes/CH₂Cl₂ (1:5). After vacuum removal of the solvents from the above two eluates, the residues were recrystallized from hexanes at -20°C. From the first fraction, 17 mg (8%, based on 1) of the orange oily solid **13** was obtained as a mixture of three isomers. The ¹H NMR (400 MHz, C₆D₆) spectrum displays a complicated pattern of signals due to the presence of three unique geometrical isomers (see Discussion). IR (hexanes): ν(CO) (cm⁻¹) 1977 (w), 1968 (vs). From the second fraction, 107 mg (72%, based on 1) of yellow crystalline **12** were obtained. ¹H NMR (400 MHz, CD₂Cl₂): δ 0.40 (s, 3 H, Si(CH₃)), 0.49 (s, 3 H, Si(CH₃)), 0.55 (s, 3 H, Si(CH₃)), 0.68 (s, 3 H, Si(CH₃)), 5.59 (m, 1 H, Cp-H), 5.61 (m, 1 H, Cp-H), 5.70 (m, 1 H, Cp-H), 5.73 (m, 1 H, Cp-H), 6.23 (m, 1 H, Cp-H), 6.37 (m, 1 H, Cp-H), 7.10 (m, 1 H, Ph), 7.30 (m, 2 H, Ph), 7.61 (s, 1 H, C=CPh-H), 7.62 (m, 2 H, Ph). ¹³C NMR (100 MHz, CD₂Cl₂): δ -3.27 (CH₃), -3.00 (CH₃), 2.64 (2 CH₃), 91.81, 92.07, 93.03, 94.21, 94.71, 95.50, 107.98, 108.03, 109.48, 110.125 (Cp), 125.44, 128.47, 138.68, 141.00 (Ph), 201.02, 202.11, 241.36 (CO), 247.42 (C=CPh-H). IR (hexanes): ν(CO) (cm⁻¹) 2008 (vs), 1982 (m), 1819 (m).

Crystallographic Structural Determination of 1. A yellow crystal of **1** with approximate dimensions 0.38 × 0.34 × 0.32 mm was selected under oil under ambient conditions and attached to the tip of a glass capillary. The crystal was mounted in a stream of cold nitrogen at 183(2) K and centered in the X-ray beam by using a video camera. The crystal evaluation and data collection were performed on a Bruker CCD-1000 diffractometer with Mo K_α (λ = 0.71073 Å) radiation and diffractometer to crystal distance of 5.08 cm. The

initial cell constants were obtained from three series of ω scans at different starting angles. Each series consisted of 20 frames collected at intervals of 0.3° in a 6° range about ω with an exposure time of 10 seconds per frame. A total of 93 reflections was obtained. Reflections were successfully indexed by an automated indexing routine in the SMART program. The final cell constants were calculated from a set of 5689 strong reflections from the actual data collection. The data were collected by using the hemisphere data collection routine. Reciprocal space was surveyed to the extent of 1.8 hemispheres to a resolution of 0.80 \AA . A total of 8075 data were harvested by collecting three sets of frames with 0.3° scans in ω with an exposure time of 20 sec per frame. These highly redundant datasets were corrected for Lorentz and polarization effects. The absorption correction was based on fitting a function to the empirical transmission surface as sampled by multiple equivalent measurements.²⁵

Systematic absences in the diffraction data were consistent with space groups Cc and C2/c, but only the latter centrosymmetric space group C2/c yielded chemically reasonable and computationally stable results in refinement.²⁶ A successful solution by direct methods provided most non-hydrogen atoms from the E-map. The remaining non-hydrogen atoms were located in an alternating series of least-squares cycles and difference Fourier maps. All non-hydrogen atoms were refined with anisotropic displacement coefficients. All hydrogen atoms were included in the structure factor calculation at idealized positions and were allowed to ride on the neighboring atoms with relative isotropic displacement coefficients. Each molecule occupies a crystallographic twofold axis. The final least-squares refinement of 120 parameters against 2063 data resulted in residuals R (based on F^2 for $I \geq 2\sigma$) and wR (based on F^2 for all data) of 0.0174 and 0.0457, respectively. The final difference Fourier

map was featureless.

X-ray data for complexes **2a**, **3c**, **5**, **9**, **10** and **12** were obtained in a similar manner.

Acknowledgment

This work was supported by the National Science Foundation through Grant No. CHE-9816342.

References

- (1) For general reviews of linked bis(cyclopentadienyl) organometallic complexes, see: (a) Barlow, S.; O'Hare, D. *Chem. Rev.* **1997**, *97*, 637. (b) Werner, H. *Inorg. Chim. Acta* **1992**, *198-200*, 715. (c) Bonifaci, C.; Ceccon, A.; Gambaro, A.; Mantovani, L.; Ganis, P.; Santi, S.; Venzo, A. *J. Organomet. Chem.* **1998**, *557*, 97. (d) Cuenca, T.; Royo, P. *Coord. Chem. Rev.* **1999**, *193-195*, 447. (e) Royo, P. *New J. Chem.* **1997**, *21*, 791.
- (2) (a) Gómez-García, R.; Royo, P. *J. Organomet. Chem.* **1999**, *583*, 86. (b) Cano, A.; Cuenca, T.; Gómez-Sal, P.; Royo, B.; Royo, P. *Organometallics* **1994**, *13*, 1688. (c) Corey, J. Y.; Huhmann, J. L.; Rath, N. P. *Inorg. Chem.* **1995**, *34*, 3203. (d) Cano, A. M.; Cano, J.; Cuenca, T.; Gómez-Sal, P.; Manzanero, A.; Royo, P. *Inorg. Chim. Acta* **1998**, *280*, 1.
- (3) (a) Amor, F.; Gómez-Sal, P.; de Jesús, E.; Royo, P.; Vázquez de Miguel, A. *Organometallics* **1994**, *13*, 4322. (b) Amor, F.; de Jesús, E.; Pérez, A. I.; Royo, P.; Vázquez de Miguel, A. *Organometallics* **1996**, *15*, 365. (c) Amor, F.; de Jesús, E.; Royo, P.; Vázquez de Miguel, A. *Inorg. Chem.* **1996**, *35*, 3440. (d) Galakhov, M. V.; Gil, A.; de Jesús, E.; Royo, P. *Organometallics* **1995**, *14*, 3746. (e) Amor, F.; Gómez-

- Sal, P.; de Jesús, E.; Martín, A.; Pérez, A. I.; Royo, P.; Vázquez de Miguel, A. *Organometallics* **1996**, *15*, 2103. (f) Calvo, M.; Galakhov, M. V.; Gómez-García, R.; Gómez-Sal, P.; Martín, A.; Royo, P.; Vázquez de Miguel, A. *J. Organomet. Chem.* **1997**, *548*, 157.
- (4) (a) Siemeling, U.; Jutzi, P.; Neumann, B.; Stammeler, H. G.; Hursthouse, M. B. *Organometallics* **1992**, *11*, 1328. (b) Hiermeier, J.; Koehler, F. H.; Mueller, G. *Organometallics* **1991**, *10*, 1787.
- (5) (a) Ovchinnikov, M. V.; Angelici, R. J. *J. Am. Chem. Soc.* **2000**, *122*, 6130. (b) Ovchinnikov, M. V.; Guzei, I. A.; Angelici, R. J. *Organometallics* **2001**, *20*, 691.
- (6) Boese, R.; Cammack, J. K.; Matzger, A. J.; Pflug, K.; Tolman, W. B.; Vollhardt, K. P. C.; Weidman, T. W. *J. Am. Chem. Soc.* **1997**, *119*, 6757.
- (7) Mills, D. S.; Nice, J. P. *J. Organomet. Chem.* **1967**, *9*, 339.
- (8) Knox, S. A. R.; Macpherson, K. A.; Orpen, A. G.; Rendle, M. C. *J. Chem. Soc., Dalton Trans.* **1989**, 1807.
- (9) Nataro, C.; Angelici, R. J. *Inorg. Chem.* **1998**, *37*, 2975.
- (10) Bennett, M. A.; Bruce, M. I.; Matheson, T. W. In *Comprehensive Organometallic Chemistry*, Wilkinson, G., Stone F. G. A., Abel, E. W., Eds., Pergamon Press: Oxford, New York 1982; Vol. 4, p. 821.
- (11) Haines, R. J.; duPreez, A. L. C. *J. Chem. Soc. Dalton Trans.* **1972**, 944.
- (12) Fröhlich, R.; Gimeno, J.; González-Cueva, M.; Lastra, E.; Borge, J.; García-Granda, S. *Organometallics* **1999**, *18*, 3008.

- (13) Zhang, Y.; Xu, S.; Tian, G.; Zhang, W.; Zhou, X. *J. Organomet. Chem.* **1997**, *544*, 43 and references therein.
- (14) Casey, C. P.; Jordan, R. F.; Rheinhold, A. L. *Organometallics* **1984**, *3*, 504.
- (15) (a) Albers, M. O.; Robinson, D. J.; Singleton, E. *Coord. Chem. Rev.* **1987**, *79*, 1. (b) Davies, D. L.; Dyke, A. F.; Knox, S. A. R.; Morris, M. J. *J. Organomet. Chem.* **1981**, *215*, C30
- (16) (a) Nelson, G. O.; Wright, M. E.; *J. Organomet. Chem.* **1981**, *206*, C21. (b) Knox, S. A. R.; Macpherson, K. A.; Orpen, A. G.; Rendle, M. C. *J. Chem. Soc. Dalton Trans.* **1989**, 1807.
- (17) (a) Chrisholm, M. H.; Hoffman, D. M.; Huffman, J. C. *J. Am. Chem. Soc.* **1984**, *106*, 6806. (b) Bruce, M. I.; Matison, J. G.; Skelton, B. W.; White, A. H. *J. Organomet. Chem.* **1983**, *251*, 249.
- (18) Champion, B. K.; Heyn, R. H.; Tilley, T. D. *Organometallics* **1990**, *9*, 1106.
- (19) Matsuzaka, H.; Ichikawa, K.; Ishioka, T.; Sato, H.; Okubo, T.; Ishii, T.; Yamashita, M.; Kondo, M.; Kitagawa, S. *J. Organomet. Chem.* **2000**, *596*, 121.
- (20) He, X. D.; Chaudret, B.; Dahan, F.; Huang, Y.-S. *Organometallics* **1991**, *10*, 970.
- (21) Colborn, R. E.; Davies, D. L.; Dyke, A. F.; Endesfelder, A.; Knox, S. A. R.; Orpen, A. G.; Plaas, D. *J. Chem. Soc. Dalton Trans.* **1983**, 2661.
- (22) Errington, R. J. *Advanced Practical Inorganic and Metalorganic Chemistry*, 1st ed.; Chapman & Hall: New York, 1997.
- (23) Pangborn, A. B.; Giardello, M. A.; Grubbs, R. H.; Rosen, R. K.; Timmers, F. J. *Organometallics* **1996**, *15*, 1518.

- (24) Perrin, D. D.; Armarego, W. L. F.; Perrin, D. R. *Purification of Laboratory Chemicals*, 2nd ed.; Pergamon: New York, 1980.
- (25) Blessing, R.H. *Acta Cryst.* **1995**, *A51*, 33-38.
- (26) All software and sources of the scattering factors are contained in the SHELXTL (version 5.1) program library (G. Sheldrick, Bruker Analytical X-Ray Systems, Madison, WI).

Table 1. Crystallographic Data for **1**, **2a**, **3c**, **5**, **9**, **10** and **12**.

	1	2a
formula	C ₁₈ H ₁₈ O ₄ Ru ₂ Si ₂	C ₂₀ H ₂₇ O ₃ PRu ₂ Si ₂ ·½C ₆ H ₁₄
fw	556.64	647.79
crystal syst	monoclinic	monoclinic
space group	<i>C2/c</i>	<i>P2₁/c</i>
<i>a</i> , Å	15.1911(9)	10.3672(4)
<i>b</i> , Å	10.1057(6)	17.6827(7)
<i>c</i> , Å	14.3573(9)	15.2779(6)
α , deg	90	90
β , deg	113.475(1)	109.273(1)
γ , deg	90	90
<i>V</i> , Å ³	2021.7(2)	2643.78(18)
<i>Z</i>	4	4
crystal color, habit	yellow block	yellow block
crystal size, mm	0.38 × 0.34 × 0.32	0.40 × 0.30 × 0.30
<i>D</i> (calcd), g cm ⁻³	1.829	1.627
wavelength, Å	0.71073	0.71073
μ (Mo, K α), mm ⁻¹	1.632	1.315
temp, K	293(2)	173(2)
diffractometer	Bruker CCD-1000	Bruker CCD-1000
abs cor	empirical	empirical
theta range	2.49 to 26.37°	1.82 to 26.37°
no. of rflns collected	8075	22306
no. of indep rflns	2063 [R(int) = 0.0181]	5374 [R(int) = 0.0208]
<i>R</i> (<i>F</i>) (<i>I</i> ≥ 2 σ (<i>I</i>)), %	R1 = 0.0174, wR2 = 0.0457	R1 = 0.0204, wR2 = 0.0532
R indices (all data)	R1 = 0.0197, wR2 = 0.0465	R1 = 0.0226, wR2 = 0.0541

Table 1. Continued.

	3c	5
formula	$C_{18}H_{18}I_2O_4Ru_2Si_2$	$C_{18}H_{18}Cl_2O_4Ru_2Si_2Sn$
fw	810.44	746.23
crystal syst	monoclinic	monoclinic
space group	$P2_1$	$P2_1/c$
a , Å	9.0042(4)	17.5165(10)
b , Å	39.9004(16)	17.0163(10)
c , Å	10.1932(4)	24.5775(14)
α , deg	90	90
β , deg	91.4325(10)	93.123(1)
γ , deg	90	90
V , Å ³	3661.0(3)	7314.8(7)
Z	6	12
crystal color, habit	yellow block	yellow block
crystal size, mm	0.40 × 0.35 × 0.30	0.45 × 0.40 × 0.40
D (calcd), g cm ⁻³	2.206	2.033
wavelength, Å	0.71073	0.71073
μ (Mo, $K\alpha$), mm ⁻¹	3.886	2.578
temp, K	173(2)	273(2)
diffractometer	Bruker CCD-1000	Bruker CCD-1000
abs cor	empirical	empirical
theta range	1.02 to 26.37°	1.16 to 28.28°
no. of rflns collected	30328	64369
no. of indep rflns	14717 [R(int) = 0.0309]	17373 [R(int) = 0.0448]
$R(F)$ ($I \geq 2\sigma(I)$), %	R1 = 0.0293, wR2 = 0.0570	R1 = 0.0301, wR2 = 0.0463
R indices (all data)	R1 = 0.0336, wR2 = 0.0615	R1 = 0.0615, wR2 = 0.0499

Table 1. Continued.

	9	10
formula	C ₄₃ H ₃₈ ORu ₂ Si ₂	C ₄₄ H ₃₈ O ₂ Ru ₂ Si ₂ ·½CH ₂ Cl ₂
fw	829.05	899.53
crystal syst	triclinic	triclinic
space group	$P\bar{1}$	$P\bar{1}$
<i>a</i> , Å	12.5711(16)	8.6733(14)
<i>b</i> , Å	12.7517(16)	12.709(2)
<i>c</i> , Å	12.7791(16)	35.391(6)
<i>α</i> , deg	99.449(2)	96.629(3)
<i>β</i> , deg	111.366(2)	96.898(3)
<i>γ</i> , deg	92.545(2)	93.476(3)
<i>V</i> , Å ³	1869.7(4)	3835.9(11)
<i>Z</i>	2	4
crystal color, habit	orange plate	dark red rod
crystal size, mm	0.36 × 0.12 × 0.04	0.55 × 0.12 × 0.06
<i>D</i> (calcd), g cm ⁻³	1.473	1.558
wavelength, Å	0.71073	0.71073
<i>μ</i> (Mo, K α), mm ⁻¹	0.904	0.957
temp, K	233(2)	293(2)
diffractometer	Bruker CCD-1000	Bruker CCD-1000
abs cor	empirical	empirical
theta range	1.74 to 23.00°	1.62 to 25.15°
no. of rflns collected	11583	28494
no. of indep rflns	5186 [R(int) = 0.0487]	13641 [R(int) = 0.0525]
<i>R</i> (<i>F</i>) (<i>I</i> ≥ 2 σ (<i>I</i>)), %	R1 = 0.0433, wR2 = 0.0732	R1 = 0.0412, wR2 = 0.0668
R indices (all data)	R1 = 0.0718, wR2 = 0.0784	R1 = 0.0818, wR2 = 0.0743

Table 1. Continued.

12	
formula	$C_{25}H_{24}O_3Ru_2Si_2 \cdot CH_2Cl_2$
fw	715.69
crystal syst	monoclinic
space group	$P2_1/c$
a , Å	18.8600(8)
b , Å	9.6259(5)
c , Å	15.3656(11)
α , deg	90
β , deg	92.119(1)
γ , deg	90
V , Å ³	2787.6(3)
Z	4
crystal color, habit	orange plate
crystal size, mm	0.43 × 0.35 × 0.03
D (calcd), g cm ⁻³	1.705
wavelength, Å	0.71073
μ (Mo, $K\alpha$), mm ⁻¹	1.387
temp, K	173(2)
diffractometer	Bruker CCD-1000
abs cor	empirical
theta range	2.38 to 25.00°
no. of rflns collected	9719
no. of indep rflns	4849 [R(int) = 0.0450]
$R(F)$ ($I \geq 2\sigma(I)$), %	R1 = 0.0474, wR2 = 0.0930
R indices (all data)	R1 = 0.0849, wR2 = 0.0993

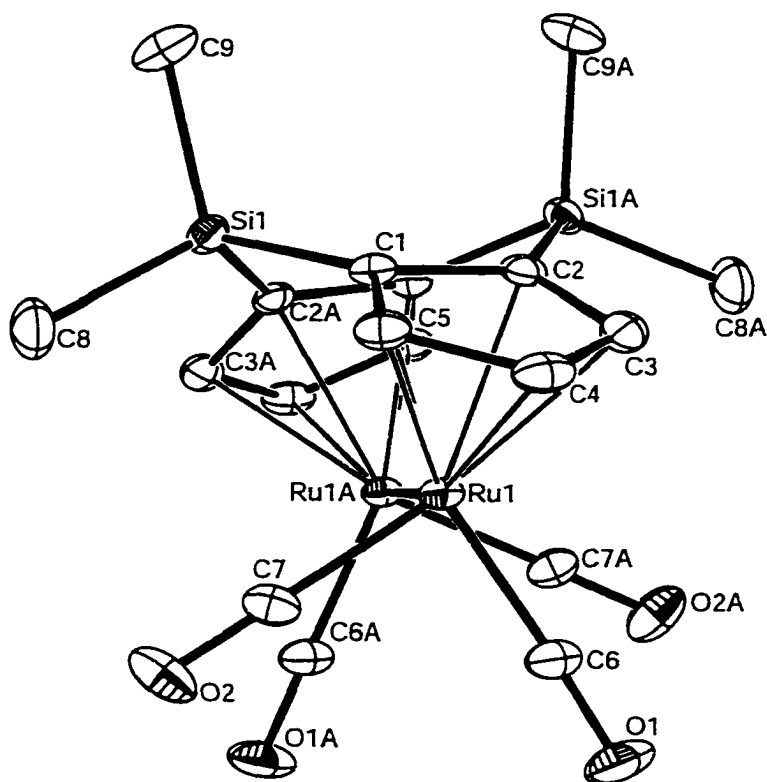


Figure 1. Thermal ellipsoid drawing of $\{(\eta^5\text{-C}_5\text{H}_3)_2(\text{SiMe}_2)_2\}\text{Ru}_2(\text{CO})_4$ (**1**) showing the labeling scheme and 30% probability ellipsoids; hydrogens are omitted for clarity. Selected bond distances (Å) and angles (deg) are as follows: Ru(1)-Ru(1A), 2.8180(3); Ru(1)-C(6), 1.868(2); Ru(1)-C(7), 1.854(2); Ru(1)-Cp(centroid), 1.907; $\angle\text{C}(6)\text{-Ru}(1)\text{-C}(7)$, 87.45(9); $\angle\text{Ru}(1\text{A})\text{-Ru}(1)\text{-C}(6)$, 93.04(7); $\angle\text{Ru}(1\text{A})\text{-Ru}(1)\text{-C}(7)$, 85.15(6); $\angle\text{Cp}(\text{centroid})\text{-Ru}(1)\text{-Ru}(1\text{A})\text{-Cp}(\text{centroid})$, 24.2; $\angle\text{C}(7)\text{-Ru}(1)\text{-Ru}(1\text{A})\text{-C}(6\text{A})$, 32.3; $\angle\text{Cp-Cp}$ fold angle, 122.86.

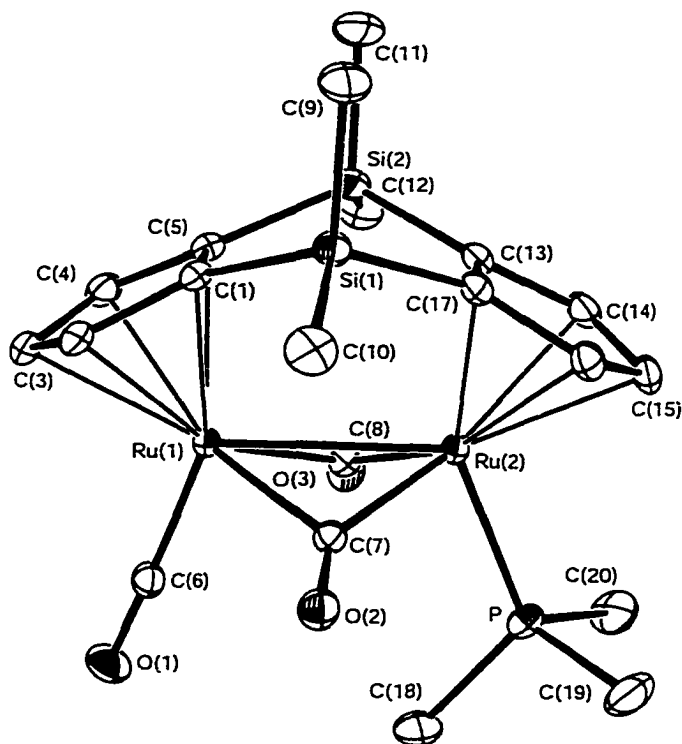


Figure 2. Thermal ellipsoid drawing of $\{(\eta^5\text{-C}_5\text{H}_3)_2(\text{SiMe}_2)_2\}\text{Ru}_2(\text{CO})(\mu\text{-CO})_2(\text{PMe}_3)$ (**2a**) showing the labeling scheme and 30% probability ellipsoids; hydrogens are omitted for clarity. Selected bond distances (Å) and angles (deg) are as follows: Ru(1)-Ru(2), 2.6579(2); Ru(1)-C(6), 1.848(2); Ru(1)-C(7), 2.104(2); Ru(1)-C(8), 2.088(2); Ru(2)-C(7), 1.992(2); Ru(2)-C(8), 1.998(2); Ru(2)-P, 2.2770(6); Ru(1)-Cp(centroid), 1.936(2); Ru(2)-Cp(centroid), 1.910; $\angle\text{C}(6)\text{-Ru}(1)\text{-C}(7)$, 86.45(9); $\angle\text{C}(6)\text{-Ru}(1)\text{-C}(8)$, 86.96(9); $\angle\text{C}(7)\text{-Ru}(1)\text{-C}(8)$, 84.78(8); $\angle\text{P-Ru}(2)\text{-C}(7)$, 85.98(6); $\angle\text{P-Ru}(2)\text{-C}(8)$, 86.27(6); $\angle\text{C}(7)\text{-Ru}(2)\text{-C}(8)$, 90.20(8); $\angle\text{Ru}(1)\text{-Ru}(2)\text{-P}$, 111.833(17); $\angle\text{Ru}(2)\text{-Ru}(1)\text{-C}(6)$, 110.21(7); $\angle\text{Cp(centroid)-Ru}(1)\text{-Ru}(2)\text{-Cp(centroid)}$, 0.1; $\angle\text{C}(6)\text{-Ru}(1)\text{-Ru}(2)\text{-P}$, 0.5; $\angle\text{Cp-Cp fold angle}$, 119.0.

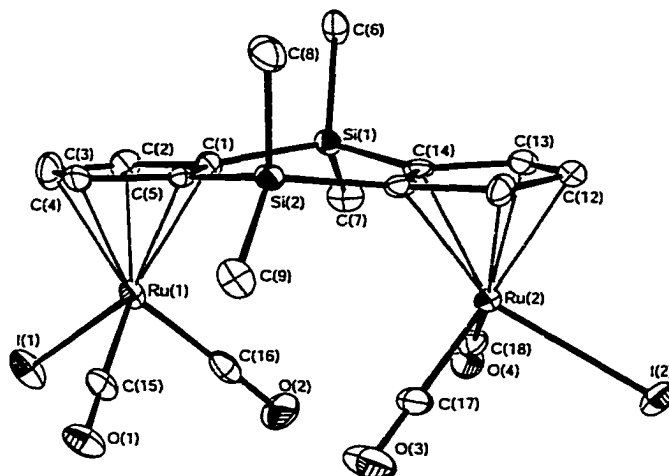


Figure 3. Thermal ellipsoid drawing of $\{(\eta^5\text{-C}_5\text{H}_3)_2(\text{SiMe}_2)_2\}\text{Ru}_2(\text{CO})_4(\text{I})_2$ (**3c**) showing the labeling scheme and 30% probability ellipsoids; hydrogens are omitted for clarity. Selected bond distances (Å) and angles (deg) are as follows: Ru(1)-Ru(2), 4.9762; Ru(1)-I(1), 2.7070(7); Ru(1)-C(15), 1.878(7); Ru(1)-C(16), 1.882(9); Ru(1)-Cp(centroid), 1.883; Ru(2)-Cp(centroid), 1.872; \angle I(1)-Ru(1)-C(15), 90.7(2); \angle I(1)-Ru(1)-C(16), 85.7(4); \angle C(16)-Ru(1)-C(15), 88.2(3); \angle Cp(centroid)-Ru(1)-Ru(2)-Cp(centroid), 5.3; \angle Cp-Cp fold angle, 175.9.

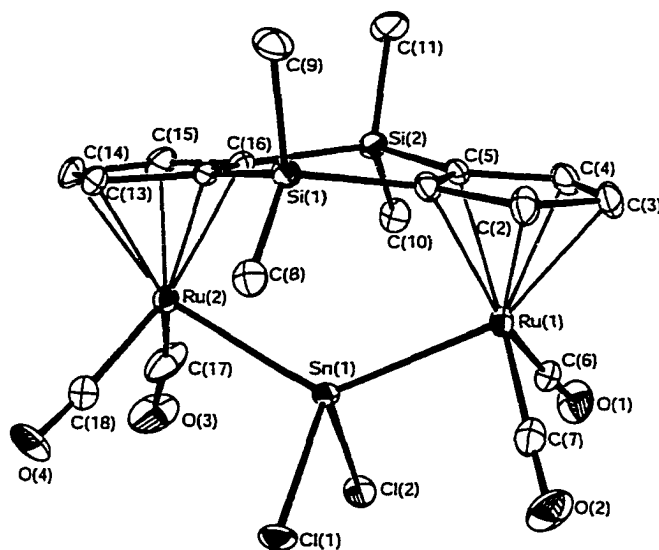


Figure 4. Thermal ellipsoid drawing of $\{(\eta^5\text{-C}_5\text{H}_3)_2(\text{SiMe}_2)_2\}(\text{CO})_4(\mu\text{-SnCl}_2)$ (**5**) showing the labeling scheme and 30% probability ellipsoids; hydrogens are omitted for clarity.

Selected bond distances (Å) and angles (deg) are as follows: Ru(1)-Ru(2), 4.625; Ru(1)-C(6), 1.874(4); Ru(1)-C(7), 1.887(4); Ru(1)-Sn(1), 2.6066(4); Ru(2)-C(17), 1.875(4); Ru(2)-C(18), 1.864(5); Ru(2)-Sn(1), 2.6034(4); Sn(1)-Cl(1), 2.4497(9); Sn(1)-Cl(2), 2.4465(9); Ru(1)-Cp(centroid), 1.895; Ru(2)-Cp(centroid), 1.887; $\angle\text{C}(7)\text{-Ru}(1)\text{-C}(6)$, 92.68(17); $\angle\text{C}(6)\text{-Ru}(1)\text{-Sn}(1)$, 87.02(12); $\angle\text{C}(7)\text{-Ru}(1)\text{-Sn}(1)$, 88.29(12); $\angle\text{Cl}(1)\text{-Sn}(1)\text{-Cl}(2)$, 92.73(3); $\angle\text{Ru}(1)\text{-Sn}(1)\text{-Ru}(2)$, 125.162(13); $\angle\text{Ru}(1)\text{-Sn}(1)\text{-Cl}(1)$, 109.24(3); $\angle\text{Cp(centroid)-Ru}(1)\text{-Ru}(2)\text{-Cp(centroid)}$, 3.1; $\angle\text{Cp-Cp fold angle}$, 171.1.

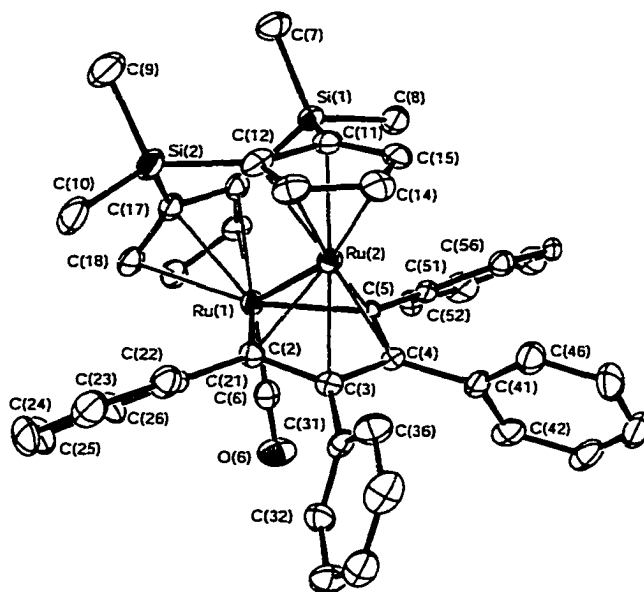


Figure 5. Thermal ellipsoid drawing of $\{(\eta^5\text{-C}_5\text{H}_3)_2(\text{SiMe}_2)_2\}\text{Ru}_2(\text{CO})\{\eta^2:\eta^4\text{-}\mu_2\text{-C(Ph)C(Ph)C(Ph)C(Ph)}\}$ (**9**) showing the labeling scheme and 30% probability ellipsoids; hydrogens are omitted for clarity. Selected bond distances (Å) and angles (deg) are as follows: Ru(1)-Ru(2), 2.6221(6); Ru(1)-C(6), 1.845(6); Ru(1)-C(5), 2.096(4); Ru(1)-C(2), 2.100(4); C(2)-C(3), 1.428(6); C(3)-C(4), 1.438(6); C(4)-C(5), 1.424(6); Ru(1)-Cp(centroid), 1.936; Ru(2)-Cp(centroid), 1.829; Ru(2)-Ruthenacyclopentadiene(Ru(1), C(2)-C(5))(centroid), 1.753; C(8)-Phenyl(C51-C56)(centroid), 3.435; $\angle\text{C(6)-Ru(1)-C(5)}$, 80.8(2); $\angle\text{C(6)-Ru(1)-C(2)}$, 79.9(2); $\angle\text{C(5)-Ru(1)-C(2)}$, 78.05(17); $\angle\text{Cp(centroid)-Ru(2)-Ruthenacyclopentadiene(Ru(1), C(2)-C(5))(centroid)}$, 172.17; $\angle\text{Cp-Cp fold angle}$, 118.83.

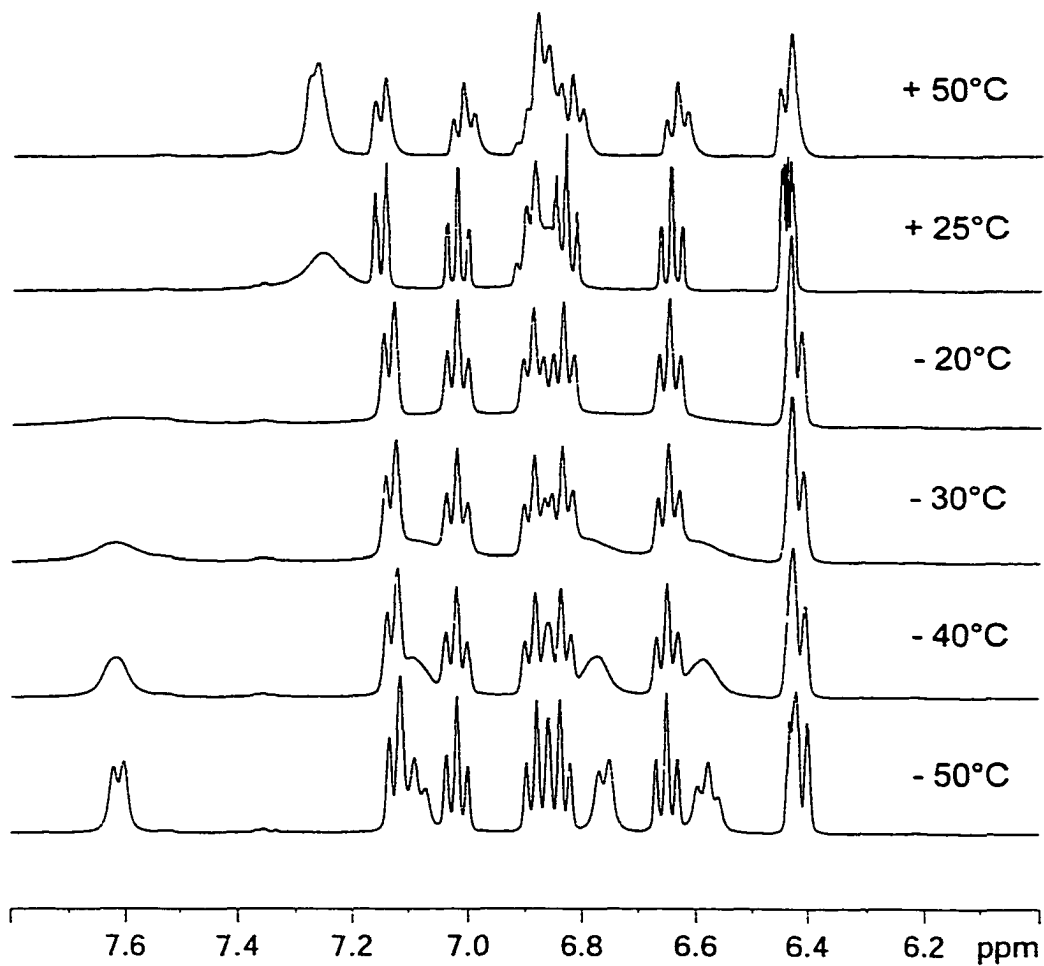


Figure 6. Variable-temperature ^1H NMR spectrum in the aromatic region of **9** in CD_2Cl_2 at 400 MHz.

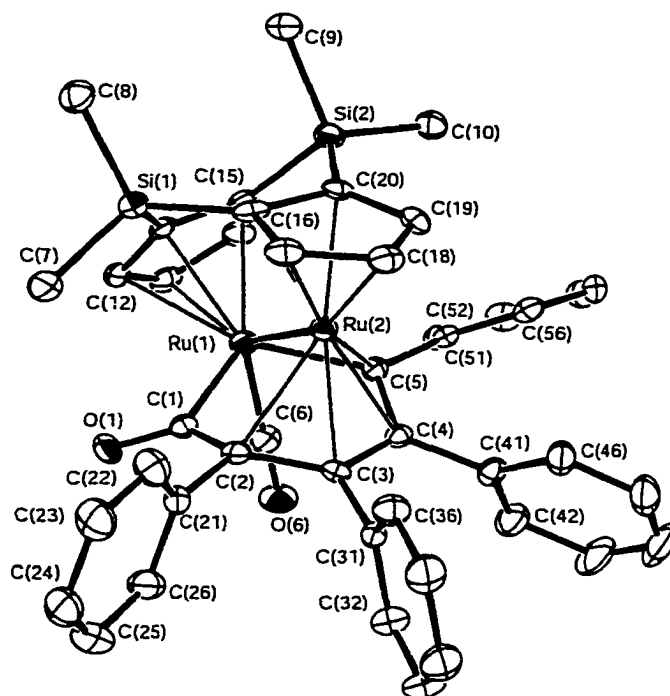


Figure 7. Thermal ellipsoid drawing of $\{(\eta^5\text{-C}_5\text{H}_3)_2(\text{SiMe}_2)_2\}\text{Ru}_2(\text{CO})\{\eta^2\text{-}\eta^4\text{-}\mu_2\text{-C(=O)C(Ph)C(Ph)C(Ph)C(Ph)}\}$ (**10**) showing the labeling scheme and 30% probability ellipsoids; hydrogens are omitted for clarity. Selected bond distances (Å) and angles (deg) are as follows: Ru(1)-Ru(2), 2.7118(6); Ru(1)-C(6), 1.856(5); Ru(1)-C(5), 2.083(4); Ru(1)-C(1), 2.029(4); C(1)-O(1), 1.219(5); C(1)-C(2), 1.482(6); C(2)-C(3), 1.444(5); C(3)-C(4), 1.431(5); C(4)-C(5), 1.431(5); Ru(2)-C(1), 2.796; Ru(2)-C(2), 2.274(4); Ru(2)-C(3), 2.211(4); Ru(2)-C(4), 2.226(4); Ru(2)-C(5), 2.110(4); Ru(1)-Cp(centroid), 1.967; Ru(2)-Cp(centroid), 1.848; Ru(2)-Ruthenacyclopentadiene(Ru(1),C(2)-C(5))(centroid), 1.769; C(10)-Phenyl(C51-C56)(centroid), 3.476; $\angle\text{C(6)-Ru(1)-C(5)}$, 78.47(17); $\angle\text{C(6)-Ru(1)-C(1)}$, 78.54(17); $\angle\text{C(5)-Ru(1)-C(1)}$, 95.00(17); $\angle\text{Cp(centroid)-Ru(2)-Ruthenacyclopentadiene(Ru(1),C(2)-C(5))(centroid)}$, 174.27; $\angle\text{Cp-Cp fold angle}$, 123.53.

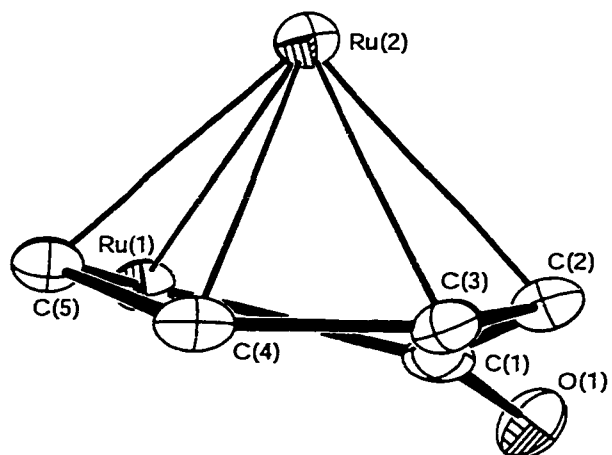


Figure 8. Structure of the core of $\{(\eta^5\text{-C}_5\text{H}_3)_2(\text{SiMe}_2)_2\}\text{Ru}_2(\text{CO})\{\eta^2:\eta^4\text{-}\mu_2\text{-C(=O)C(Ph)C(Ph)C(Ph)C(Ph)}\}$ (**10**).

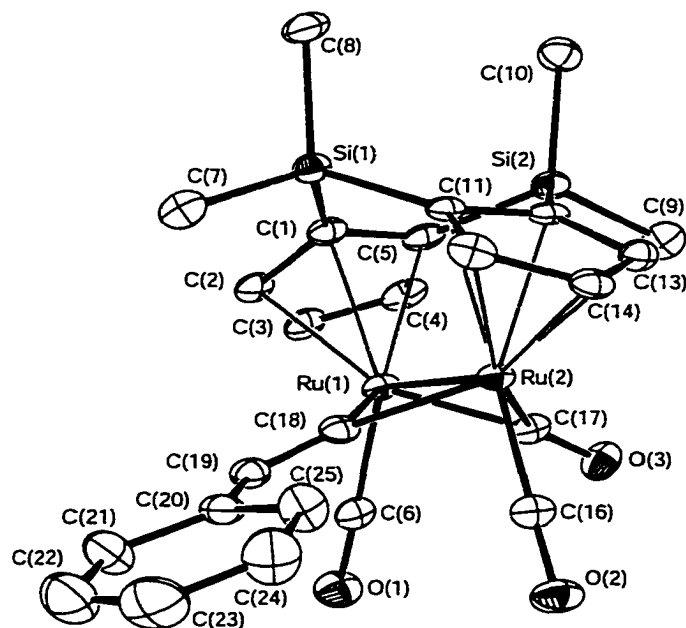


Figure 9. Thermal ellipsoid drawing of $\{(\eta^5\text{-C}_5\text{H}_3)_2(\text{SiMe}_2)_2\}\text{Ru}_2(\text{CO})_2(\mu\text{-CO})(\mu\text{-C=CHPh})$ (**12**) showing the labeling scheme and 30% probability ellipsoids; hydrogens are omitted for clarity. Selected bond distances (Å) and angles (deg) are as follows: Ru(1)-Ru(2), 2.6551(7); Ru(1)-C(18), 2.049(6); Ru(2)-C(18), 2.028(7); C(18)-C(19), 1.312(8); C(19)-C(20), 1.475(8); Ru(1)-C(17), 2.023(7); Ru(2)-C(17), 2.060(6); Ru(1)-Cp(centroid), 1.919; Ru(2)-Cp(centroid), 1.918; $\angle\text{C(6)-Ru(1)-C(17)}$, 86.4(3); $\angle\text{C(6)-Ru(1)-C(18)}$, 83.8(2); $\angle\text{C(18)-Ru(1)-C(17)}$, 87.9(2); $\angle\text{C(16)-Ru(2)-C(17)}$, 83.8(2); $\angle\text{C(16)-Ru(2)-C(18)}$, 86.5(3); $\angle\text{C(18)-Ru(2)-C(17)}$, 87.4(2); $\angle\text{Ru(1)-Ru(2)-C(16)}$, 108.76(18); $\angle\text{Ru(2)-Ru(1)-C(6)}$, 108.78(19); $\angle\text{Ru(1)-C(18)-Ru(2)}$, 81.3(2); $\angle\text{Ru(1)-C(17)-Ru(2)}$, 81.1(3); $\angle\text{C(6)-Ru(1)-Ru(2)-C(16)}$, 0.2; $\angle\text{Cp(centroid)-Ru(1)-Ru(2)-Cp(centroid)}$, 0.9; $\angle\text{Cp-Cp fold angle}$, 118.5.

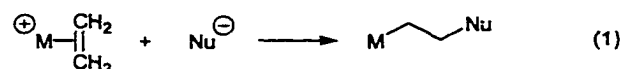
**CHAPTER 4. HYDROFUNCTIONALIZATION OF ALKENES
PROMOTED BY DIRUTHENIUM COMPLEXES [$\{(\eta^5\text{-C}_5\text{H}_3)_2(\text{SiMe}_2)_2\}\text{Ru}_2(\text{CO})_3(\eta^2\text{-CH}_2=\text{CH-R})(\mu\text{-H})\}^+$ FEATURING A
KINETICALLY INERT PROTON ON A METAL-METAL BOND**

A paper to be submitted to the Journal of the American Chemical Society¹

Maxim V. Ovchinnikov, Eric LeBlanc, Ilia A. Guzei,[‡] and Robert J. Angelici

Introduction

Metal-assisted nucleophilic attack on unsaturated ligands is a reaction of great synthetic importance and represents one of the most common and well-studied reactions in organometallic chemistry.¹ For example, amines and alkoxides attack a carbon of coordinated alkenes in transition metal complexes if the metal is sufficiently electropositive to promote such an attack (eq 1).² One of the simplest approaches to making the metal in a complex more positive is to add

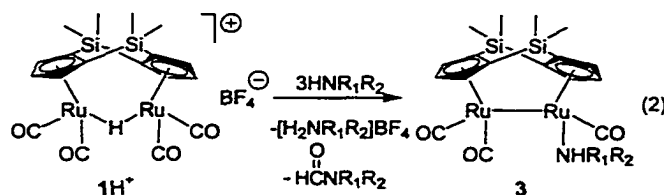


a proton (H^+) to the metal center.³ However, most protonated metal complexes containing unsaturated ligands either do not react with nucleophiles because the metal is not sufficiently

¹ Reproduced with permission from the Journal of the American Chemical Society, to be submitted for publication. Unpublished work copyright 2000 American Chemical Society.

[‡] Current address: Department of Chemistry, University of Wisconsin, Madison, WI 53706.

electropositive or the nucleophiles simply deprotonate the metal to give the unreactive neutral metal complex. We recently reported⁴ the synthesis of the cationic dinuclear complex $[\{(\eta^5\text{-C}_5\text{H}_3)_2(\text{SiMe}_2)_2\}\text{Ru}_2(\text{CO})_4(\mu\text{-H})\text{]}^+$ (1H^+) whose carbon monoxide ligands are activated to attack by amine nucleophiles (eq 2) because of the positive charge on the complex and the slow rate of



deprotonation of the bridging hydride by the amines. In this communication we report the synthesis of protonated alkene complexes $[\{(\eta^5\text{-C}_5\text{H}_3)_2(\text{SiMe}_2)_2\}\text{Ru}_2(\text{CO})_3(\eta^2\text{-CH}_2=\text{CH-R})(\mu\text{-H})\text{]}^+$ ($2\mathbf{a}\text{-bH}^+$) and the activation of the alkene ligand in these complexes to attack by amines and other nucleophiles to give the alkylated nucleophiles. This type of reaction with amine nucleophiles is a key step in the catalytic intermolecular hydroamination of alkenes, a process of great current interest and importance.⁵

Results and Discussion

The reaction of $[\{(\eta^5\text{-C}_5\text{H}_3)_2(\text{SiMe}_2)_2\}\text{Ru}_2(\text{CO})_4(\mu\text{-H})\text{]}^+$ (1H^+) with $\text{Me}_3\text{NO}\cdot 2\text{H}_2\text{O}$ in the presence of the desired alkene forms complexes $\{(\eta^5\text{-C}_5\text{H}_3)_2(\text{SiMe}_2)_2\}\text{Ru}_2(\text{CO})_3(\eta^2\text{-CH}_2=\text{CH-R})$ ($2\mathbf{a}\text{-b}$; $\text{R} = \text{H}, \text{Me}$) in 72 and 65% isolated yields, respectively, as air- and moisture-sensitive yellow solids (Scheme 1; see supporting information for experimental details). Addition of 1 equiv of $\text{CF}_3\text{SO}_3\text{H}$ or $\text{CF}_3\text{SO}_3\text{D}$ to solutions of complexes $2\mathbf{a}\text{-b}$ in CH_2Cl_2 at room temperature gives the hydride-bridged dinuclear Ru complexes $2\mathbf{a}\text{-bH}^+\text{TfO}^-$

in quantitative yields. Complex $2\mathbf{bH}^+\text{TfO}^-$ exists as a mixture (2.3:1 ratio) of two isomers with Ru coordinated to different faces of the propylene ligand. The CO stretching frequencies of $2\mathbf{a-bH}^+\text{TfO}^-$ are approximately 40 cm^{-1} higher than those of 2 and fall within the range where amine attack on coordinated alkenes is expected to occur.² An X-ray diffraction study of $2\mathbf{aH}^+\text{BF}_4^-$ (Figure 1)⁶ reveals an eclipsed orientation of the terminal CO and ethylene ligands on the two Ru atoms. The Ru-Ru distance in $2\mathbf{aH}^+\text{BF}_4^-$ ($3.1306(6)\text{ \AA}$) is similar to that in complex $1\mathbf{H}^+\text{BF}_4^-$ ($3.1210(5)\text{ \AA}$).⁷ Complexes $2\mathbf{a-bH}^+\text{TfO}^-$ are slow to undergo deprotonation relative to reaction of the alkene with nucleophiles as the unprotonated complexes $2\mathbf{a-b}$ are not detected among the products of reactions of $2\mathbf{a-bH}^+\text{TfO}^-$ with nucleophiles (vide infra). The deuterated complex $2\mathbf{aD}^+\text{TfO}^-$ in wet acetone- d_6 solution ($\sim 5\%$ H_2O) did not undergo measurable H-D exchange after 1 day at $25\text{ }^\circ\text{C}$. As for $1\mathbf{H}^+$,⁴ this low kinetic acidity is attributed to a combination of the bulkiness of the dimethylsilyl linkers in the $(\eta^5\text{-C}_5\text{H}_3)_2(\text{SiMe}_2)_2$ bridging ligand and the rigidity of the molecule.

Reactions of $2\mathbf{a-bH}^+\text{TfO}^-$ with amines (NH_3 , MeNH_2 , Me_2NH , morpholine, *p*- $\text{CH}_3\text{C}_6\text{H}_4\text{NH}_2$) yield amine complexes $\{(\eta^5\text{-C}_5\text{H}_3)_2(\text{SiMe}_2)_2\}\text{Ru}_2(\text{CO})_3(\text{NHR}_1\text{R}_2)$ ($\text{NHR}_1\text{R}_2 = \text{NH}_3$, MeNH_2 , Me_2NH)⁸ (3) and the corresponding alkylated amines in a 1:1 ratio as determined by ^1H NMR spectroscopy (Table 1; entry 1; Scheme 2). The reactions of $2\mathbf{bH}^+\text{TfO}^-$ give Markovnikov addition products with $>95\%$ regioselectivity. In contrast to reactions of $1\mathbf{H}^+$ (eq 2),⁴ even weakly nucleophilic amines (*p*- $\text{CH}_3\text{C}_6\text{H}_4\text{NH}_2$, $\text{p}K_{\text{a}} = 5.10$)⁹ react with $2\mathbf{aH}^+\text{TfO}^-$. Rates of reactions of $2\mathbf{aH}^+\text{TfO}^-$ with morpholine are approximately $10^2\text{-}10^3$ times faster than those of complex $1\mathbf{H}^+$ ($t_{1/2} = 45\text{ min}$ for $1\mathbf{H}^+$, $t_{1/2} < 1\text{ sec}$ for

$2\mathbf{aH}^+\text{TfO}^-$);⁴ the reaction of $2\mathbf{aH}^+\text{TfO}^-$ with *p*-CH₃C₆H₄NH₂ was found to be slowest ($t_{1/2} = 35$ min, 25 °C, CDCl₃) among the amines studied. The absence of the deprotonated complexes $2\mathbf{a-b}$ and formamides among the products in these reactions is consistent with relatively slow rates of deprotonation of $2\mathbf{a-bH}^+\text{TfO}^-$ and faster rates of nucleophilic attack on the coordinated alkene than on CO.²

The scope of this reaction is relatively broad: complexes $2\mathbf{a-bH}^+\text{TfO}^-$ react with several representative nucleophiles (PMe₃, ⁻OMe, ⁻SMe) to give the hydrofunctionalized alkenes and, in most cases (Table 1; entries 2, 4), readily identifiable Ru-containing products.¹⁰ Reactions of $2\mathbf{a-bH}^+\text{TfO}^-$ with these nucleophiles occur rapidly ($t_{1/2} < 1$ sec) to give organic products with high Markovnikov regioselectivities (except PMe₃). Surprisingly, the reaction of complex $2\mathbf{bH}^+\text{TfO}^-$ gives a mixture of *n*-PrPMe₃⁺ and *i*-PrPMe₃⁺ in a 1.6:1 ratio.

Although a detailed mechanism for the reactions of $2\mathbf{a-bH}^+\text{TfO}^-$ with nucleophiles is yet to be established, on the basis of experiments with deuterium-labeled complex $2\mathbf{aD}^+\text{TfO}^-$, we propose the mechanism shown in Scheme 2. It involves initial nucleophilic attack by the amine on the coordinated alkene to produce the cationic intermediate **A**, which is either deprotonated to **B** or undergoes reductive elimination of the alkylated ammonium salt to form an unsaturated di-ruthenium intermediate that coordinates an amine to give **3**. Intermediate **B** could also undergo reductive elimination of the alkylated amine. This mechanism is consistent with the reaction of the deuterium-labeled $2\mathbf{aD}^+\text{TfO}^-$ with morpholine which gives *N*-ethylmorpholine (CH₂D-CH₂-N(CH₂CH₂)₂O) that is $\sim 93 \pm 5\%$ deuterated at the methyl position and no other. No intermediates were observed by FT-IR or

^1H NMR spectroscopy during the course of the reactions. Reductive eliminations involving a $\mu\text{-H}$ have only recently been characterized¹¹ in the formation of alkanes and arenes from $\text{Pd}_2\text{R}_2(\mu\text{-H})(\text{dppm})_2^+$ and proposed in the formation of formamides in reaction (2).⁴

Conclusions

In conclusion, we have demonstrated that the alkene complexes $2\mathbf{a}\text{-bH}^+\text{TfO}^-$, featuring a kinetically inert bridging proton on a metal-metal bond and a doubly-linked dicyclopentadienyl ligand, react with a variety of nucleophiles to give hydrofunctionalized alkenes with predominantly Markovnikov regioselectivity. Future studies will be directed toward hydroamination and other hydrofunctionalization reactions of alkenes that are catalyzed by $2\mathbf{a}\text{-bH}^+\text{TfO}^-$ and its derivatives.

Experimental Part

General Procedures. All reactions were performed under an argon atmosphere in reagent grade solvents, using standard Schlenk or dry-box techniques.¹² Methylene chloride and diethyl ether were purified by the Grubbs method prior to use.¹³ All other solvents were purified by published methods.¹⁴ Chemicals were purchased from Aldrich Chemical Co., unless otherwise mentioned, or prepared by literature methods, as referenced below. Alumina (neutral, activity I, Aldrich) was degassed under vacuum for 12 h and treated with Ar-saturated water (7.5 % w/w). ^1H and ^{13}C NMR spectra were recorded on a Bruker DRX-400 spectrometer using deuterated solvents as internal references. Solution infrared spectra were recorded on a Nicolet-560 spectrometer using NaCl cells with 0.1 mm spacers.

Elemental analyses were performed on a Perkin Elmer 2400 series II CHNS/O analyzer. Unless stated otherwise, organic products were identified by comparison of their ^1H NMR spectra with authentic samples obtained from Aldrich Chemical Co.

Synthesis of $\{(\eta^5\text{-C}_5\text{H}_3)_2(\text{SiMe}_2)_2\}\text{Ru}_2(\text{CO})_3(\eta^2\text{-CH}_2=\text{CH-R})$ (2a-b**).** In a typical procedure, a solution of $1\text{H}^+\text{BF}_4^-$ (100.0 mg, 0.16 mmol) in CH_2Cl_2 (50 mL) was treated with a flow of gaseous ethylene for 1 min. Then solid $\text{Me}_3\text{NO}\cdot 2\text{H}_2\text{O}$ (18.0 mg, 0.17 mmol) was added, and the mixture was stirred for 10 min under an ethylene flow. After the solvent was removed under vacuum, the mixture was chromatographed on an alumina column (1 \times 20 cm) first with hexanes and then with a 1:5 (v/v) mixture of CH_2Cl_2 and hexanes which eluted a yellow band containing **2a** (72 mg, 84%). ^1H NMR (400 MHz, CDCl_3): δ 0.35 (s, 6 H, $\text{Si}(\text{CH}_3)$), 0.44 (s, 6 H, $\text{Si}(\text{CH}_3)$), 2.30 (s, 4 H, $\text{CH}_2=\text{CH}_2$), 4.88 (br s, 2 H, Cp-*H*), 5.48 (br s, 2 H, Cp-*H*), 5.79 (br s, 2 H, Cp-*H*). ^{13}C NMR (100 MHz, CDCl_3): δ -2.72, 5.00 (CH_3), 30.03 ($\text{CH}_2=\text{CH}_2$), 87.32, 91.73, 93.18, 94.47, 95.72, 96.19 (Cp), 207.07 (CO). IR (hexanes): $\nu(\text{CO})$ (cm^{-1}) 2000 (vs), 1950 (vs), 1923 (w). Complex **2b** was prepared in the same manner and used for the synthesis of $2\text{bH}^+\text{TfO}^-$ without isolation and purification.

Synthesis of $[\{(\eta^5\text{-C}_5\text{H}_3)_2(\text{SiMe}_2)_2\}\text{Ru}_2(\text{CO})_3(\eta^2\text{-CH}_2=\text{CH-R})(\mu\text{-H or D})]^+$ (2a-bH⁺**, **2aD⁺**).** A solution of **2a-b** (0.10 mmol) in CH_2Cl_2 (10 mL) was treated with $\text{CF}_3\text{SO}_3\text{H}$, $\text{HBF}_4\cdot\text{OEt}_2$ or $\text{CF}_3\text{SO}_3\text{D}$ (0.11 mmol) at room temperature. An orange air-stable precipitate of the corresponding product was obtained in nearly quantitative yield (>95%) by diluting the reaction solution with a 10-fold excess of diethyl ether (100 mL). $2\text{aH}^+\text{TfO}^-$: ^1H NMR (400 MHz, CD_2Cl_2): δ -19.59 (s, 1 H, Ru-*H*-Ru), 0.42 (s, 3 H, $\text{Si}(\text{CH}_3)$), 0.56 (s, 3 H, $\text{Si}(\text{CH}_3)$), 0.58 (s, 3 H, $\text{Si}(\text{CH}_3)$), 0.62 (s, 3 H, $\text{Si}(\text{CH}_3)$), 3.30 (m, 2 H, $\text{CH}_2=\text{CH}_2$), 3.41 (m, 2 H,

$\text{CH}_2=\text{CH}_2$), 4.96 (m, 1 H, Cp-*H*), 5.99 (m, 2 H, Cp-*H*), 6.03 (m, 2 H, Cp-*H*), 6.08 (m, 1 H, Cp-*H*). ^{13}C NMR (100 MHz, CD_2Cl_2): δ -2.77, -2.54, 2.54, 4.28 (CH_3), 45.05 ($\text{CH}_2=\text{CH}_2$), 84.92, 88.14, 93.42, 93.55, 95.28, 98.19, 99.96, 101.43, 103.5, 104.42 (Cp), 195.28, 196.31, 200.76 (CO). IR (CH_2Cl_2): $\nu(\text{CO})$ (cm^{-1}) 2060 (s), 2017 (vs), 1990 (w). Anal. Calcd for $\text{C}_{20}\text{H}_{23}\text{F}_3\text{O}_6\text{Ru}_2\text{SSi}_2$: C, 33.99; H, 3.28. Found: C, 34.07; H, 3.20. $2\text{bH}^+\text{TfO}^-$: ^1H NMR (400 MHz, CD_2Cl_2): (major isomer) δ -19.48 (s, 1 H, Ru-*H*-Ru), 0.36 (s, 3 H, Si(CH_3)), 0.55 (s, 3 H, Si(CH_3)), 0.56 (s, 3 H, Si(CH_3)), 0.61 (s, 3 H, Si(CH_3)), 1.86 (d, $J = 6.0$ Hz, 3 H, CH_3 -CH), 3.04 (d, $J = 13.2$ Hz, 1 H, CH=CHH), 3.53 (d, $J = 8.4$ Hz, 1 H, CH=CHH), 4.76 (ddq, $J = 13.2, 8.4, 6.0$ Hz, 1 H, CH=CH $_2$), 4.95 (br s, 1 H, Cp-*H*), 5.96 (m, 3 H, Cp-*H*), 6.07 (br s, 1 H, Cp-*H*), 6.13 (br s, 1 H, Cp-*H*); (minor isomer) δ -20.54 (s, 1 H, Ru-*H*-Ru), 0.44 (s, 3 H, Si(CH_3)), 0.55 (s, 3 H, Si(CH_3)), 0.57 (s, 3 H, Si(CH_3)), 0.58 (s, 3 H, Si(CH_3)), 1.81 (d, $J = 6.0$ Hz, 3 H, CH_3 -CH), 3.46 (d, $J = 13.2$ Hz, 1 H, CH=CHH), 3.64 (d, $J = 8.0$ Hz, 1 H, CH=CHH), 4.42 (ddq, $J = 13.2, 8.0, 6.0$ Hz, 1 H, CH=CH $_2$), 5.27 (br s, 1 H, Cp-*H*), 5.67 (br s, 1 H, Cp-*H*), 5.91 (br s, 1 H, Cp-*H*), 5.95 (m, 2 H, Cp-*H*), 6.04 (br s, 1 H, Cp-*H*), 6.13 (br s, 1 H, Cp-*H*). IR (CH_2Cl_2): $\nu(\text{CO})$ (cm^{-1}) 2060 (s), 2015 (vs), 1986 (w). Anal. Calcd for $\text{C}_{21}\text{H}_{25}\text{F}_3\text{O}_6\text{Ru}_2\text{SSi}_2$: C, 34.99; H, 3.50. Found: C, 35.34; H, 3.54.

Reactions of $2\text{a-bH}^+\text{TfO}^-$ and $2\text{aD}^+\text{TfO}^-$ with Amines. In a typical experiment, amine (2-3 equiv) was added to a solution of $2\text{a-bH}^+\text{TfO}^-$ (or $2\text{aD}^+\text{TfO}^-$) (~10 mg) and triphenylmethane (~3 mg, internal standard) in CDCl_3 (1 mL) in a Young-type NMR tube (gaseous amines were bubbled through the suspension for 5 min; then a stream of dry argon was bubbled through the solution in order to remove the excess amine). During the addition of amine, the reaction mixture changed color from yellow to wine-red. Complexes 2a-

bH^+TfO^- or $2\text{aD}^+\text{TfO}^-$ reacted completely, and yields of the alkylated amines and complexes $\{(\eta^5\text{-C}_5\text{H}_3)_2(\text{SiMe}_2)_2\}\text{Ru}_2(\text{CO})_3(\text{NHR}_1\text{R}_2)$ (**3**) ($\text{NHR}_1\text{R}_2 = \text{NH}_3, \text{MeNH}_2, \text{Me}_2\text{NH}$)¹⁵ were close to stoichiometric as determined by means of ^1H NMR spectroscopy. Complexes $\{(\eta^5\text{-C}_5\text{H}_3)_2(\text{SiMe}_2)_2\}\text{Ru}_2(\text{CO})_3(\text{NHR}_1\text{R}_2)$ (**3**) ($\text{NR}_1\text{R}_2 = \text{morpholine}, p\text{-CH}_3\text{C}_6\text{H}_4\text{NH}_2$) undergo rapid decomposition in CDCl_3 solution. When the reactions with these amines are performed in the presence of CO or ethylene, complexes **1** or **2a** are formed in stoichiometric amounts.

Reactions of 2a-bH⁺TfO⁻ with PMe₃. In a typical experiment, PMe_3 (2 equiv) was added to a solution of $2\text{a-bH}^+\text{TfO}^-$ (~10 mg) and triphenylmethane (~3 mg, internal standard) in CD_2Cl_2 (1 mL) in a Young-type NMR tube. During the addition of PMe_3 , the reaction mixture changed color from yellow to orange. Yields of the alkylated phosphonium salts RPMe_3^+ and complex $\{(\eta^5\text{-C}_5\text{H}_3)_2(\text{SiMe}_2)_2\}\text{Ru}_2(\text{CO})_3(\text{PMe}_3)$ ¹⁶ were close to stoichiometric as determined by means of ^1H NMR spectroscopy. $n\text{-PrPMe}_3^+$: ^1H NMR (400 MHz, CD_2Cl_2): δ 1.13 (t, $J = 7.2$ Hz, 3 H, $\text{CH}_3\text{-CH}_2$), 1.62 (m, 2 H, $\text{CH}_3\text{-CH}_2$), 1.88 (d, $J = 14.0$ Hz, 9 H, $\text{CH}_3\text{-P}$), 2.14 (m, 2 H, $\text{CH}_2\text{-P}$). $i\text{-PrPMe}_3^+$: ^1H NMR (400 MHz, CD_2Cl_2): δ 1.28 (dd, $J = 7.2, 18.8$ Hz, 6 H, $\text{CH}_3\text{-CH}$), 1.84 (d, $J = 12.4$ Hz, 9 H, $\text{CH}_3\text{-P}$), 2.47 (m, 1 H, CH-P).

Reactions of 2a-bH⁺TfO⁻ with NaOMe. In a typical experiment, solid NaOMe (~5 equiv) was added to a suspension of $2\text{a-bH}^+\text{TfO}^-$ (~10 mg) and triphenylmethane (~3 mg, internal standard) in C_6D_6 (1 mL) in a Young-type NMR tube. The tube was placed in a ultrasonic bath and sonicated for 20 min. The reaction mixture changed color from colorless to brown. Yields of the methyl ethers MeOEt and MeO-*i*-Pr were close to stoichiometric as determined by ^1H NMR spectroscopy. Ruthenium-containing products underwent rapid decomposition to form unidentifiable products.

Reactions of 2a-bH⁺TfO⁻ with NaSMe. In a typical experiment, solid NaSMe (~5 equiv) was added to a suspension of 2a-bH⁺TfO⁻ (~10 mg) and triphenylmethane (~3 mg, internal standard) in C₆D₆ (1 mL) in a Young-type NMR tube. The tube was placed in an ultrasonic bath and sonicated for 40 min. The reaction mixture changed color from colorless to red. Complexes $\{(\eta^5\text{-C}_5\text{H}_3)_2(\text{SiMe}_2)_2\}\text{Ru}_2(\text{CO})(\mu\text{-CO})_2(\eta^1\text{-MeSEt})$ and $\{(\eta^5\text{-C}_5\text{H}_3)_2(\text{SiMe}_2)_2\}\text{Ru}_2(\text{CO})(\mu\text{-CO})_2(\eta^1\text{-MeS-i-Pr})$ were the only products which were formed in 82% and 67% yields respectively as determined by means of ¹H NMR spectroscopy. $\{(\eta^5\text{-C}_5\text{H}_3)_2(\text{SiMe}_2)_2\}\text{Ru}_2(\text{CO})(\mu\text{-CO})_2(\eta^1\text{-MeSEt})$: ¹H NMR (400 MHz, C₆D₆): δ 0.17 (s, 6 H, Si(CH₃)), 0.51 (s, 6 H, Si(CH₃)), 1.28 (t, $J = 7.5$ Hz, 3 H, CH₃-CH₂), 1.41 (s, 3 H, CH₃-S), 1.55 (q, $J = 7.5$ Hz, 2 H, CH₂-S), 4.48 (br s, 2 H, Cp-H), 5.04 (m, 2 H, Cp-H), 5.17 (m, 1 H, Cp-H), 5.34 (m, 1 H, Cp-H). IR (hexanes): $\nu(\text{CO})$ (cm⁻¹) 1981 (s), 1923 (vs), 1776 (w). $\{(\eta^5\text{-C}_5\text{H}_3)_2(\text{SiMe}_2)_2\}\text{Ru}_2(\text{CO})(\mu\text{-CO})_2(\eta^1\text{-MeS-i-Pr})$: ¹H NMR (400 MHz, C₆D₆): δ 0.19 (s, 6 H, Si(CH₃)), 0.53 (s, 6 H, Si(CH₃)), 1.35 (d, $J = 6.6$ Hz, 6 H, CH₃-CH), 1.42 (br s, 3 H, CH₃-S), 1.78 (m, 1 H, CH-S), 4.46 (br s, 2 H, Cp-H), 5.10 (br s, 2 H, Cp-H), 5.14 (m, 1 H, Cp-H), 5.44 (br s, 1 H, Cp-H). IR (hexanes): $\nu(\text{CO})$ (cm⁻¹) 1980 (s), 1923 (vs), 1774 (w).

Acknowledgment

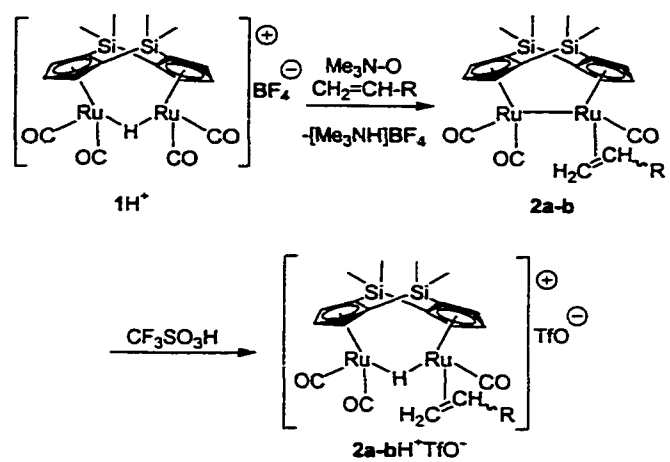
This work was supported by the National Science Foundation through Grant No. CHE-9816342.

References

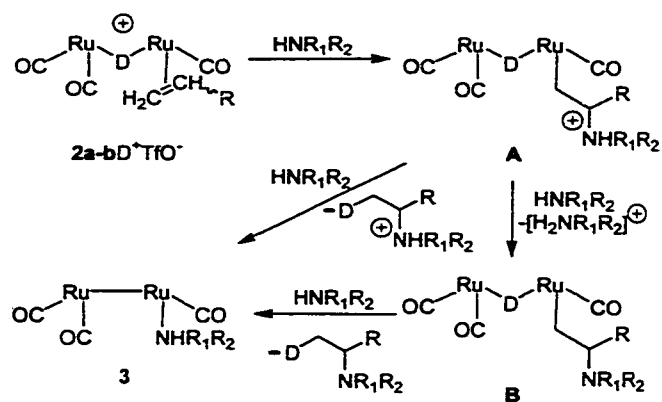
- (1) (a) McDaniel, K. F. In *Comprehensive Organometallic Chemistry*, Wilkinson, G., Stone F. G. A., Abel, E. W., Eds., Pergamon Press: Oxford, New York 1995; Vol. 12, p. 601. (b) Collman, J. P.; Hegedus, L. S.; Norton, J. R.; Finke, R. G. *Principles and Applications of Organotransition Metal Chemistry*; University Science Books: Mills Valley, CA, 1987; Chapter 7. (c) Yamamoto, A. *J. Organomet. Chem.* **2000**, *600*, 159. (d) Brunet, J. J.; Neibecker, D.; Niedercorn, F. *J. Mol. Catal.* **1989**, *49*, 235.
- (2) Bush, R. C.; Angelici, R. J. *J. Am. Chem. Soc.* **1986**, *108*, 2735.
- (3) (a) Angelici, R. J. *Acc. Chem. Res.* **1995**, *28*, 52. (b) Kristjánsdóttir, S. S.; Norton, J. R. In *Transition Metal Hydrides: Recent Advances in Theory and Experiments*; Dedieu, A., Ed.; VCH: New York, 1991; Chapter 10. (c) Bullock, R. M. *Comments Inorg. Chem.* **1991**, *12*, 1.
- (4) (a) Ovchinnikov, M. V.; Angelici, R. J. *J. Am. Chem. Soc.* **2000**, *122*, 6130. (b) Ovchinnikov, M. V.; Guzei, I. A.; Angelici, R. J. *Organometallics* **2001**, *20*, 691.
- (5) For leading references, see: (a) Kawatsura, M.; Hartwig, J. F. *J. Am. Chem. Soc.* **2000**, *122*, 9546. (b) Beller, M.; Eichberger, M.; Trauthwein, H. *Angew. Chem., Int. Ed. Engl.* **1997**, *36*, 2225. (c) Tian, S.; Arredondo, V. M.; Stern, C. L.; Marks, T. J. *Organometallics* **1999**, *18*, 2568. (d) Muller, T. E.; Beller, M. *Chem. Rev.* **1998**, *98*, 675. (e) Casalnuovo, A. L.; Calabrese, J. C.; Milstein, D. *J. Am. Chem. Soc.* **1988**, *110*, 6738.
- (6) Crystallographic data (excluding structure factors) for the structure in this paper have been deposited with the Cambridge Crystallographic Data Centre as supplementary publication no. CCDC-162940 ($2\mathbf{aH}^+\mathbf{BF}_4^-$). Copies of the data can be obtained, free of

charge, on application to CCDC, 12 Union Road, Cambridge CB2 1EZ, UK, (fax: +44 1223 336033 or e-mail: deposit@ccdc.cam.ac.uk).

- (7) Details of the X-ray and neutron diffraction studies of $1\text{H}^+\text{BF}_4^-$ will be published separately: Ovchinnikov, M. V.; Wang, X.; Schultz, A. J.; Angelici, R. J. Manuscript in preparation.
- (8) Complexes $\{(\eta^5\text{-C}_5\text{H}_3)_2(\text{SiMe}_2)_2\}\text{Ru}_2(\text{CO})_3(\text{NHR}_1\text{R}_2)$ (**3**) ($\text{NHR}_1\text{R}_2 = \text{morpholine, } p\text{-CH}_3\text{C}_6\text{H}_4\text{NH}_2$) undergo rapid decomposition in CDCl_3 solution
- (9) Perrin, D. D. *Dissociation Constants of Organic Bases in Aqueous Solution*; Butterworths: London, 1972.
- (10) See Supporting Information.
- (11) Stockland, R. A. Jr.; Anderson, G. K.; Rath, N. P. *J. Am. Chem. Soc.* **1999**, *121*, 7945.
- (12) Errington, R. J. *Advanced Practical Inorganic and Metalorganic Chemistry*, 1st ed.; Chapman & Hall: New York, 1997.
- (13) Pangborn, A. B.; Giardello, M. A.; Grubbs, R. H.; Rosen, R. K.; Timmers, F. J. *Organometallics* **1996**, *15*, 1518.
- (14) Perrin, D. D.; Armarego, W. L. F.; Perrin, D. R. *Purification of Laboratory Chemicals*, 2nd ed.; Pergamon: New York, 1980.
- (15) Ovchinnikov, M. V.; Guzei, I. A.; Angelici, R. J. *Organometallics* **2001**, *20*, 691.
- (16) Details of the NMR characterization and X-ray diffraction study of $\{(\eta^5\text{-C}_5\text{H}_3)_2(\text{SiMe}_2)_2\}\text{Ru}_2(\text{CO})_3(\text{PMe}_3)$ will be published separately: Ovchinnikov, M. V.; Guzei, I. A.; Angelici, R. J. Manuscript in preparation.

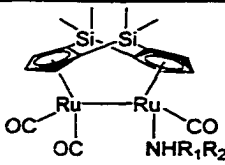
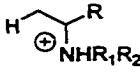
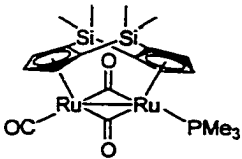
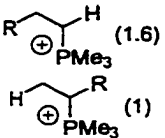
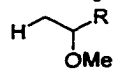
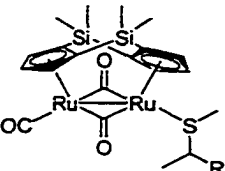


Scheme 1. Synthesis of complexes **2a-b**H⁺TfO⁻ (R = H (**a**), CH₃ (**b**)).



Scheme 2. Proposed mechanism for the reaction of $2a-bD^+TfO^-$ with amines. (η^5 - $C_5H_3)_2(SiMe_2)_2$ ligands are omitted.

Table 1. Hydrofunctionalization of alkenes promoted by **2a-bH⁺** (R = H (**a**), CH₃ (**b**)).

	Nucleophile	Ru-cont. Product	Organic Product(s) (ratio)
1	NHR ₁ R ₂ (CDCl ₃) (2 equiv.)		
2	PMe ₃ (CD ₂ Cl ₂) (2 equiv.)		
3	NaOMe (C ₆ D ₆) (1-5 equiv.)	Decomp. products	
4	NaSMe (C ₆ D ₆) (1-5 equiv.)		-

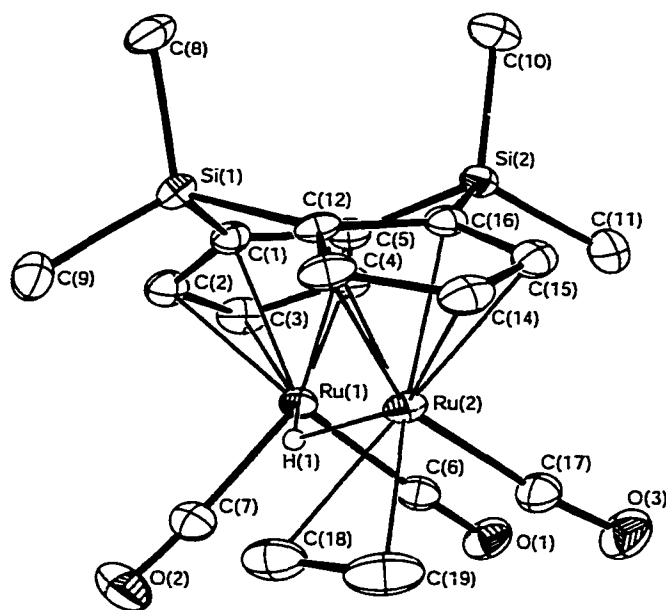


Figure 1. Thermal ellipsoid drawing, with 30% probability ellipsoids, [$\{(\eta^5\text{-C}_5\text{H}_3)_2(\text{SiMe}_2)_2\}\text{Ru}_2(\text{CO})_3(\eta^2\text{-CH}_2\text{=CH}_2)(\mu\text{-H})\}^+$ in $2\text{aH}^+\text{BF}_4^-$ showing the labeling scheme. Selected bond distances (\AA) and angles (deg) are as follows: Ru(1)-Ru(2), 3.1306(6); Ru(1)-H(1) = Ru(2)-H(1), 1.743(1); Ru(1)-C(6), 1.901(7); Ru(1)-C(7), 1.899(7); Ru(2)-C(17), 1.889(7); Ru(2)-C(18), 2.237(7); Ru(2)-C(19), 2.242(7); C(18)-C(19), 1.340(12); Ru(1)-Cp(centroid), 1.872(3); Ru(2)-Cp(centroid), 1.868(3); $\angle\text{Ru(1)-H(1)-Ru(2)}$, 128(1); $\angle\text{Ru(2)-Ru(1)-C(6)}$, 89.28(19); $\angle\text{Ru(2)-Ru(1)-C(7)}$, 101.6(2); $\angle\text{C(6)-Ru(1)-C(7)}$, 91.2(3); $\angle\text{Ru(1)-Ru(2)-C(17)}$, 88.8(2); $\angle\text{C(6)-Ru(1)-Ru(2)-C(17)}$, 5.5(3); $\angle\text{C(7)-Ru(1)-Ru(2)-C(17)}$, 96.5(3); $\angle\text{Cp(centroid)-Ru(1)-Ru(2)-Cp(centroid)}$, 3.16(17); $\angle\text{Cp-Cp fold angle (angle between the planes of the Cp rings)}$, 131.3(3).

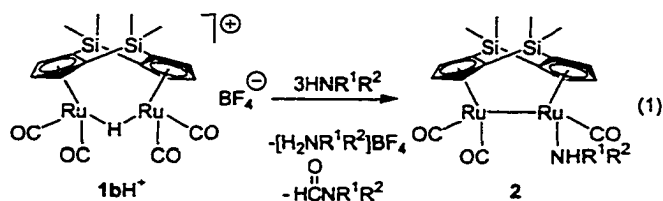
**CHAPTER 5. METAL CONTROL OF THE REACTION SITE IN
REACTIONS OF $[\{(\eta^5\text{-C}_5\text{H}_3)_2(\text{SiMe}_2)_2\}\text{M}_2(\text{CO})_4(\mu\text{-H})\}^+$ (M = Fe, Ru, Os)
WITH NUCLEOPHILIC AMINES**

A paper to be submitted to *Angewandte Chemie, International English Edition*

Maxim V. Ovchinnikov, Xiaoping Wang, Arthur J. Schultz, and Robert J. Angelici

Introduction

Transition metal hydrides have attracted a considerable amount of attention because they are important components of many catalytic and stoichiometric reactions.¹ The acidities of transition metal mono- and polyhydrides depend upon the electronic and steric properties of the complexes.² It has also been noted³ that there may be significant differences in the thermodynamic acidities (equilibrium for proton transfer) and kinetic acidities (the rate of proton transfer) of transition metal hydrides. We recently reported⁴ the synthesis of the protonated dinuclear complex $[\{(\eta^5\text{-C}_5\text{H}_3)_2(\text{SiMe}_2)_2\}\text{Ru}_2(\text{CO})_4(\mu\text{-H})\}^+ (\mathbf{1bH}^+\text{BF}_4^-)$ whose



carbon monoxide ligands are activated to attack by amine nucleophiles (eq 1) because of the positive charge on the complex and the slow rate of deprotonation of the bridging hydride by the amines. The unusually low kinetic acidity of $\mathbf{1bH}^+\text{BF}_4^-$ was explained by the bulkiness of the dimethylsilyl linkers of the $(\eta^5\text{-C}_5\text{H}_3)_2(\text{SiMe}_2)_2$ ligand and the rigidity of the molecule.

Herein we report a more detailed investigation of $\mathbf{1bH^+BF_4^-}$ and its Fe and Os analogs which lead to a more complete understanding of the low kinetic acidity of $\mathbf{1bH^+BF_4^-}$ as compared with its reactions with amines that lead to nucleophilic attack on its CO ligands (eq. 1).

Results and Discussion

An X-ray crystallographic study of complex $\mathbf{1bH^+BF_4^-}$ suggested that the bridging hydride ligand is not in the plane defined by Ru(1), Ru(2) and the centroids of the two Cp rings.⁵ Because the location of the bridging hydride ligand between the Ru atoms, as deduced from X-ray data, has a large uncertainty, a neutron diffraction study of $\mathbf{1bD^+TfO^-}$ was undertaken.^{6,7,8} The neutron diffraction data clearly establish the “off-center” position of the bridging hydride which is reflected in the angle (112.3°) between the Cp(centroid)-Ru(1)-Ru(2)-Cp(centroid) and Ru(1)-D(1)-Ru(2) planes. (Fig. 1). The “off-center” site of the hydride ligand is also supported by a long C(15)-C(18) distance (4.089 \AA) compared to the much shorter C(16)-C(17) distance (3.031 \AA). The bridging hydride ligand is located above (toward the SiMe_2 group) the C(15)-Ru(1)-Ru(2)-C(18) plane as indicated by the angle (20.66°) between this plane and the Ru(1)-D(1)-Ru(2) plane. The “off-center” location may be controlled by the tendency of both Ru atoms to adopt a pseudo-octahedral geometry, with angles of approximately 90° between the adjacent carbonyls and the Ru-H-Ru bond, and at the same time achieve a relatively short Ru-Ru distance. The bridging hydride is fluxional in solution as inferred from the ^1H and ^{13}C NMR spectra, which show, even at -50°C , only two signals for the $\text{Si}(\text{CH}_3)_2$ methyl groups in accord with the rapid movement of the bridging hydride ligand from one side to the other of the Ru-Ru vector. On the other hand, the solid-state ^{13}C NMR spectrum of $\mathbf{1bH^+BF_4^-}$ exhibits four signals (δ 0.26 br, 2.73, 8.63) for the

Si(CH₃)₂ methyl groups and ten partially overlapped Cp resonances (δ 91.79-111.34 range), as expected for the solid state structure.

Complexes **1aH⁺BF₄⁻** and **1cH⁺BF₄⁻**, the Fe and Os analogs of **1bH⁺BF₄⁻**, were synthesized as shown in Scheme 1. The structures (X-ray crystallography) and spectroscopic (NMR, IR) characteristics (Table 1, Figure 2) of **1aH⁺BF₄⁻** and **1cH⁺BF₄⁻** are very similar to those of **1bH⁺BF₄⁻**. The “off-center” location of the bridging hydride in **1aH⁺BF₄⁻** and **1cH⁺BF₄⁻** is evident from the unsymmetrical positions of the CO ligands, similar to that observed in **1bH⁺BF₄⁻**, although the hydride ligand was not located in the X-ray study of **1cH⁺BF₄⁻**. The location of the bridging hydride inside the rigid cavity created by the CO ligands and the Si(CH₃)₂ groups (Figures 1, 2) suggests that complexes **1a,cH⁺BF₄⁻** should also undergo deprotonation by basic amines very slowly; as a result, their CO ligands should be susceptible to nucleophilic attack. Surprisingly, compounds **1a,cH⁺BF₄⁻** react with amines (ammonia, MeNH₂, Me₂NH, Et₃N, morpholine) to yield only the deprotonated complexes **1a,c**. There was no evidence for nucleophilic attack on CO, such as formation of formamides or complexes of type **2** (Scheme 2), although Et₃N deprotonates the **1a,cH⁺BF₄⁻** complexes slowly ($t_{1/2} \sim 21$ h in CDCl₃).⁹

In order to understand why **1bH⁺BF₄⁻** reacts with primary and secondary amines by attack at a CO ligand (eq 1) while **1aH⁺BF₄⁻** and **1cH⁺BF₄⁻** undergo simple deprotonation with the same amines, it is necessary to consider both the relative rates of deprotonation (path 1, Scheme 2) and nucleophilic attack on the CO ligands (path 2). The rate of deprotonation, i.e. the kinetic acidity, is similar for all three complexes **1a-cH⁺BF₄⁻**.¹⁰ On the other hand, the rate of nucleophilic attack on a CO ligand depends on the electrophilicity of the CO group. The relative electrophilicities of the CO ligands in **1a-cH⁺BF₄⁻** may be estimated

from their average $\nu(\text{CO})$ values.¹¹ The higher $\nu(\text{CO})$ value for the Ru complex $\mathbf{1bH}^+\text{BF}_4^-$ (average $\nu(\text{CO}) = 2051 \text{ cm}^{-1}$) indicates that its CO ligands are more electrophilic than those in its Fe and Os analogs (average $\nu(\text{CO}) = 2044, 2038 \text{ cm}^{-1}$ respectively, Table 1). Thus, it is reasonable that $\mathbf{1bH}^+\text{BF}_4^-$ reacts with primary and secondary amines by nucleophilic attack on a CO ligand (path 2); only a small amount of deprotonation (path 1) occurs.⁴ On the other hand, the observation that $\mathbf{1aH}^+$ and $\mathbf{1cH}^+$ react with amines to give only deprotonation products (path 1) is consistent with a slower rate of amine attack on the CO ligand, as expected for these complexes with lower $\nu(\text{CO})$ values. Thus, it is the electronic activation of the CO ligands by Ru in $\mathbf{1bH}^+$ that leads to products resulting from nucleophilic attack on CO.

Conclusions

In conclusion, we have demonstrated that a CO ligand in the protonated complex $\{(\eta^5\text{-C}_5\text{H}_3)_2(\text{SiMe}_2)_2\}\text{Ru}_2(\text{CO})_4(\mu\text{-H})^+$ ($\mathbf{1bH}^+\text{BF}_4^-$) is the site of reaction with amines because of the high electrophilicity of the CO ligands and the low kinetic acidity of the bridging hydride – a unique combination of kinetic properties that are not found in the Fe and Os analogs.

Experimental Section

General procedures and syntheses of $\mathbf{1bH}^+\text{BF}_4^-$ and $\mathbf{1bD}^+\text{TfO}^-$ are reported elsewhere.^{4b}

1a: The synthesis of **1a** was adapted and improved from the literature method.¹² A mixture of $\text{Fe}_2(\text{CO})_9$ (2.00 g, 5.49 mmol) and $(\text{C}_5\text{H}_4)_2(\text{SiMe}_2)_2$ ¹³ (0.71 g, 2.86 mmol) in toluene (100 mL) was heated to reflux for 32 hours. The resulting brown precipitate was removed by filtration, and the brownish green solution was reduced to dryness. The remaining dark solid was chromatographed on an alumina column (5 × 20 cm) first with hexanes and then with a 1:10 (v/v) mixture of CH_2Cl_2 and hexanes which eluted an emerald-green band containing **1a**. Evaporation gave **1a** as a brown solid (1.80 g, 70%). ¹H NMR (400 MHz, C_6D_6): δ 0.23 (s, 6 H, Si(CH_3)), 0.41 (s, 6 H, Si(CH_3)), 4.31 (t, $J = 2.2$ Hz, 2 H, Cp- H), 4.66 (d, $J = 2.2$ Hz, 4 H, Cp- H). ¹³C NMR (100 MHz, C_6D_6): δ -3.13 (CH_3), 4.00 (CH_3), 82.84, 92.61, 94.48 (Cp), the CO resonance was not observed. IR (hexanes): $\nu(\text{CO})$ (cm^{-1}) 2015 (vs), 1961 (s). IR (solid on teflon film): $\nu(\text{CO})$ (cm^{-1}) 1982 (vs), 1942 (s), 1770 (s). Anal. Calcd for $\text{C}_{18}\text{H}_{18}\text{O}_4\text{Fe}_2\text{Si}_2$: C, 46.37; H, 3.89. Found: C, 46.25; H, 3.99.

1aH⁺BF₄⁻: A green solution of **1a** (100 mg, 0.21 mmol) in CH_2Cl_2 (20 mL) was treated with $\text{HBF}_4 \cdot \text{Et}_2\text{O}$ (28 μL , 0.25 mmol) at room temperature. A dark purple precipitate of **1aH⁺BF₄⁻** was obtained in nearly quantitative yield (107 mg, 92%) by diluting the solution with a 10-fold excess of ether (200 mL). ¹H NMR (400 MHz, CD_2Cl_2): δ -29.47 (s, 1 H, Fe- H -Fe), 0.62 (s, 6 H, Si(CH_3)), 0.75 (s, 6 H, Si(CH_3)), 5.15 (t, $J = 2.0$ Hz, 2 H, Cp- H), 5.84 (d, $J = 2.0$ Hz, 4 H, Cp- H). ¹³C NMR (100 MHz, CD_2Cl_2): δ -3.50 (CH_3), 2.07 (CH_3), 81.73, 96.38, 98.27 (Cp), 210.04 (CO). Anal. Calcd for $\text{C}_{18}\text{H}_{19}\text{BF}_4\text{O}_4\text{Fe}_2\text{Si}_2$: C, 39.02; H, 3.46. Found: C, 38.63; H, 3.20.

1c: A mixture of $\text{Os}_3(\text{CO})_{12}$ (1.00 g, 1.10 mmol), $(\text{C}_5\text{H}_4)_2(\text{SiMe}_2)_2$ (179 mg, 0.73 mmol) and methylisobutylketone (4 mL) in decane (100 mL) was heated at 150 °C for 72 hours. The black solution was filtered, and chromatographed on an alumina column (5 × 20

cm) first with hexanes and then with a 1:10 (v/v) mixture of CH₂Cl₂ and hexanes which eluted a pale yellow band containing **1c** (yellow solid; 187 mg, 35%). ¹H NMR (400 MHz, CD₃NO₂): δ 0.31 (s, 6 H, Si(CH₃)), 0.53 (s, 6 H, Si(CH₃)), 5.73 (d, *J* = 2.0 Hz, 4 H, Cp-*H*), 6.00 (t, *J* = 2.0 Hz, 2 H, Cp-*H*). IR (hexanes): ν(CO) (cm⁻¹) 2008 (vs), 1940 (s).

1cH⁺BF₄⁻: A yellow solution of **1c** (100 mg, 136 mmol) in CH₂Cl₂ (20 mL) was treated with HBF₄·Et₂O (16 μL, 149 mmol) at room temperature. A yellow precipitate of **1cH⁺BF₄⁻** was obtained in nearly quantitative yield (112 mg, 95%) by diluting the solution with a 10-fold excess of ether (200 mL). ¹H NMR (400 MHz, CD₃NO₂): δ -20.80 (s, 1 H, Os-*H*-Os), 0.54 (s, 6 H, Si(CH₃)), 0.67 (s, 6 H, Si(CH₃)), 6.23 (t, *J* = 2.0 Hz, 2 H, Cp-*H*), 6.34 (d, *J* = 2.0 Hz, 4 H, Cp-*H*). ¹³C NMR (100 MHz, CD₃NO₂): δ -2.80 (CH₃), 2.46 (CH₃), 85.92, 97.98, 99.19 (Cp), 175.09 (CO). Anal. Calcd for C₁₈H₁₉BF₄O₄Os₂Si₂·CH₂Cl₂: C, 25.14; H, 2.33. Found: C, 25.62; H, 2.38.

References

- (1) (a) Kristjánssdóttir, S. S.; Norton, J. R. In *Transition Metal Hydrides: Recent Advances in Theory and Experiments*; Dedieu, A., Ed.; VCH: New York, 1991; Chapter 10. (b) Pearson, R. G. *Chem. Rev.* **1985**, *85*, 41. (c) Martinho-Simões, J. A.; Beauchamp, J. L. *Chem. Rev.* **1990**, *90*, 629. (d) Bullock, R. M. *Comments Inorg. Chem.* **1991**, *12*, 1.
- (2) (a) Angelici, R. J. *Acc. Chem. Res.* **1995**, *28*, 52. (b) Edidin, R. T.; Sullivan, J. M.; Norton, J. R. *J. Am. Chem. Soc.* **1987**, *109*, 3945. (c) Moore, E. J.; Sullivan, J. M.; Norton, J. R. *J. Am. Chem. Soc.* **1986**, *108*, 2257. (d) Jordan, R. F.; Norton, J. R. *J. Am. Chem. Soc.* **1982**, *104*, 1255.

- (3) (a) Darensbourg, M. Y.; Ludvig, M. M. *Inorg. Chem.* **1986**, *25*, 2894. (b) Hanckel, J. M.; Darensbourg, M. Y. *J. Am. Chem. Soc.* **1983**, *105*, 6979. (c) Kristjánssdóttir, S. S.; Moody, A E.; Weberg, R. T.; Norton, J. R. *Organometallics* **1988**, *7*, 1983.
- (4) (a) Ovchinnikov, M. V.; Angelici, R. J. *J. Am. Chem. Soc.* **2000**, *122*, 6130. (b) Ovchinnikov, M. V.; Guzei, I. A.; Angelici, R. J. *Organometallics* **2001**, *20*, 691.
- (5) Crystallographic data (excluding structure factors) for the structures in this paper have been deposited with the Cambridge Crystallographic Data Centre as supplementary publication no. CCDC-163489 (**1aH⁺BF₄⁻**), CCDC-163488 (**1bH⁺BF₄⁻**; X-Ray diffraction), CCDC-163102 (**1bD⁺TfO⁻**; neutron diffraction), CCDC-163490 (**1cH⁺BF₄⁻**). Copies of the data can be obtained, free of charge, on application to CCDC, 12 Union Road, Cambridge CB2 1EZ, UK, (fax: +44 1223 336033 or e-mail: deposit@ccdc.cam.ac.uk).
- (6) Deuterated complex [$\{(\eta^5\text{-C}_5\text{H}_3)_2(\text{SiMe}_2)_2\}\text{Ru}_2(\text{CO})_4(\mu\text{-D})\}]^+\text{TfO}^-$ (**1bD⁺TfO⁻**) was used in order to simplify the refinement of the neutron diffraction data.
- (7) Yellow block, $2.8 \times 1.4 \times 0.8$ mm ($V = 3.14$ mm³), monoclinic $P2_1/n$, $a = 11.750(2)$ Å, $b = 15.488(3)$ Å, $c = 13.194(2)$ Å, $\alpha = 90^\circ$, $\beta = 92.67(1)^\circ$, $\gamma = 90^\circ$, $V = 2416.7(7)$ Å³, $Z = 4$, $\rho_{\text{calcd}} = 1.945$ g cm⁻³, $T = 20$ K, radiation: neutrons, $\lambda = 0.71 - 4.2$ Å. Neutron diffraction data were collected from a single crystal of **1bD⁺TfO⁻** at the Intense Pulsed Neutron Source (IPNS), Argonne National Laboratory. The IPNS single-crystal diffractometer (SCD) is a time-of-flight (TOF) instrument with a time- and position-sensitive detector.¹⁴ A wavelength-dependent spherical absorption correction was applied with $\mu(\lambda) = 0.908 + 0.582 \cdot \lambda$ cm⁻¹. Symmetry related reflections were not

averaged because of the wavelength dependence of extinction. A total of 4209 independent reflections were used in the structural refinement. The structure was refined with the program SHELXL97.¹⁵ In the final least-squares cycle, carbon, oxygen, fluorine and hydrogen atoms were refined with anisotropic temperature factors. The remaining heavy atoms were refined isotropically. Final $R1 = 0.084$, $wR2 = 0.156$ (for observed data with $I > 2\sigma(I)$).

- (8) For a recent review on neutron diffraction studies of transition metal hydrides, see: Bau, R.; Drabnis, M. H. *Inorg. Chim. Acta* **1997**, *259*, 27.
- (9) The acidities of $\mathbf{1a}\text{-cH}^+\text{BF}_4^-$, estimated as $\text{p}K_a(\text{H}_2\text{O})$ values from studies of the equilibrium constants for proton transfer reactions between $\mathbf{1a}\text{-cH}^+\text{BF}_4^-$ and 2-bromoaniline in CD_3CN at 25 °C, are virtually the same ($\text{p}K_a(\text{H}_2\text{O}) = 1.7(\pm 0.9)$ ($\mathbf{1aH}^+\text{BF}_4^-$), $1.0(\pm 0.5)$ ($\mathbf{1bH}^+\text{BF}_4^-$), $1.1(\pm 0.8)$ ($\mathbf{1aH}^+\text{BF}_4^-$)). However, these $\text{p}K_a(\text{H}_2\text{O})$ values represent *only approximate* thermodynamic acidities of $\mathbf{1a}\text{-cH}^+\text{BF}_4^-$ due to the long reaction times (several months) and the uncertainty about their completion.
- (10) All of the complexes $\mathbf{1a}\text{-cH}^+\text{BF}_4^-$ undergo complete deprotonation in $\text{DMSO-}d_6$ solution, where the $\text{DMSO-}d_6$ is both the solvent and the base ($\text{p}K_a(\text{H}_2\text{O}) = -1.8$); Perrin, D. D. *Dissociation Constants of Organic Bases in Aqueous Solution*; Butterworths: London, 1972), at approximately the same rate ($t_{1/2} \sim 7.5$ h).
- (11) Angelici, R. J. *Acc. Chem. Res.* **1972**, *5*, 335.
- (12) Siemeling, U.; Jutzi, P.; Neumann, B.; Stammer, H. G.; Hursthouse, M. B. *Organometallics* **1992**, *11*, 1328.
- (13) Hiermeier, J.; Koehler, F. H.; Mueller, G. *Organometallics* **1991**, *10*, 1787.

- (14) Schultz, A. J. *Trans. Am. Cryst. Assoc.* **1993**, 29, 29.
- (15) *SHELXL-97 – A program for crystal structure refinement*. Release 97-2. Sheldrick, G. M., Institut für Anorganische Chemie der Universität, Göttingen, Germany, 1998.

Table 1. Selected Properties of $[\{(\eta^5\text{-C}_5\text{H}_3)_2(\text{SiMe}_2)_2\}\text{M}_2(\text{CO})_4(\mu\text{-H})]^+ \mathbf{1a}\text{-cH}^+\text{BF}_4^-$ (M = Fe (a), Ru (b), Os (c)).

	1aH⁺BF₄⁻	1bH⁺BF₄⁻	1cH⁺BF₄⁻
M-M, Å	2.999	3.1210(5)	3.0933(3)
M-H, Å	1.601, 1.660	1.728(5)	-
C(16)-C(17), Å	2.935	3.031	2.982
C(15)-C(18), Å	3.695	4.089	4.118
$\nu(\text{CO}), \text{cm}^{-1}$ (CH ₂ Cl ₂)	2069 (vs), 2039 (w), 2025 (s)	2077 (vs), 2050 (w), 2027 (s)	2067 (vs), 2036 (w), 2011 (s)
Average $\nu(\text{CO}), \text{cm}^{-1}$	2044	2051	2038

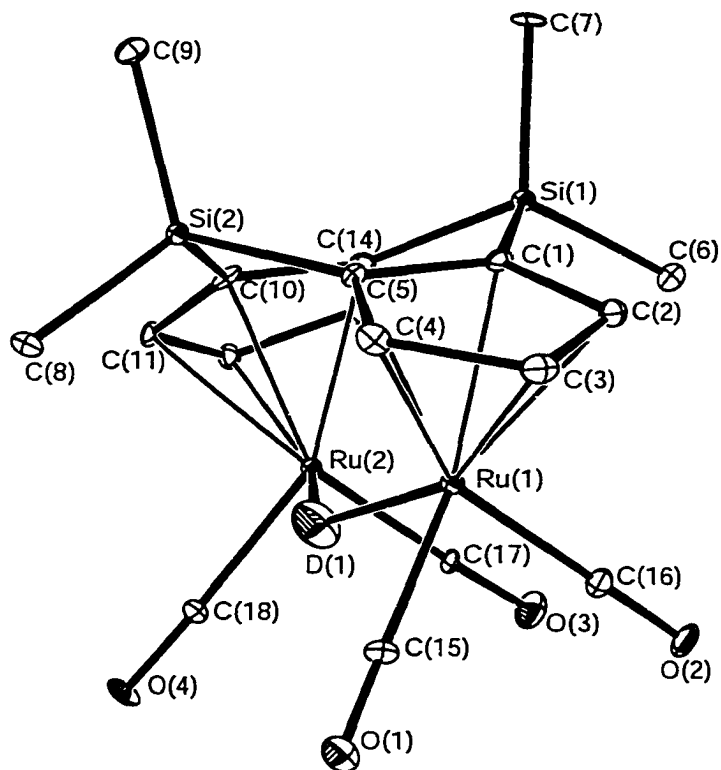


Figure 1. Molecular structure of $1bD^+TfO^-$ as determined by neutron diffraction. Thermal ellipsoid drawing, with 50% probability ellipsoids, of $[\{(\eta^5-C_5H_3)_2(SiMe_2)_2\}Ru_2(CO)_4(\mu-D)]^+$ in $1bD^+TfO^-$ showing the labeling scheme. Selected bond distances [\AA] and angles [$^\circ$] are as follows: Ru(1)-Ru(2), 3.103(3); Ru(1)-D(1), 1.741(4); Ru(2)-D(1), 1.768(5); Ru(1)-C(15), 1.909(4); Ru(1)-C(16), 1.889(4); Ru(2)-C(17), 1.904(4); Ru(1)-C(18), 1.910(4); Ru(1)-Cp(centroid), 1.880(2); Ru(2)-Cp(centroid), 1.877(3); $\angle Ru(1)-D(1)-Ru(2)$, 124.3(3); $\angle C(15)-Ru(1)-D(1)$, 80.2(2); $\angle C(16)-Ru(1)-D(1)$, 96.4(2); $\angle C(15)-Ru(1)-C(16)$, 89.3(2); $\angle C(17)-Ru(2)-D(1)$, 100.4(2); $\angle C(18)-Ru(2)-D(1)$, 77.4(2); $\angle C(17)-Ru(2)-C(18)$, 91.0(2); $\angle C(16)-Ru(1)-Ru(2)-C(17)$, 0.25(19); $\angle C(15)-Ru(1)-Ru(2)-C(18)$, 2.75(19); $\angle Cp(\text{centroid})-Ru(1)-Ru(2)-Cp(\text{centroid})$, 1.3(2); $\angle Cp-Cp$ fold angle (angle between the planes of the Cp rings), 131.1(1).

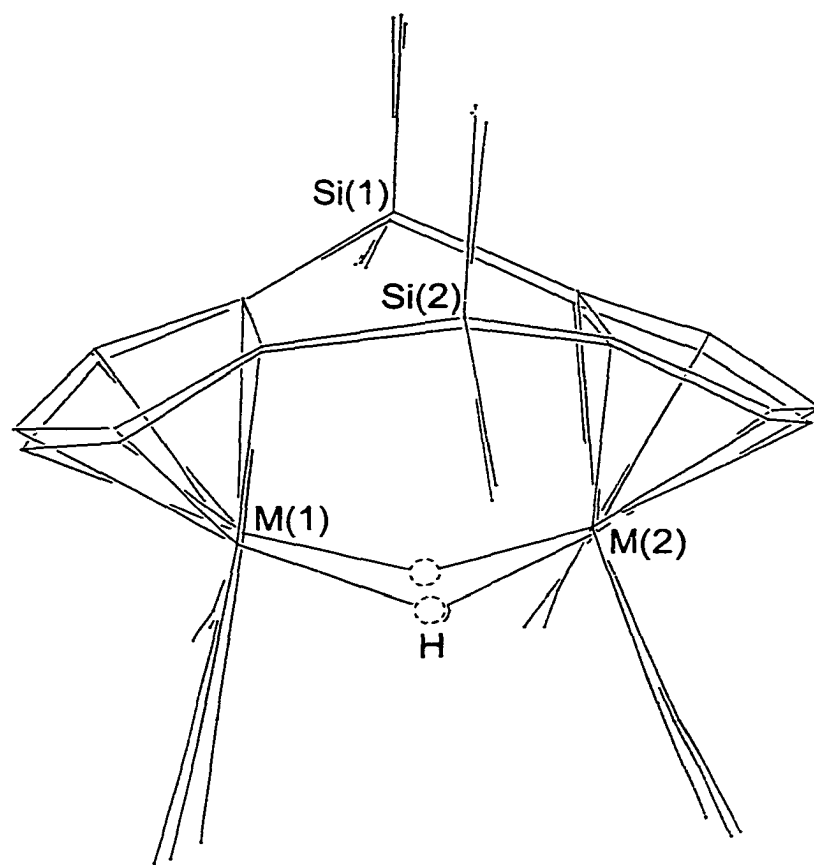
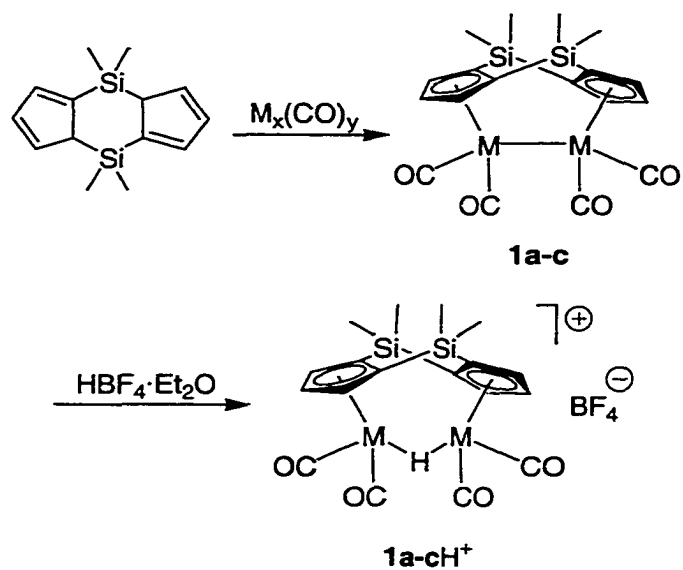
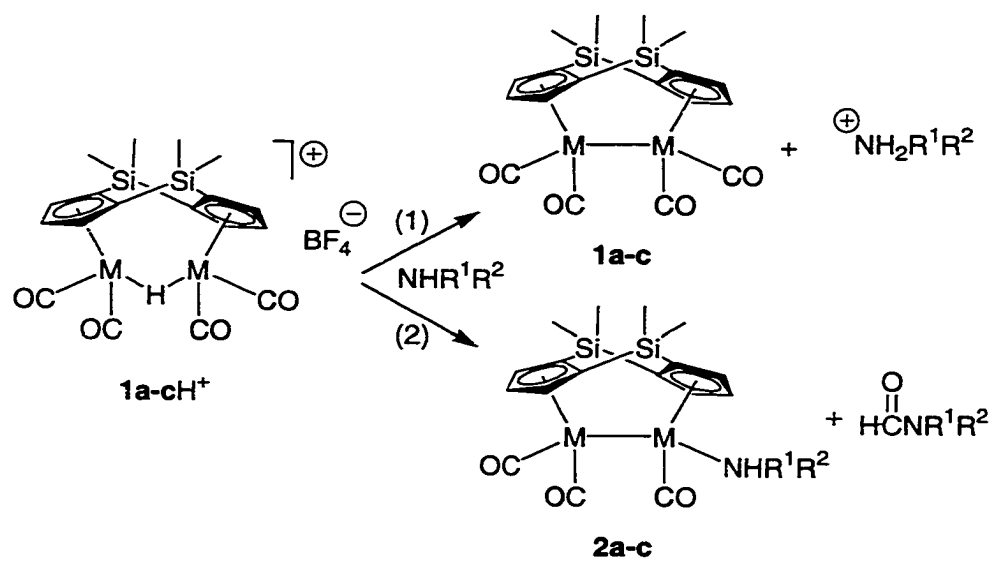


Figure 2. Overlay of the structures of $1aH^+BF_4^-$, $1bD^+TfO^-$, and $1cH^+BF_4^-$ illustrating the similarities in their molecular structures.



Scheme 1. Synthesis of complexes **1a-c** and **1a-cH⁺BF₄⁻** (M = Fe (a), Ru (b), Os (c)).



Scheme 2

**CHAPTER 6. REACTIONS OF THE PROTONATED DINUCLEAR
RUTHENIUM COMPLEX $[\{(\eta^5\text{-C}_5\text{H}_3)_2(\text{SiMe}_2)_2\}\text{Ru}_2(\text{CO})_4(\mu\text{-H})]^+$ WITH
NUCLEOPHILES**

A paper to be submitted to *Inorganic Chemistry*¹

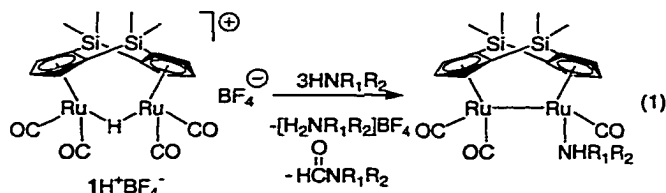
Maxim V. Ovchinnikov, Arkady M. Ellern, Ilia A. Guzei, and Robert J. Angelici

Introduction

Nucleophilic attack on coordinated ligands is a reaction common to a number of transition metal complexes and constitutes a transformation of synthetic importance.¹ One of the simplest approaches to making a complex more positive, and thus more susceptible to nucleophilic attack, is to add a proton (H^+) to the metal center and/or the metal-metal bond.² However, most protonated metal complexes either do not undergo nucleophilic attack because they are not electrophilic enough or basic nucleophiles, which are usually also good bases, simply deprotonate the metal to give the unreactive neutral metal complex. We recently reported³ the synthesis of the cationic dinuclear complex $[\{(\eta^5\text{-C}_5\text{H}_3)_2(\text{SiMe}_2)_2\}\text{Ru}_2(\text{CO})_4(\mu\text{-H})]^+\text{BF}_4^-$ ($\text{1H}^+\text{BF}_4^-$) whose carbon monoxide ligands are activated to nucleophilic attack by amines (eq 1) because of the positive charge on the complex and the relatively slow rate of deprotonation of the bridging hydride by the amines.

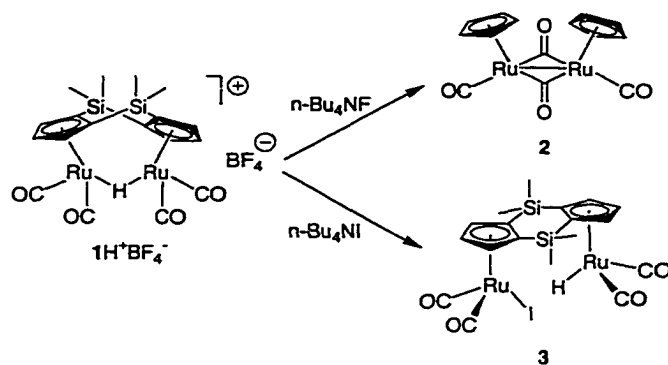
¹ Reproduced with permission from *Inorganic Chemistry*, to be submitted for publication.

In this paper we report different types of reactions of $1\text{H}^+\text{BF}_4^-$ with nucleophiles (halide anions, nucleophilic phosphines, ^-OMe , ^-SMe) to give a variety of new complexes. While the reaction in eq (1) illustrates amine attack on a CO ligand of $1\text{H}^+\text{BF}_4^-$, the reactions in the present paper show that other nucleophiles add to the Ru or to the Si atom of the linking (η^5 - C_5H_3) $_2(\text{SiMe}_2)_2$ ligand.



Results and Discussion

Reactions of $\{[(\eta^5\text{-C}_5\text{H}_3)_2(\text{SiMe}_2)_2]\text{Ru}_2(\text{CO})_4(\mu\text{-H})\}^+\text{BF}_4^-$ ($1\text{H}^+\text{BF}_4^-$) with Halide Anions ($n\text{-Bu}_4\text{NX}$; X = F, Cl, Br, I). Synthesis of $\{[(\eta^5\text{-C}_5\text{H}_3)_2(\text{SiMe}_2)_2]\text{Ru}_2(\text{CO})_4(\text{H})(\text{I})\}$ (3). Complex $1\text{H}^+\text{BF}_4^-$ reacts with an excess of $n\text{-Bu}_4\text{NF}$ in THF to give the simple (η^5 - C_5H_3) $_2\text{Ru}_2(\text{CO})_4$ (2)⁴ complex (Scheme 1) as the only Ru-containing product. The reaction is very fast and exothermic. Presumably, this reaction proceeds by initial F^- cleavage of the SiMe_2 groups followed by fast deprotonation of the protonated intermediate complex $\{[(\eta^5\text{-C}_5\text{H}_3)_2\text{Ru}_2(\text{CO})_4(\mu\text{-H})]^+\}$ by F^- . Water, which is present in and cannot be removed from the commercial solution of $n\text{-Bu}_4\text{NF}$ in THF, serves as the proton source for this reaction. Formation of complex **2** is not surprising since F^- is a known reagent for the deprotection of silylated substrates;⁵ the deprotonated complex $\{[(\eta^5\text{-C}_5\text{H}_3)_2(\text{SiMe}_2)_2]\text{Ru}_2(\text{CO})_4$ (**1**) also reacts rapidly with $n\text{-Bu}_4\text{NF}$ to give **2**.

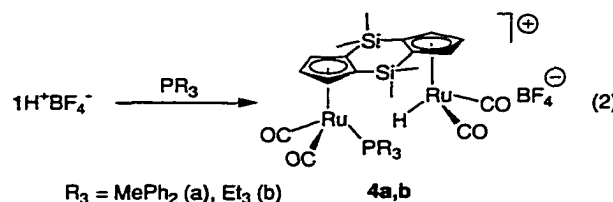


Scheme 1

Reactions of $1\text{H}^+\text{BF}_4^-$ with Cl^- or Br^- proceed to give the deprotonated complex **1** as the only product at extremely slow rates ($t_{1/2} > 24$ h) at room temperature. On the other hand, reaction of $1\text{H}^+\text{BF}_4^-$ with I^- gives within 24 h a 55% yield of $\{(\eta^5\text{-C}_5\text{H}_3)_2(\text{SiMe}_2)_2\}\text{-Ru}_2(\text{CO})_4(\text{H})(\text{I})$ (**3**) as a mildly air-sensitive solid (Scheme 1). The only other Ru-containing product is the deprotonated complex **1** (30%) resulting from the deprotonation of $1\text{H}^+\text{BF}_4^-$ by I^- . The IR spectrum of **3** in hexanes solutions shows the expected four strong $\nu(\text{CO})$ absorptions of equal intensities corresponding to the $(\eta^5\text{-C}_5\text{H}_3)\text{Ru}(\text{CO})_2(\text{I})$ ($2050, 2004\text{ cm}^{-1}$) and $(\eta^5\text{-C}_5\text{H}_3)\text{Ru}(\text{CO})_2(\text{H})$ ($2035, 1977\text{ cm}^{-1}$) portions of the molecule; these assignments are based on a comparison with $\nu(\text{CO})$ bands for $\text{CpRu}(\text{CO})_2(\text{I})$ ($2048, 1997\text{ cm}^{-1}$)⁶ and $\text{CpRu}(\text{CO})_2(\text{H})$ ($2023, 1958\text{ cm}^{-1}$).⁴ The ^1H NMR spectrum of **3** at room temperature shows two sets of doublets and triplets in the range δ 5.34–5.91 ppm for the protons of each cyclopentadienyl ring, consistent with two nonequivalent ABB' spin systems. The Ru-H resonance occurs as a singlet at δ –10.84 ppm.

Reactions of $\{(\eta^5\text{-C}_5\text{H}_3)_2(\text{SiMe}_2)_2\}\text{Ru}_2(\text{CO})_4(\mu\text{-H})^+\text{BF}_4^-$ ($1\text{H}^+\text{BF}_4^-$) with

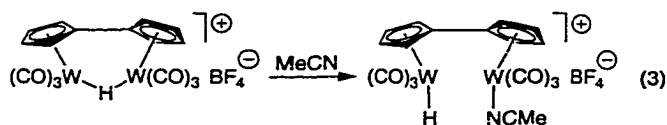
Phosphines (PEt₃, PMePh₂). Synthesis of $[(\eta^5\text{-C}_5\text{H}_3)_2(\text{SiMe}_2)_2]\text{Ru}_2(\text{CO})_4(\text{H})(\text{PR}_3)]^+$ (4a,b**).** We reported³ that the $\text{p}K_a$ of $1\text{H}^+\text{BF}_4^-$ could be determined by studying the proton transfer reaction between PPh_3 and $1\text{H}^+\text{BF}_4^-$. Over the course of these studies we observed trace sideproducts that appeared to contain both $\eta^1\text{-H}$ and $\eta^1\text{-PPh}_3$ ligands. Therefore we sought to investigate the reactivity of $1\text{H}^+\text{BF}_4^-$ with more nucleophilic and less bulky phosphines.



When $1\text{H}^+\text{BF}_4^-$ and PR_3 (PMe_3 , PEt_3 , PMe_2Ph , PMePh_2) are allowed to react in acetonitrile (5-50 min for PMe_3 , PEt_3 ; 2-6 h for PMe_2Ph ; 6-48 h for PMePh_2), complexes $[(\eta^5\text{-C}_5\text{H}_3)_2(\text{SiMe}_2)_2]\text{Ru}_2(\text{CO})_4(\text{H})(\text{PR}_3)]^+$ (**4a,b**; $\text{R}_3 = \text{MePh}_2$ (**a**), Et_3 (**b**)) are obtained in 95% yields as air-sensitive colorless crystalline solids (eq 2). Their IR spectra in CH_3CN solution show the expected four strong $\nu(\text{CO})$ absorptions corresponding to the $[(\eta^5\text{-C}_5\text{H}_3)\text{Ru}(\text{CO})_2(\text{PR}_3)]^{+7}$ and $(\eta^5\text{-C}_5\text{H}_3)\text{Ru}(\text{CO})_2(\text{H})$ moieties. An X-ray structural determination of **4a** shows (Figure 1, Table 1) that the asymmetric unit contains two different molecules. In each of these molecules the Ru atoms exhibit a three-legged piano-stool geometry. The most interesting feature of the structure is the almost flat conformation of the $(\eta^5\text{-C}_5\text{H}_3)_2(\text{SiMe}_2)_2$ ligand ($\angle\text{Cp-Cp}$ fold angle = 170.09°), which is consistent with the long Ru-Ru nonbonding distance ($4.662(9)$ Å). The cyclopentadienyl rings of the bridging ligand are not twisted with respect to each other, which is evident in the torsion angle $\angle\text{Cp}(\text{centroid})\text{-Ru}(1)\text{-Ru}(2)\text{-Cp}(\text{centroid})$ (0.7°). Such a small twist may reflect the lack of

steric repulsions between the cisoid $\text{Ru}(\text{CO})_2\text{H}$ and $\text{Ru}(\text{CO})_2(\text{PMePh}_2)$ units. The absence of the deprotonated complex **1** product in eq (2) indicates that the cleavage reactions are faster than the rates of deprotonation of $1\text{H}^+\text{BF}_4^-$ by phosphines. It is worth mentioning that the reaction completion times were inconsistent from run to run under identical experimental conditions and varied greatly for unknown reasons. Because of this, attempted kinetic studies of the reaction of $1\text{H}^+\text{BF}_4^-$ with PMePh_2 were unsuccessful. Presumably, these reactions are catalyzed by unidentified reaction sideproduct(s), which are not observed during the course of or at the end of the reaction.

The observed cleavage (Scheme 1 and eq 2) of the protonated Ru-Ru bond in $[\{(\eta^5\text{-C}_5\text{H}_3)_2(\text{SiMe}_2)_2\}\text{Ru}_2(\text{CO})_4(\mu\text{-H})]^+ (\text{1H}^+\text{BF}_4^-)$ by Γ and phosphines is a relatively rare type of reaction. To the best of our knowledge, only one other example of this type of cleavage has been reported (eq 3).⁸ It involves a hydride-bridged fulvalene di-tungsten complex which reacts with

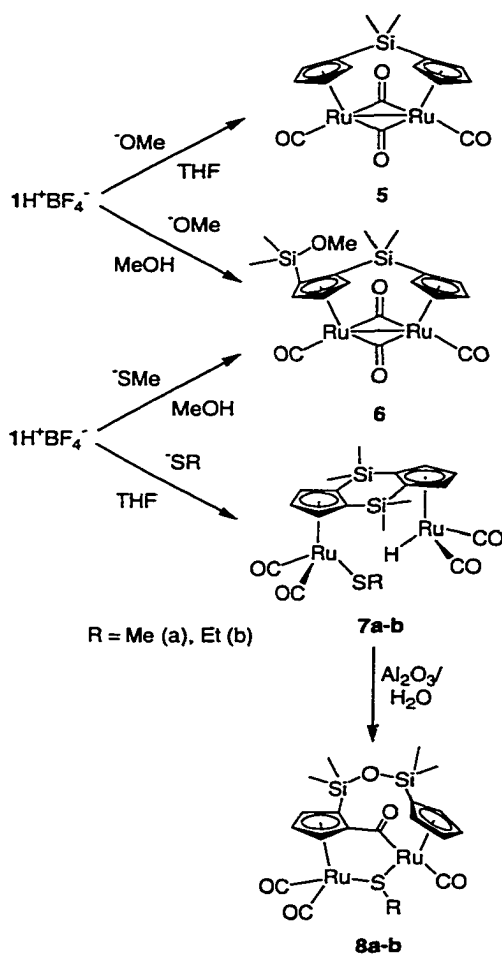


acetonitrile to give the cleavage product. There was no reaction of the following potential ligands with $1\text{H}^+\text{BF}_4^-$ at room temperature within 24 hours: pyridine, MeCN, C_2H_4 , phenylacetylene.

Reactions of $[\{(\eta^5\text{-C}_5\text{H}_3)_2(\text{SiMe}_2)_2\}\text{Ru}_2(\text{CO})_4(\mu\text{-H})]^+\text{BF}_4^-$ ($1\text{H}^+\text{BF}_4^-$) with NaOMe and NaSMe. Synthesis of $\{\mu\text{-}\eta^5:\eta^5\text{-(C}_5\text{H}_3\text{SiMe}_2\text{OMe)(C}_5\text{H}_4\text{)SiMe}_2\}\text{Ru}_2(\text{CO})_4$ (6**) and $\{\mu\text{-}\eta^5:\eta^1:\eta^5\text{-(C}_5\text{H}_3\text{C=O)(C}_5\text{H}_4\text{)(SiMe}_2\text{)O}\}\text{Ru}_2(\mu\text{-SR})(\text{CO})_3$ (**8a,b**; $\text{R} = \text{Me, Et}$). It is well-known^{1a} that electropositive transition metal complexes undergo nucleophilic attack by**

alkoxide anions on coordinated alkene and CO ligands. In contrast, when complex and NaOMe are reacted in THF for 10 min, $\{(\eta^5\text{-C}_5\text{H}_4)_2\text{SiMe}_2\}\text{Ru}_2(\text{CO})_4$ (**5**) is obtained as the only isolated product in 42% yield as an air-stable yellow crystalline solid (Scheme 2).

Complex **5**, which was previously reported,⁹ is readily identified by its IR spectrum (2005 (vs), 1966 (vs), 1936 (m) and 1758 (m) cm^{-1}) and the characteristic AA'BB' (δ 5.66-5.06 ppm range) spin system in its ^1H NMR spectrum. It is unclear how this reaction proceeds from a mechanistic point of view since the formation of each molecule of **5** requires



Scheme 2

two protons and the starting complex $1\text{H}^+\text{BF}_4^-$ can provide only one proton. Assuming the yield of **5** would be higher if the reaction were conducted in a protic medium, we investigated the reaction of $1\text{H}^+\text{BF}_4^-$ with NaOMe in MeOH solvent. Surprisingly, a mixture of **1** and the monolinked complex $\{\mu\text{-}\eta^5\text{:}\eta^5\text{-(C}_5\text{H}_3\text{SiMe}_2\text{OMe)(C}_5\text{H}_4\text{)SiMe}_2\}\text{Ru}_2(\text{CO})_4$ (**6**) was isolated in an approximately 1:2 ratio (Scheme 2). Complex **6**, which is isolated in 58% yield as yellow, air-sensitive crystals, was identified by the characteristic patterns in its ^1H NMR and IR spectra. The IR spectrum of **6** in hexanes shows $\nu(\text{CO})$ absorptions at 2019 (vs), 2008 (s), 1971 (s), 1950 (s), 1940 (m), 1795 (m) cm^{-1} which corresponds to both terminal and bridging CO ligands. The ^1H NMR spectrum of **6** exhibits resonances for the inequivalent “ C_5H_3 ” and “ C_5H_4 ” Cp rings (each displays a unique ABC and ABCD splitting pattern) and four signals for the $\text{Si}(\text{CH}_3)_2$ methyl groups in the δ 0.26-0.47 range. The δ 3.56 singlet is assigned to the MeO group. Although a detailed mechanism for the reaction of $1\text{H}^+\text{BF}_4^-$ with MeO^- is undoubtedly complex, it presumably involves initial attack by the MeO^- on a linking SiMe_2 group followed by proton transfer to the Cp ring.

A single crystal X-ray structural determination (Figure 2, Table 1)¹⁰ of **6** shows that the Ru-Ru distance in **6** (2.7049(3) Å) is the same as that (2.7042(4) Å) in complex **5**. In fact both structures are almost identical in terms of the corresponding bond distances and angles. There is only a small twist around the Ru-Ru axis; this is reflected in the small $\angle\text{Cp}(\text{centroid})\text{-Ru}(1)\text{-Ru}(2)\text{-Cp}(\text{centroid})$ torsion angle (8.0°).

Complex $1\text{H}^+\text{BF}_4^-$ reacts with NaSMe in MeOH to give the same products as those obtained from the reactions of $1\text{H}^+\text{BF}_4^-$ with NaOMe in MeOH: a mixture of complexes **1** (33%) and **6** (51%) in approximately the same 1:2 ratio. This observation suggests that MeO^-

acts as the nucleophile in both reactions. However, the reaction between $\text{1H}^+\text{BF}_4^-$ and NaSMe in THF leads to $\{(\eta^5\text{-C}_5\text{H}_3)_2(\text{SiMe}_2)_2\}\text{Ru}_2(\text{CO})_4(\text{H})(\text{SMe})$ (**7a**). Spectroscopic features of **7a** are similar to those of complex **3**. The ^1H NMR spectrum of **7a** exhibits resonances for the inequivalent Cp rings (each displays a unique AB_2 splitting pattern), two signals for the $\text{Si}(\text{CH}_3)_2$ methyl groups at δ 0.33 and 0.59, and a characteristic upfield signal for the hydride ligand at δ -10.66. The IR spectrum of **7a** in hexanes solutions shows the expected four strong $\nu(\text{CO})$ absorptions of equal intensities corresponding to the $(\eta^5\text{-C}_5\text{H}_3)\text{Ru}(\text{CO})_2(\text{SMe})$ (2044, 1995 cm^{-1}) and $(\eta^5\text{-C}_5\text{H}_3)\text{Ru}(\text{CO})_2(\text{H})$ (2035, 1977 cm^{-1}) moieties. Attempts to isolate pure **7a** were unsuccessful due in part to the fact that this compound undergoes structural rearrangement on contact with neutral and basic alumina or silica during routine column chromatography to give complex **8a**. Complex **7b** undergoes the same transformation.

The structure of **8a** (Figure 3, Table 1) was conclusively established by an X-ray crystallographic analysis. The two ruthenium atoms are bridged by the $\mu\text{-SMe}$ group and by the $\{\mu\text{-}\eta^5\text{:}\eta^1\text{:}\eta^5\text{-(C}_5\text{H}_3\text{C=O)(C}_5\text{H}_4\text{)(SiMe}_2\text{)}_2\text{O}\}$ ligand, which binds in a η^5 fashion to Ru(1) and $\eta^5\text{:}\eta^1$ to Ru(2). The Ru(1)-S(1) and Ru(2)-S(1) distances are slightly different (2.3809(6) and 2.3450(6) Å); the $\mu\text{-SMe}$ ligand exhibits a trigonal-pyramidal geometry about the sulfur (pseudo- sp^3 hybridization). This geometry is indicated by the sum of the angles around the S atom (325.8°), which is considerably smaller than the 360° expected for an sp^2 -hybridized sulfur. Both Ru atoms exhibit a three-legged piano-stool geometry with approximately 90° ($\pm 5^\circ$) angles between the non-cyclopentadienyl ligands.

The IR spectrum of **8a** in hexanes shows $\nu(\text{CO})$ absorptions at 2038 (vs), 1992 (vs),

1934 (m) cm^{-1} , which corresponds to the three terminal CO ligands, and at 1591 (w) cm^{-1} , which is assigned to the acyl CO group. The ^1H NMR spectrum of **8a** exhibits seven resonances for the inequivalent Cp rings (they display unique ABC and ABCD splitting patterns), four signals for the $\text{Si}(\text{CH}_3)_2$ methyl groups in the δ 0.35-0.42 range, and a signal at δ 2.41 which corresponds to the μ -SMe group.

The observed conversion of **7** to **8** is a complicated transformation for which a mechanism is not obvious. Presumably, water on the alumina surface serves as the source of the oxygen atom for the construction of the $\text{SiMe}_2\text{OSiMe}_2$ link.

Conclusions

The dinuclear ruthenium complex $[\{(\eta^5\text{-C}_5\text{H}_3)_2(\text{SiMe}_2)_2\}\text{Ru}_2(\text{CO})_4(\mu\text{-H})]^+\text{BF}_4^-$ ($1\text{H}^+\text{BF}_4^-$) is activated to react with nucleophiles as a result of the bridging proton, which is kinetically slow to be deprotonated by bases/nucleophiles. As shown previously (eq 1), amines react with $1\text{H}^+\text{BF}_4^-$ by attacking a CO ligand. On the other hand, I^- , RS^- and phosphines add (Schemes 1, 2; eq 2) at one of the Ru centers, resulting in cleavage of the Ru-H-Ru bond. The final type of addition to $1\text{H}^+\text{BF}_4^-$ is that exhibited by MeO^- and F^- , which results in cleavage of Si-C(cyclopentadienyl) bonds to give **6** and $(\eta^5\text{-C}_5\text{H}_5)_2\text{Ru}_2(\text{CO})_4$. Except for the reaction with F^- , all of these types of reactions depend on the presence of the proton on the Ru-Ru bond (Scheme 1). The unprotonated $(\eta^5\text{-C}_5\text{H}_3)_2(\text{SiMe}_2)_2\text{Ru}_2(\text{CO})_4$ (**1**) undergoes no reactions with these nucleophiles (except F^-) under the mild room-temperature conditions of these studies.

Experimental Part

General Procedures. All reactions were performed under an argon atmosphere in reagent grade solvents, using standard Schlenk or dry-box techniques.¹¹ Hexanes, methylene chloride and diethyl ether were purified by the Grubbs method prior to use.¹² All other solvents were purified by published methods.¹³ Chemicals were purchased from Aldrich Chemical Co., unless otherwise mentioned, or prepared by literature methods, as referenced below. Alumina (neutral, activity I, Aldrich) was degassed under vacuum for 12 h and treated with Ar-saturated water (7.5 % w/w). ¹H and ¹³C NMR spectra were recorded on a Bruker DRX-400 spectrometer using deuterated solvents as internal references. Solution infrared spectra were recorded on a Nicolet-560 spectrometer using NaCl cells with 0.1 mm spacers. Elemental analyses were performed on a Perkin Elmer 2400 series II CHNS/O analyzer.

Reaction of 1H⁺ with n-Bu₄NF. A suspension of 1H⁺BF₄⁻ (10.0 mg, 15.5 μmol) in THF (50 mL) was treated with a solution of n-Bu₄NF in THF (0.2 mL, 1.0 M). The resulting orange solution contained mainly (η^5 -C₅H₅)₂Ru₂(CO)₄ (**2**), as indicated by IR bands at 2005 (vs), 1966 (vs), 1936 (m) and 1758 (m) cm⁻¹, which are characteristic of **2**.⁴

Reaction of 1H⁺ with n-Bu₄NI. Synthesis of {(η^5 -C₅H₃)₂(SiMe₂)₂}Ru₂(CO)₄(H)(I) (3**).** A solution of 1H⁺BF₄⁻ (50.0 mg, 77.5 μmol) and n-Bu₄NI (300 mg, 0.8 mmol) in CH₂Cl₂ (30 mL) was stirred for 24 hours. Solvent was removed under vacuum; the resulting yellow residue was redissolved in hexanes/CH₂Cl₂ (10:1) (5 mL) and chromatographed on an alumina column (20 × 1 cm) with hexanes/CH₂Cl₂ (10:1) as the eluent. A yellow band was eluted and collected. Then, a dark-yellow band was eluted with hexanes/CH₂Cl₂ (4:1). From

the first fraction, 13 mg (30%, based on $1\text{H}^+\text{BF}_4^-$) of **1** were obtained. From the second fraction, 29 mg (55%, based on $1\text{H}^+\text{BF}_4^-$) of pale yellow crystalline **3** were obtained. ^1H NMR (400 MHz, CDCl_3): δ -10.84 (s, 1 H, Ru-*H*), 0.36 (s, 6 H, Si(CH_3)), 0.57 (s, 6 H, Si(CH_3)), 5.34 (d, $J = 2.4$ Hz, 2 H, Cp), 5.55 (d, $J = 2.4$ Hz, 2 H, Cp), 5.77 (t, $J = 2.4$ Hz, 1 H, Cp), 5.91 (t, $J = 2.4$ Hz, 1 H, Cp). IR (hexanes): $\nu(\text{CO})$ (cm^{-1}) 2050 (vs), 2035 (vs), 2004 (vs), 1977 (vs). Anal. Calcd for $\text{C}_{18}\text{H}_{19}\text{IO}_4\text{Ru}_2\text{Si}_2 \cdot \frac{1}{2}\text{CH}_2\text{Cl}_2$: C, 30.56; H, 2.77. Found: C, 30.95; H, 2.74.

Synthesis of $[(\eta^5\text{-C}_5\text{H}_3)_2(\text{SiMe}_2)_2]\text{Ru}_2(\text{CO})_4(\text{H})(\text{PMePh}_2)]\text{BF}_4$ (4a**).** A yellow solution of $1\text{H}^+\text{BF}_4^-$ (120 mg, 0.19 mmol) and PMePh_2 (39 μL , 0.20 mmol) in CH_3CN (50 mL) was stirred for 6-20 h at ambient temperature. The reaction was followed by IR until the starting complex $1\text{H}^+\text{BF}_4^-$ disappeared. The resulting pale yellow solution was filtered through a short pad of Celite, and the filtrate was layered with Et_2O (200 mL) to precipitate (**4a**) as colorless crystals (149 mg, 95%). ^1H NMR (400 MHz, CD_3CN): δ -10.34 (s, 1 H, Ru-*H*), 0.39 (s, 6 H, Si(CH_3)), 0.60 (s, 6 H, Si(CH_3)), 2.44 (d, $J = 10.8$ Hz, 3 H, PCH_3), 5.70 (m, 5 H, Cp-*H*), 5.89 (t, $J = 2.4$ Hz, 1 H, Cp-*H*), 5.56 (m, 10 H, PPh_2). $^{31}\text{P}\{^1\text{H}\}$ NMR (162 MHz, CD_3CN): δ 30.68 (s, PMePh_2). IR (CH_3CN): $\nu(\text{CO})$ (cm^{-1}) 2058 (vs), 2025 (vs), 2009 (vs), 1961 (vs). Anal. Calcd for $\text{C}_{31}\text{H}_{32}\text{BF}_4\text{O}_4\text{PRu}_2\text{Si}_2 \cdot \text{CH}_3\text{CN}$: C, 44.75; H, 3.98. Found: C, 44.59; H, 3.93. Crystals of **4a** suitable for X-ray diffraction analysis were obtained by slow cooling of a saturated solution of **4a** in $\text{Et}_2\text{O}/\text{CH}_2\text{Cl}_2/\text{MeCN}$ (10:2:1) to -20°C .

Synthesis of $[(\eta^5\text{-C}_5\text{H}_3)_2(\text{SiMe}_2)_2]\text{Ru}_2(\text{CO})_4(\text{H})(\text{PEt}_3)]\text{BF}_4$ (4b**).** By reacting PEt_3 (19 μL , 0.17 mmol) with complex $1\text{H}^+\text{BF}_4^-$ (100 mg, 0.16 mmol) in CH_3CN (30 mL), **4b** (112 mg, 95%; colorless solid) was prepared and isolated using the same methods as for the

preparation of **4a**. ^1H NMR (400 MHz, CD_3CN): δ -10.77 (s, 1 H, Ru-*H*), 0.39 (s, 6 H, Si(CH_3)), 0.59 (s, 6 H, Si(CH_3)), 1.13 (dt, $J = 7.2, 20.8$ Hz, 9 H, PCH_2CH_3), 2.07 (dq, $J = 7.2, 9.6$ Hz, 6 H, PCH_2CH_3), 5.69 (d, $J = 2.4$ Hz, 2 H, Cp-*H*), 5.76 (d, $J = 2.4$ Hz, 2 H, Cp-*H*), 5.90 (t, $J = 2.4$ Hz, 1 H, Cp-*H*), 6.00 (m, 1 H, Cp-*H*). $^{31}\text{P}\{^1\text{H}\}$ NMR (162 MHz, CD_3CN): δ 47.52 (s, PEt_3). IR (CH_3CN): $\nu(\text{CO})$ (cm^{-1}) 2052 (vs), 2024 (vs), 2001 (vs), 1961 (vs).

Reaction of $1\text{H}^+\text{BF}_4^-$ with NaOMe. Method 1. Solid NaOMe (10.0 mg, 185 μmol) was added to a suspension of $1\text{H}^+\text{BF}_4^-$ (50.0 mg, 77.6 μmol) in THF (50 mL), and the mixture was stirred for 10 min. The resulting orange solution contained mainly $\{(\eta^5\text{-C}_5\text{H}_4)_2\text{SiMe}_2\}\text{Ru}_2(\text{CO})_4$ (**5**), as indicated by IR bands at 2005 (vs), 1966 (vs), 1936 (m) and 1758 (m) cm^{-1} . After the solvent was removed under vacuum, the mixture was chromatographed on an alumina column (20 \times 1 cm) first with hexanes and then with hexanes/ CH_2Cl_2 (5:1) which eluted a yellow band containing **5** (17 mg, 42%). Its IR and ^1NMR spectra are the same as those previously reported⁹ for this compound.

Method 2. Synthesis of $\{\mu\text{-}\eta^5\text{:}\eta^5\text{-}(\text{C}_5\text{H}_3\text{SiMe}_2\text{OMe})(\text{C}_5\text{H}_4)\text{SiMe}_2\}\text{Ru}_2(\text{CO})_4$ (6**).** Solid NaOMe (10.0 mg, 185 μmol) was added to a solution of $1\text{H}^+\text{BF}_4^-$ (50.0 mg, 77.6 μmol) in MeOH (50 mL), and the mixture was stirred for 10 min. Solvent was removed under vacuum; the resulting yellow residue was dissolved in hexanes (2 mL) and chromatographed on an alumina column (20 \times 1 cm) with hexanes/ CH_2Cl_2 (10:1) as the eluent. A yellow band was eluted and collected. Then, a second yellow band was eluted with hexanes/ CH_2Cl_2 (5:1). From the first fraction, 12 mg (27%, based on $1\text{H}^+\text{BF}_4^-$) of **1** were obtained. From the second fraction, 26 mg (58%, based on $1\text{H}^+\text{BF}_4^-$) of pale yellow crystalline $\{\mu\text{-}\eta^5\text{:}\eta^5\text{-}(\text{C}_5\text{H}_3\text{SiMe}_2\text{OMe})(\text{C}_5\text{H}_4)\text{SiMe}_2\}\text{Ru}_2(\text{CO})_4$ (**6**) were obtained. ^1H NMR (400 MHz, CDCl_3): δ

0.26 (s, 3 H, Si(CH₃)), 0.43 (s, 3 H, Si(CH₃)), 0.46 (s, 3 H, Si(CH₃)), 0.47 (s, 3 H, Si(CH₃)), 3.56 (s, 3 H, OCH₃), 5.22 (m, 1 H, Cp-H), 5.37 (m, 1 H, Cp-H), 5.60 (m, 1 H, Cp-H), 5.63 (m, 1 H, Cp-H), 5.71 (m, 1 H, Cp-H), 5.77 (m, 1 H, Cp-H), 5.82 (m, 1 H, Cp-H). ¹³C NMR (100 MHz, CDCl₃): δ -2.55, -2.06, 0.02, 0.17 (CH₃), 49.71 (OCH₃), 84.72, 88.45, 89.13, 90.73, 91.18, 93.69, 95.99, 100.59, 101.49, 104.31 (Cp), 216.36 (CO). IR (hexanes): ν(CO) (cm⁻¹) 2019 (vs), 2008 (s), 1971 (s), 1950 (s), 1940 (m), 1795 (m). Anal. Calcd for C₁₉H₂₂O₅PRu₂Si₂: C, 36.83; H, 3.58. Found: C, 36.98; H, 4.01. Crystals of **6** suitable for X-ray diffraction analysis were obtained by slow cooling of a saturated solution of **6** in hexanes/CH₂Cl₂ (10:1) to -20°C.

Reaction of 1H⁺BF₄⁻ with NaSMe. Method 1. Solid NaSMe (12.0 mg, 169 μmol) was added to a solution of 1H⁺BF₄⁻ (50.0 mg, 77.6 μmol) in MeOH (50 mL), and the mixture was stirred for 10 min. The resulting orange solution contained mainly {μ-η⁵:η⁵-(C₅H₃SiMe₂OMe)(C₅H₄)SiMe₂}Ru₂(CO)₄ (**6**) (see above) and **1**. After the solvent was removed under vacuum, the resulting yellow residue was dissolved in hexanes (2 mL) and chromatographed on an alumina column (20 × 1 cm) with hexanes/CH₂Cl₂ (10:1) as the eluent. A yellow band, containing **1** (14 mg, 33%, based on 1H⁺BF₄⁻), was eluted and collected. Then, a second yellow band containing **6** (23 mg, 51%, based on 1H⁺BF₄⁻) was eluted with hexanes/CH₂Cl₂ (5:1).

Method 2. Synthesis of {μ-η⁵:η¹:η⁵-(C₅H₃C=O)(C₅H₄)(SiMe₂)₂O}Ru₂(μ-SMe)(CO)₃ (8a**).** Solid NaSMe (12.0 mg, 169 μmol) was added to a suspension of 1H⁺BF₄⁻ (50.0 mg, 77.6 μmol) in THF (50 mL), and the mixture was stirred for 30 min. The resulting orange solution contained some **1** but mainly {(η⁵-C₅H₃)₂(SiMe₂)₂}Ru₂(CO)₄(H)(SMe) (**7a**),

as indicated by the IR ($\nu(\text{CO})$ 2044 (vs), 2035 (vs), 1995 (vs), 1977 (vs) cm^{-1}) and ^1H NMR spectra (400 MHz, CDCl_3 , δ -10.66 (s, 1 H, Ru-*H*), 0.33 (s, 6 H, Si(CH_3)), 0.59 (s, 6 H, Si(CH_3)), 2.03 (s, 3 H, SCH₃), 5.47 (d, $J = 2.4$ Hz, 2 H, Cp), 5.55 (m, 2 H, Cp), 5.97 (t, $J = 2.4$ Hz, 1 H, Cp), 5.99 (t, $J = 2.4$ Hz, 1 H, Cp)). After the solvent was removed under vacuum, the resulting orange-brown residue was dissolved in hexanes/ CH_2Cl_2 (5:1) (2 mL) and chromatographed on an alumina column (20 \times 1 cm) with hexanes/ CH_2Cl_2 (10:1) as the eluent. A yellow band was eluted and collected. Then, an orange band was eluted with $\text{CH}_2\text{Cl}_2/\text{MeOH}$ (5:1). From the first fraction, 9 mg (21%, based on $1\text{H}^+\text{BF}_4^-$) of **1** were obtained. From the orange fraction, 30 mg (62%, based on $1\text{H}^+\text{BF}_4^-$) of orange crystalline $\{\mu\text{-}\eta^5\text{:}\eta^1\text{:}\eta^5\text{-}(\text{C}_5\text{H}_3\text{C}=\text{O})(\text{C}_5\text{H}_4)(\text{SiMe}_2)_2\text{O}\}\text{Ru}_2(\mu\text{-SMe})(\text{CO})_3$ (**8a**) were obtained. ^1H NMR (400 MHz, CDCl_3): δ 0.35 (s, 3 H, Si(CH_3)), 0.35 (s, 3 H, Si(CH_3)), 0.42 (s, 6 H, Si(CH_3)), 2.41 (s, 3 H, SCH₃), 4.83 (m, 1 H, Cp-*H*), 4.86 (m, 1 H, Cp-*H*), 4.88 (m, 1 H, Cp-*H*), 4.95 (m, 2 H, Cp-*H*), 5.18 (m, 1 H, Cp-*H*), 5.80 (t, $J = 2.0$ Hz, 1 H, Cp-*H*). ^{13}C NMR (100 MHz, CDCl_3): δ 1.20, 1.84, 1.88, 3.54 (CH_3), 32.92 (SCH₃), 78.23, 80.17, 82.22, 84.23, 84.43, 84.69, 85.38, 101.71, 105.27 (Cp; 9 out of 10 peaks), 191.65, 197.72, 207.84 (CO), 254.72 (Cp-C=O). IR (hexanes): $\nu(\text{CO})$ (cm^{-1}) 2038 (vs), 1992 (vs), 1934 (m), 1591 (w). Anal. Calcd for $\text{C}_{19}\text{H}_{22}\text{O}_5\text{Ru}_2\text{SSi}_2$: C, 36.76; H, 3.57. Found: C, 36.95; H, 3.71. Crystals of **8a** suitable for X-ray diffraction analysis were obtained by slow cooling of a saturated solution of **8a** in hexanes to -20°C .

Synthesis of $\{\mu\text{-}\eta^5\text{:}\eta^1\text{:}\eta^5\text{-}(\text{C}_5\text{H}_3\text{C}=\text{O})(\text{C}_5\text{H}_4)(\text{SiMe}_2)_2\text{O}\}\text{Ru}_2(\mu\text{-SEt})(\text{CO})_3$ (8b**).** By reacting NaSEt (14 mg, 0.17 mmol) with complex $1\text{H}^+\text{BF}_4^-$ (50 mg, 77.6 μmol), **8b** (27 mg, 54%; orange solid) was prepared and isolated using the same method as in the preparation of

8a. ^1H NMR (400 MHz, CDCl_3): δ 0.35 (s, 3 H, Si(CH_3)), 0.36 (s, 3 H, Si(CH_3)), 0.42 (s, 3 H, Si(CH_3)), 0.43 (s, 3 H, Si(CH_3)), 1.09 (t, $J = 7.2$ Hz, 3 H, SCH_2CH_3), 2.63 (m, 2 H, SCH_2CH_3), 4.85 (m, 1 H, Cp-H), 4.90 (m, 3 H, Cp-H), 5.01 (m, 1 H, Cp-H), 5.13 (m, 1 H, Cp-H), 5.77 (m, 1 H, Cp-H). IR (hexanes): $\nu(\text{CO})$ (cm^{-1}) 2036 (vs), 1990 (vs), 1934 (m), 1589 (w).

General Procedure for X-ray Structure Determinations. Data were collected on a Bruker CCD-1000 diffractometer. The structures were solved using direct methods and standard difference map techniques, and refined by full matrix least-squares procedures using SHELXTL.¹⁴ All hydrogen atoms were placed in the structure factor calculation at idealized positions. Complete details of the crystallographic study of **4a**, **6** and **8a** (CIF) are available free of charge via the Internet at <http://pubs.acs.org>.

Acknowledgment

This work was supported by the National Science Foundation through Grant No. CHE-9816342.

References

- (1) (a) McDaniel, K. F. In *Comprehensive Organometallic Chemistry*, Wilkinson, G., Stone F. G. A., Abel, E W., Eds., Pergamon Press: Oxford, New York 1995; Vol. 12, p. 601. (b) Collman, J. P.; Hegedus, L. S.; Norton, J. R.; Finke, R. G. *Principles and Applications of Organotransition Metal Chemistry*; University Science Books: Mills Valley, CA, 1987; Chapter 7. (c) Müller, T. E.; Beller, M. *Chem. Rev.* **1998**, 98, 67.

- (2) (a) Angelici, R. J. *Acc. Chem. Res.* **1995**, *28*, 52. (b) Kristjánisdóttir, S. S.; Norton, J. R. In *Transition Metal Hydrides: Recent Advances in Theory and Experiments*; Dedieu, A., Ed.; VCH: New York, 1991; Chapter 10. (c) Pearson, R. G. *Chem. Rev.* **1985**, *85*, 41. (d) Martinho Simões, J. A.; Beauchamp, J. L. *Chem. Rev.* **1990**, *90*, 629. (e) Bullock, R. M. *Comments Inorg. Chem.* **1991**, *12*, 1.
- (3) (a) Ovchinnikov, M. V.; Angelici, R. J. *J. Am. Chem. Soc.* **2000**, *122*, 6130. (b) Ovchinnikov, M. V.; Guzei, I. A.; Angelici, R. J. *Organometallics* **2001**, *20*, 691.
- (4) Doherty, N. M.; Knox, S. A. R.; Morris, M. J. *Inorg. Synth.* **1990**, *28*, 189.
- (5) Greene, T. W.; Wuts, P. G. M. *Protective Groups in Organic Synthesis*; John Wiley & Sons, Inc.: New York, 1999.
- (6) Joseph, M. F.; Page, J. A.; Baird, M. C. *Organometallics* **1984**, *3*, 1749.
- (7) Treichel, P. M.; Komar, D. A. *Synth. React. Inorg. Met.-Org. Chem.* **1980**, *10*, 205.
- (8) Tilset, M.; Vollhardt, K. P. C.; Boese, R. *Organometallics* **1994**, *13*, 3146.
- (9) Bitterwolf, T. E.; Leonard, M. B.; Horine, P. A.; Shade, J. E.; Rheingold, A. L.; Staley, D. J.; Yap, G. P. A. *J. Organomet. Chem.* **1996**, *512*, 11.
- (10) Crystallographic data (excluding structure factors) for the structure in this paper have been deposited with the Cambridge Crystallographic Data Centre as supplementary publication no. CCDC-165288 (**4a**), no. CCDC-165287 (**6**), no. CCDC-165286 (**8a**). Copies of the data can be obtained, free of charge, on application to CCDC, 12 Union Road, Cambridge CB2 1EZ, UK, (fax: +44 1223 336033 or e-mail: deposit@ccdc.cam.ac.uk).

- (11) Errington, R. J. *Advanced Practical Inorganic and Metalorganic Chemistry*, 1st ed.; Chapman & Hall: New York, 1997.
- (12) Pangborn, A. B.; Giardello, M. A.; Grubbs, R. H.; Rosen, R. K.; Timmers, F. J. *Organometallics* **1996**, *15*, 1518.
- (13) Perrin, D. D.; Armarego, W. L. F.; Perrin, D. R. *Purification of Laboratory Chemicals*, 2nd ed.; Pergamon: New York, 1980.
- (14) All software and sources of the scattering factors are contained in the SHELXTL (version 5.1) program library (G. Sheldrick, Bruker Analytical X-Ray Systems, Madison, WI).

Table 1. Crystallographic Data for **4a**, **6** and **8a**.

	4a	6
formula	$C_{31}H_{32}BF_4O_4PRu_2Si_2$ $\cdot \frac{1}{2}CH_2Cl_2$	$C_{19}H_{22}O_5Ru_2Si_2$
fw	887.13	588.69
crystal syst	monoclinic	orthorhombic
space group	$P2_1$	$Pbca$
a , Å	12.781(7)	16.7840(11)
b , Å	21.254(11)	13.2842(8)
c , Å	14.342(8)	19.9675(13)
α , deg	90	90
β , deg	104.886(9)	90
γ , deg	90	90
V , Å ³	3765(3)	4452.0(5)
Z	4	8
crystal color, habit	colorless prism	orange prism
crystal size, mm	0.40 × 0.20 × 0.20	0.30 × 0.30 × 0.20
μ (Mo, $K\alpha$), mm ⁻¹	1.032	1.491
temp, K	298(2)	298(2)
abs cor	empirical	empirical
theta range	191 to 23.25°	2.37 to 26.37°
no. of rflns collected	31150	24731
no. of indep rflns	10786 [R(int) = 0.0694]	4556 [R(int) = 0.0289]
$R(F)$ ($I \geq 2\sigma(I)$), %	R1 = 0.0527, wR2 = 0.1227	R1 = 0.0230, wR2 = 0.0535

Table 1. Continued.

	8a
formula	$C_{19}H_{22}O_5Ru_2SSi_2$
fw	620.75
crystal syst	triclinic
space group	$P\bar{1}$
a , Å	10.5499(4)
b , Å	14.3296(6)
c , Å	16.4601(7)
α , deg	92.7868(10)
β , deg	106.5317(10)
γ , deg	102.3499(10)
V , Å ³	2314.31(16)
Z	4
crystal color, habit	orange block
crystal size, mm	0.40 × 0.30 × 0.30
μ (Mo, $K\alpha$), mm ⁻¹	1.526
temp, K	173(2)
abs cor	empirical
theta range	1.46 to 26.37°
no. of rflns collected	20646
no. of indep rflns	9379 [R(int) = 0.0161]
$R(F)$ ($I \geq 2\sigma(I)$), %	R1 = 0.0201, wR2 = 0.0504

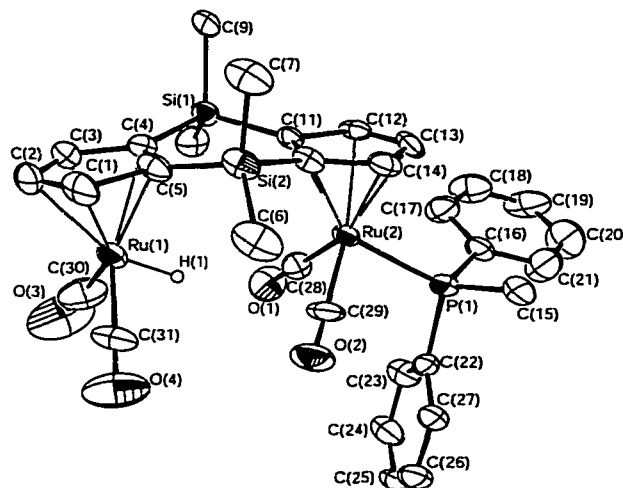


Figure 1. Thermal ellipsoid drawing of $[\{(\eta^5\text{-C}_5\text{H}_3)_2(\text{SiMe}_2)_2\}\text{Ru}_2(\text{CO})_4(\text{H})(\text{PMePh}_2)]^+$ (**4a**) showing the labeling scheme and 30% probability ellipsoids; hydrogens are omitted for clarity. Selected bond distances (Å) and angles (deg) are as follows: Ru(1)-Ru(2), 4.662(9); Ru(1)-C(30), 1.813(16); Ru(1)-C(31), 1.861(13); Ru(2)-C(28), 1.882(12); Ru(2)-C(29), 1.888(11); Ru(2)-P(1), 2.334(3); P(1)-C(15), 1.820(11); Ru(1)-Cp(centroid), 1.916(3); Ru(2)-Cp(centroid), 1.903(3); $\angle\text{C}(30)\text{-Ru(1)-C(31)}$, 89.6(6); $\angle\text{C}(28)\text{-Ru(2)-C(29)}$, 90.9(5); $\angle\text{C}(28)\text{-Ru(2)-P(1)}$, 89.6(3); $\angle\text{C}(29)\text{-Ru(2)-P(1)}$, 88.3(4); $\angle\text{Cp(centroid)-Ru(1)-Ru(2)-Cp(centroid)}$, 0.7; $\angle\text{Cp-Cp fold angle}$, 170.09.

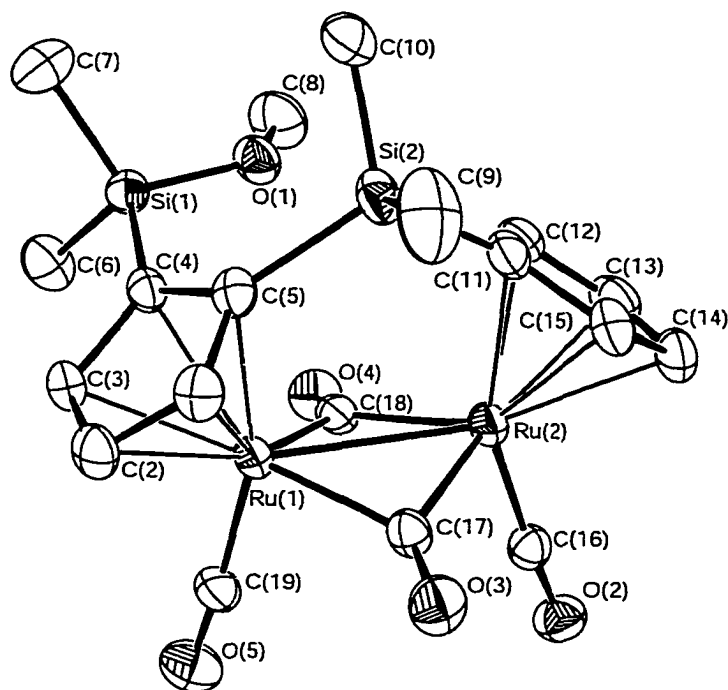


Figure 2. Thermal ellipsoid drawing of $\{\mu\text{-}\eta^5\text{:}\eta^5\text{-(C}_5\text{H}_3\text{SiMe}_2\text{OMe)(C}_5\text{H}_4\text{)SiMe}_2\}\text{Ru}_2(\text{CO})_4$ (**6**) showing the labeling scheme and 30% probability ellipsoids; hydrogens are omitted for clarity. Selected bond distances (Å) and angles (deg) are as follows: Ru(1)-Ru(2), 2.7049(3); Ru(1)-C(19), 1.859(3); Ru(1)-C(17), 2.056(3); Ru(1)-C(18), 2.048(3); Ru(2)-C(16), 1.858(3); Ru(2)-C(17), 2.029(3); Ru(2)-C(18), 2.060(3); Ru(1)-Cp(centroid), 1.981(3); Ru(2)-Cp(centroid), 1.977(3); $\angle\text{C(19)-Ru(1)-C(17)}$, 90.03(12); $\angle\text{C(19)-Ru(1)-C(18)}$, 85.73(12); $\angle\text{C(17)-Ru(1)-C(18)}$, 92.34(10); $\angle\text{Ru(1)-Ru(2)-C(16)}$, 105.55(8); $\angle\text{Ru(2)-Ru(1)-C(19)}$, 104.11(9); $\angle\text{Cp(centroid)-Ru(1)-Ru(2)-Cp(centroid)}$, 8.0; $\angle\text{C(16)-Ru(1)-Ru(2)-C(16)}$, 4.30(5); $\angle\text{Cp-Cp fold angle}$, 104.83.

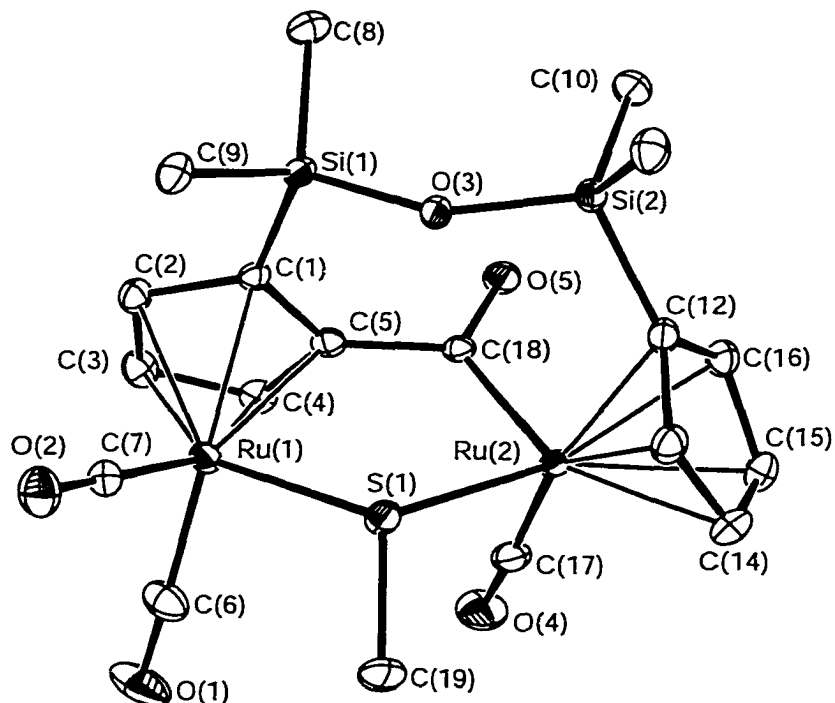


Figure 3. Thermal ellipsoid drawing of $\{\mu\text{-}\eta^5\text{:}\eta^1\text{:}\eta^5\text{-}(\text{C}_5\text{H}_3\text{C}=\text{O})(\text{C}_5\text{H}_4)(\text{SiMe}_2)_2\text{O}\}\text{Ru}_2(\mu\text{-SMe})(\text{CO})_3$ (**8a**) showing the labeling scheme and 30% probability ellipsoids; hydrogens are omitted for clarity. Selected bond distances (Å) and angles (deg) are as follows: Ru(1)-Ru(2), 3.898(3); Ru(1)-S(1), 2.3809(6); Ru(2)-S(1), 2.3450(6); C(19)-S(1), 1.813(3); Ru(1)-C(7), 1.896(2); Ru(1)-C(6), 1.880(3); Ru(2)-C(17), 1.844(3); Ru(2)-C(18), 2.026(2); C(5)-C(18), 1.521(3); C(18)-O(5), 1.232(3); Ru(1)-Cp(centroid), 1.919(6); Ru(2)-Cp(centroid), 1.884(6); $\angle\text{C(6)-Ru(1)-C(7)}$, 90.79(11); $\angle\text{C(6)-Ru(1)-S(1)}$, 94.67(10); $\angle\text{C(7)-Ru(1)-S(1)}$, 89.59(7); $\angle\text{C(17)-Ru(2)-C(18)}$, 86.52(10); $\angle\text{C(17)-Ru(2)-S(1)}$, 91.61(8); $\angle\text{C(18)-Ru(2)-S(1)}$, 91.47(6); $\angle\text{C(5)-C(18)-Ru(2)}$, 122.74(14); $\angle\text{O(5)-C(18)-Ru(2)}$, 125.02(16); $\angle\text{Ru(1)-S(1)-Ru(2)}$, 111.13(2); $\angle\text{Ru(1)-S(1)-C(19)}$, 107.89(11); $\angle\text{Ru(2)-S(1)-C(19)}$, 106.75(10).

GENERAL CONCLUSIONS

Protonation of the Ru-Ru bond in $\{(\eta^5\text{-C}_5\text{H}_3)_2(\text{SiMe}_2)_2\}\text{Ru}_2(\text{CO})_4$ (**1**) gives a cationic complex $[\{(\eta^5\text{-C}_5\text{H}_3)_2(\text{SiMe}_2)_2\}\text{Ru}_2(\text{CO})_4(\mu\text{-H})]^+$ (**1H⁺**) in which the bridging proton is removed only very slowly by bases even though the proton is thermodynamically acidic ($\text{p}K_{\text{a}}^{\text{AN}}=6.5(\pm 0.2)$). The low kinetic acidity of **1H⁺** allows it to react with alkyl amines, which attack a CO ligand that is activated to such an attack by the cationic nature of the complex. These amine reactions lead to the elimination of the $\mu\text{-H}$ which becomes incorporated into the formamide product. The proposed mechanism for this reaction is based on kinetic and isotope labeling studies. Although it is not obvious why the bridging proton is kinetically inert with respect to deprotonation, it may be due to a combination of the bulkiness and rigidity of the $(\eta^5\text{-C}_5\text{H}_3)_2(\text{SiMe}_2)_2$ ligand. Further studies of reactions of **1H⁺** with various nucleophiles revealed a general pattern for reactivity of **1H⁺**.

As an extension of this chemistry, we demonstrated that coordinated ethylene in protonated diruthenium complex $[\{(\eta^5\text{-C}_5\text{H}_3)_2(\text{SiMe}_2)_2\}\text{Ru}_2(\text{CO})_3(\eta^2\text{-CH}_2=\text{CH}_2)(\mu\text{-H})]^+$ (**2aH⁺**) undergoes nucleophilic attack by amines and phosphines to give corresponding ethylated organic products. Future studies will be directed toward hydroamination and other hydrofunctionalization reactions of alkenes that are catalyzed by **2aH⁺** and its derivatives.

ACKNOWLEDGEMENTS

I would like to thank my adviser, Professor Robert J. Angelici, for his tremendous support and guidance throughout my career in graduate school at Iowa State University. Also, I deeply appreciate the help and participation of the past and present Angelici group members. I would like to acknowledge our collaborators: Professor Moon-Gun Choi (Yonsei University, Seoul, Korea), Dr. Arthur J. Schultz and Dr. Xiaoping Wang (IPNS, Argonne National Laboratory), Dr. Iliia A. Guzei and Dr. Arkady Ellern (Molecular Structure Laboratory, University of Wisconsin, Madison). At last, but not the least, I would like to thank my family and friends for their love and support.